International Geology Review
Publication details, including instructions for authors and subscription information:
http://www.tandfonline.com/loi/tigr20

1.8 Ga magmatism in southern Finland: strongly enriched mantle and juvenile crustal sources in a post-collisional setting

Henrikki Rutanen [a], Ulf B. Andersson [b], Markku Väisänen [c], Åke Johansson [d], Sören Fröjdö [a], Yann Lahaye [e] & Olav Eklund [c]

[a] Geology & Mineralogy, Åbo Akademi University, Turku, Finland

[b] Department of Earth Sciences, Uppsala University, Uppsala, Sweden

[c] Department of Geology, University of Turku, Turku, Finland

[d] Laboratory for Isotope Geology, Swedish Museum of Natural History, Stockholm, Sweden

[e] The Finland Isotope Geosciences Laboratory, Geological Survey of Finland, Espoo, Finland

Version of record first published: 23 Jul 2010.

To cite this article: Henrikki Rutanen, Ulf B. Andersson, Markku Väisänen, Åke Johansson, Sören Fröjdö, Yann Lahaye & Olav Eklund (2011): 1.8 Ga magmatism in southern Finland: strongly enriched mantle and juvenile crustal sources in a post-collisional setting, International Geology Review, 53:14, 1622-1683

To link to this article: http://dx.doi.org/10.1080/00206814.2010.496241

International Geology Review
Vol. 53, No. 14, December 2011, 1622–1683

Taylor & Francis
Taylor & Francis Group

1.8 Ga magmatism in southern Finland: strongly enriched mantle and juvenile crustal sources in a post-collisional setting

Henrikki Rutanen[a]*, Ulf B. Andersson[b], Markku Väisänen[c], Åke Johansson[d], Sören Fröjdö[a], Yann Lahaye[e] and Olav Eklund[c]

[a]*Geology & Mineralogy, Åbo Akademi University, Turku, Finland;* [b]*Department of Earth Sciences, Uppsala University, Uppsala, Sweden;* [c]*Department of Geology, University of Turku, Turku, Finland;* [d]*Laboratory for Isotope Geology, Swedish Museum of Natural History, Stockholm, Sweden;* [e]*The Finland Isotope Geosciences Laboratory, Geological Survey of Finland, Espoo, Finland*

(*Accepted 17 May 2010*)

Whole-rock and isotope geochemistry of six ~1.8 Ga post-kinematic intrusions, emplaced along the ~1.9 Ga Southern Svecofennian Arc Complex (SSAC) and in the SW part of the Karelian Domain in Finland, was studied. The intrusive age [U–Pb secondary ion mass spectrometer (SIMS)] of one of these, the Petravaara Pluton, was determined as 1811 ± 6 Ma.

Basic-intermediate rocks are alkali-rich ($K_2O + Na_2O > 4$ wt.%) and typically shoshonitic, strongly enriched in large ion lithophile elements and light rare earth elements, but relatively depleted in high field strength elements and heavy rare earth elements. The enrichment is much higher than can be accounted for by crustal contamination and requires previously melt-depleted mantle sources, subjected to variable metasomatism by carbonate-rich fluids and sediment-derived melts. These sources are inferred to consist of phlogopite ± amphibole-bearing peridotites from depths below the spinel–garnet transition, as shown by the high Ce/Yb ratios. $^{87}Sr/^{86}Sr$(1.8 Ga) ratios in the range 0.7027–0.7031 and 'mildly depleted' ε_{Nd}(1.8 Ga) values (+0.1 to +1.4), with T_{DM} values <2.1 Ga, suggest that mantle enrichment was associated with the previous Svecofennian subduction–accretion process, when enriched sub-Svecofennian mantle sections developed, dominantly characterized by $^{147}Sm/^{144}Nd$ ratios of 0.14–0.17.

The associated granitoids are diversified. One group is marginally peraluminous, transitional between I (volcanic-arc) and S (syn-collisional) types, and was derived from mixed igneous and sedimentary, but juvenile Svecofennian source rocks, as supported by near-chondritic ε_{Nd}(1.8 Ga) and somewhat elevated $^{87}Sr/^{86}Sr$(1.8 Ga). The other group is transitional between I and A (within-plate) types in character and had dominantly igneous protoliths. The whole-rock geochemistry and isotopes suggest that the compositional variation between ~50 and 70 wt.% SiO_2 may be explained by hybridization between strongly enriched mantle-derived magmas and anatectic granitic magmas from the juvenile Svecofennian crust. One intrusion in the east contains a significant portion of Archaean, mostly igneous protolithic material (ε_{Nd}(1.8 Ga) = –2.8 and $\varepsilon_{Hf}(t)$ for zircons between +2.8 and –11.9, with an average of –4.9).

The ~1.8 Ga post-kinematic intrusions were emplaced within the SSAC subsequent to the continental collision with the Volgo-Sarmatia craton from the SE, during a shift from contraction to extension, that is, in a post-collisional setting.

Keywords: geochemistry; shoshonitic; mantle metasomatism; Nd-Sr-Hf and U–Pb isotopes; Svecofennian; Fennoscandian Shield

*Corresponding author. Email: hrutanen@abo.fi

ISSN 0020-6814 print/ISSN 1938-2839 online

DOI: 10.1080/00206814.2010.496241
http://www.informaworld.com

Introduction

Approximately 20 small (1–15 km in diameter/length), P-, F-, Ba-, Sr-, and light rare earth element (LREE)-enriched, often bi- or polymodal basic-intermediate-acid 1815–1760 Ma post-kinematic intrusive complexes and dikes/dike swarms have intruded the southeastern part of the Fennoscandian Shield. They occur in a ca. 600 km long E–W-trending belt, extending from southwestern Finland to Lake Ladoga in Russian Karelia (Figure 1; Andersson *et al.* 2006a and references therein). The surrounding bedrock comprises the essentially juvenile (<2.1 Ga; Lahtinen and Huhma 1997) Southern Svecofennian Arc Complex (SSAC; Korsman *et al.* 1997; Väisänen *et al.* 2002), which consists of pre- to late-orogenic, 1.90–1.81 Ga supracrustal and plutonic sequences (e.g. Kähkönen 2005; Nironen 2005), except in the easternmost part (Karelian Domain), where ca. 2.0 Ga supracrustals cover the Archaean craton (e.g. Laajoki 2005; Sorjonen-Ward and Luukkonen 2005).

We use the non-genetic term post-kinematic, in the sense that these intrusions post-date most of the ductile, pervasive deformation phases in southern Finland and tend to be younger than the predominantly 1.85–1.815 thousand million year-old, late Svecofennian granite intrusions that intruded the same area (e.g. Ehlers *et al.* 1993; Nironen 2005; Nironen and Kurhila 2008; Skyttä and Mänttäri 2008). They crosscut earlier structures but are often emplaced in connection with brittle-ductile, transpressional shear zones (e.g. Bergman 1986; Branigan 1987; Hubbard and Branigan 1987; Eklund *et al.* 1998; Nironen 2005; Torvela *et al.* 2008), suggesting that they do not post-date all tectonic activity (i.e. they are not strictly post-tectonic). Traditionally, these intrusions have been labelled 'post-orogenic' (e.g. Simonen 1980; Nironen 2005), because they typically lack superimposed structures. However, as they were emplaced during a shift from ductile to brittle tectonics immediately after the end of the major, late Svecofennian contractional orogeny at ca. 1.80 Ga, we consider this label inadequate.

Following collision, a gradual change from convergence to (trans)tension results in a shift from orogenic thickening to large lateral movements and escape along mega-shear zones, termed 'post-collisional' (e.g. Liégeois 1998; Bonin 2004). During a post-collisional tectonic phase in an orogeny, potassic magmas of high-K calc-alkaline and shoshonitic composition are typically emplaced (Liégeois *et al.* 1998; Bonin 2004). This last phase of an orogeny is followed by a gradual shift to post-orogenic and anorogenic settings and the stabilization of a new craton (Bonin *et al.* 1998; Bonin 2004).

The present contribution adds new geochemical and isotopic data on several of these intrusions, to complement previous studies (e.g. Eklund *et al.* 1998; Väisänen *et al.* 2000; Andersson *et al.* 2006a and references therein) and to refine the understanding of their origin and evolution. We also discuss the palaeogeodynamic environment that was prevalent at the time in this part of the Svecofennian orogen.

Regional geology

Archaean rocks (3.5–2.5 Ga; Mutanen and Huhma 2003 and references therein) form a cratonic nucleus in the northeastern part of the Fennoscandian Shield, in NE Finland and NW Russia (Figure 1). The craton was subjected to rifting in its interior and along the margins 2.45–1.95 thousand million years ago (Gaál and Gorbatschev 1987; Huhma *et al.* 1990; Peltonen *et al.* 1996). The Svecofennian Domain mainly formed at (2.1–)1.95–1.86 Ga from juvenile sources in volcanic arcs and intervening sedimentary basins, which were accreted to the Archaean cratonic nucleus from the present southerly direction (Gaál and Gorbatschev 1987; Nironen 1997). According to recent geodynamic models, the

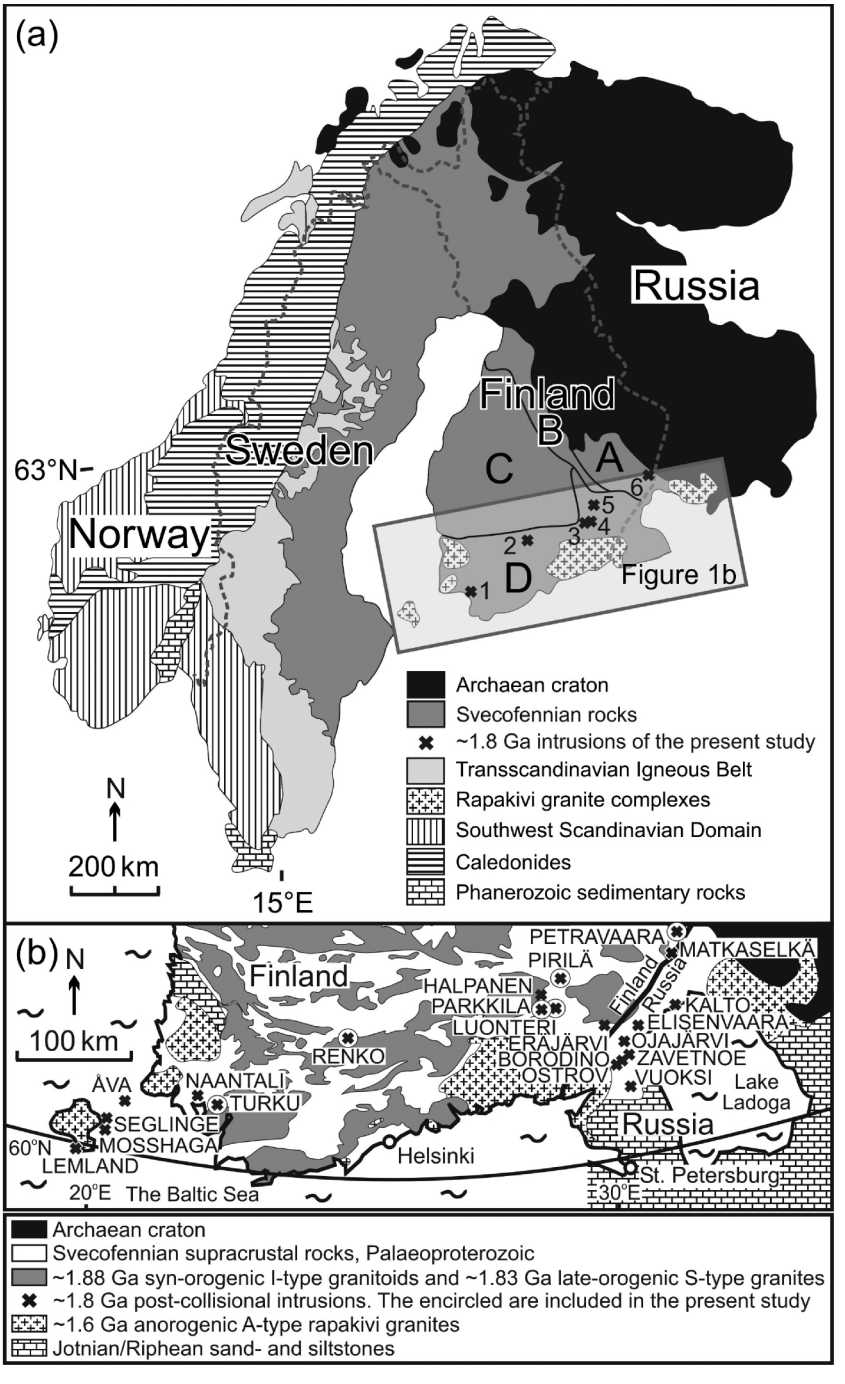

Figure 1. (a) Geological overview of the Fennoscandian Shield (modified after Högdahl and Sjöström 2001). The Palaeoproterozoic Arc Complexes under concern in Finland (e.g. after Korsman *et al.* 1997; Väisänen *et al.* 2002): A, Archaean Karelian Domain covered by Palaeoproterozoic supracrustals; B, Primitive Arc Complex; C, Central Svecofennian Arc Complex; and D, Southern Svecofennian Arc Complex. The positions of the studied intrusions are numbered: 1, Turku;

accretion involved both juvenile arcs and 'microcontinents' containing older crustal fragments that assembled during successive accretional episodes between 1.91 and 1.87 Ga (Lahtinen 1994; Korsman *et al.* 1999; Väisänen *et al.* 2002; Ehlers *et al.* 2004; Lahtinen *et al.* 2005; Korja *et al.* 2006).

According to Lahtinen *et al.* (2005), the arc accretion was followed by extension in southern Finland at ca. 1.86–1.84 Ga, whereas Nironen *et al.* (2006), Nironen and Kurhila (2008), and Skyttä and Mänttäri (2008) argued that extension continued during metamorphism and granite emplacement until 1.83–1.82 Ga. Extension was followed by convergence, with the main crustal shortening at ca. 1.82 Ga (Väisänen *et al.* 2002; Levin *et al.* 2005; Skyttä and Mänttäri 2008). This is interpreted as being related to continental collision, where Volgo-Sarmatia hit Fennoscandia obliquely from the SSE (e.g. Pesonen *et al.* 2003; Lahtinen *et al.* 2005; Bogdanova *et al.* 2008). The collision resulted in NW–SE compressional tectonics, NW-directed thrusting, and, at a later stage, partitioning of strain into around E–W dextral, transpressional shear zones and NNE–SSW reverse, E-side up shear zones (Ehlers *et al.* 1993; Skyttä *et al.* 2006; Väisänen and Skyttä 2007; Torvela *et al.* 2008).

The continental collision occurred simultaneously with high-T and low-P metamorphism and crustal melting in southern Finland and southcentral Sweden, including I- and S-type granitoid magmatism in Sweden, lasting until ca. 1.75 Ga (Huhma 1986; Ehlers *et al.* 1993; Claesson and Lundqvist 1995; Romer and Öhlander 1995; Öhlander and Romer 1996; Andersson and Öhlander 2004; Kurhila *et al.* 2005; Figure 1). Simultaneously in the west and southwest, subduction along the active Svecofennian continental margin created the voluminous Transscandinavian Igneous Belt (TIB) (e.g. Nyström 1982; Andersson 1991; Åhäll and Larson 2000; Andersson *et al.* 2004c; Rutanen and Andersson 2009).

According to Torvela *et al.* (2008) transpressional, ductile deformation along the South Finland shear zone had commenced already at ca. 1.85 Ga and was reactivated within a ductile regime at ca. 1.83 and ca. 1.79 Ga. Ehlers *et al.* (1993) and Väisänen and Skyttä (2007) suggested that the main ductile deformation was localized into transpressional shear zones in SW Finland at ca. 1.81–1.79 Ga. After ca. 1.79 Ga, the crust in southern Finland entered the brittle regime (Torvela *et al.* 2008).

Based on geophysical data, Korja and Heikkinen (2005, 2008) suggested that the collisional period was followed by a gravitational collapse of a thickened crust at ca. 1.80–1.77 Ga in southern Finland. In contrast, Cagnard *et al.* (2007) found no evidence for orogenic collapse, but proposed a compressional lateral flow of hot, ductile crust and exhumation by erosion. Based on thermal modelling, Kukkonen and Lauri (2009) proposed that collision and thickening of the crust at ca. 1.87–1.86 Ga generated the heat required for metamorphism, anatexis, and formation of the late-orogenic granitic magmas in southern Finland.

The post-kinematic intrusions penetrated the SSAC and the SW Karelian Domain shortly after the major regional thermomagmatic peak. However, at least locally, their intrusion took place during the last pulses of high heat flow (Vaasjoki and Sakko 1988; Väisänen *et al.* 2000; Mouri *et al.* 2005; Andersson *et al.* 2006b; Baltybaev *et al.* 2006; Väisänen and Kirkland 2008).

Figure 1. 2, Renko; 3, Parkkila; 4, Luonteri; 5, Pirilä; and 6, Petravaara. The rock types and the coordinates are given in Table 1. (b) All Svecofennian 1.8 Ga post-collisional intrusions and dikes in southern Finland and Russian Karelia in a simplified geological map (modified after Eklund *et al.* 1998; Koistinen *et al.* 2001; Konopelko and Eklund 2003). The circled diagonal crosses mark the intrusions studied in this article.

In the north, in Proterozoic terranes underlain by Archaean basement, crustal reworking also occurred at 1.85–1.76 Ga, including metamorphism and extensive granitoid magmatism, for example, in northern Finland (Huhma 1986; Vaasjoki 2001; Nironen 2005; Ahtonen *et al.* 2007; Heilimo *et al.* 2009) and northernmost Sweden (e.g. Öhlander *et al.* 1987, 1999; Bergman *et al.* 2001), but the connection to the tectonic processes in the south remains unknown.

1.8 Ga post-kinematic intrusions in southern Finland and Russian Karelia

Post-kinematic intrusions of 1.8 Ga in the western part of the SSAC comprise the 1797 ± 4 Ma Åva (Patchett and Kouvo 1986) and the 1785 ± 3 Ma Seglinge (Vaasjoki 1996) ring complexes, as well as the hypabyssal 1788 ± 11 Ma Mosshaga (Welin *et al.* 1983) and the 1770 ± 2 Ma Lemland (Suominen 1991) intrusions. These intrusions consist of coarse-grained porphyritic granites and monzonites. The intrusions are rounded or oval in form and from 4 to 15 km in diameter. The contacts with older rocks are sharp and contact metamorphism or chilled contacts have not been observed. The last phases of the intrusions are fine- and even-grained granites, aplites, granite pegmatites, and lamprophyres (Bergman 1986; Hubbard and Branigan 1987; Eklund 1993; Figure 1). A set of radial lamprophyre dikes is present in the Åva area (Kaitaro 1953; Andersson *et al.* 2006a). Recent zircon secondary ion mass spectrometer (SIMS) geochronology of the bimodal Åva ring complex gave intrusion ages from ca. 1790 to 1760 million years and 1801 ± 10 million years for the associated lamprophyre dikes (Eklund and Shebanov 2005). Additionally, at Naantali in SW Finland, ca. 1.80 Ga carbonatite dikes have recently been documented (Woodard and Hetherington, submitted; Figure 1).

Post-kinematic rocks included in this study comprise intrusions in the Turku (SW Finland) and Renko areas (central southern Finland), as well as the Parkkila, Luonteri, Pirilä, and Petravaara intrusions in SE Finland (described in detail below). At least two additional post-kinematic intrusions are found in SE Finland (Figure 1): (i) the Halpanen carbonatite dike (1792 ± 1 Ma, Pb–Pb zircon; Puustinen and Karhu 1999; Rukhlov and Bell 2010) and (ii) the Eräjärvi granite dike (1792 ± 5 Ma, U–Pb zircon; Nykänen 1988; Rämö *et al.* 2005).

The ca. 1.8 Ga post-kinematic intrusions in the easternmost SSAC, in Russian Karelia (Figure 1), vary significantly in their composition, with mafic rocks dominating in some intrusions whereas granites dominate in others (Ivanikov *et al.* 1995). With the exception of the 1781 ± 20 Ma (SIMS U–Pb zircon, Woodard *et al.*, submitted) Kalto lamprophyre dikes swarm (e.g. Ivashchenko and Lavrov 1993; Eklund *et al.* 1998), the intrusions are rounded and some demonstrate a well-developed ring structure, for example, the relatively large (16 km long and 6 km across) polymodal ultramafic to mesosyenitic, 1802 ± 17 Ma Vuoksi intrusion (Konopelko and Ivanikov 1996). The 1801 ± 4 Ma ultramafic to leucosyenitic Elisenvaara intrusive complex is composed of small stocks, pipe-like bodies, and dikes (Andersson *et al.* 2006a). The polymodal, approximately 13 × 5 km Ojajärvi intrusion comprises, for example, meladiorite, syenite, monzonite, granodiorite, and granite (Konopelko 1997) and has an age of ca. 1800 million years (e.g. Ivanikov *et al.* 1996), whereas the hypabyssal monzonitic Ostrov intrusion (Konopelko 1997) yielded an age of 1789 ± 3 million years (U–Pb zircon; pers. comm. O. Levchenkov 2008).

Intrusions of this study

We sampled six 1815–1794 Ma intrusions for geochemistry from an approximately 500 km E–W transect along the SSAC and the SW Karelian Domain in southern Finland

(Figure 1, Table 1) to add constraints on the tectonic setting of the post-kinematic magmatism. All ages cited below in this chapter refer to U–Pb zircon ages.

Turku

Five post-kinematic, monzodioritic, 1815 ± 2 Ma intrusions, which are closely associated with 1814 ± 3 Ma garnet-bearing peraluminous S-type granites, have been described from the Turku area in SW Finland (Figure 1; Table 1; Väisänen *et al.* 2000). The monzodiorites form dikes rather than plutonic bodies and range from 1.0 to 6.5 km in length and 0.1 to 1.0 km in width. Country-rock xenoliths and partly assimilated fragments occur within the monzodiorites near the contacts. The associated pink S-type granites may be up to 10 km long. Enclaves of mafic rocks in the granite and granitic fragments in the monzodiorites, as well as hybrid-like mixtures, attest to mingling of the magmas. Both the monzodioritic and granitic bodies are emplaced in a WSW–ENE direction, parallel to the regional structural grain. The main minerals of the monzodiorites are plagioclase, hornblende, biotite, titanite, apatite, Fe-Ti oxides (magnetite and ilmenite), and quartz, whereas the accessories are zircon and sulphides. Apatite is partly cumulus-enriched (Figure 2a; Table 1). Detailed description of the Turku intrusions and their field relationships can be found in Väisänen and Hölttä (1999) and Väisänen *et al.* (2000).

Renko

The 1812 ± 2 Ma (Vaasjoki 1995) Renko intrusion in central southern Finland (Figure 1) is composed of almost undeformed quartz-monzodiorite (sample #2a) and appears as a 3 × 1 km large positive anomaly on the aeromagnetic map. The country rock is composed of the late-orogenic Svecofennian granite. According to Lahtinen (1996), the surrounding granites show signs of mingling with the quartz-monzodiorite. Granite (sample #2b) and granite pegmatite dikes, a few centimetres to a couple of metres wide, were observed to sharply cut the monzonite and may represent back-veining of anatectic country-rock magmas (Figure 2b). The microcline phenocrystic granite dike (sample #2b) consists of plagioclase, quartz, and biotite, as well as accessory zircon, apatite, oxides, chlorite, and myrmekite.

The quartz-monzodiorite consists of plagioclase, dark brown pleochroic biotite, weakly undulating quartz, and K-feldspar (Figure 2c). Green hornblende was documented by Vaasjoki (1995), but was not found in the sample of this study (sample #2a; Table 1). The accessory minerals occur in relatively large amounts, including apatite, titanite, zircon, chlorite, sulphides, and oxides that consist mainly of magnetite. The abundance of magnetite correlates with the positive magnetic anomaly (Vaasjoki 1995; Lahtinen 1996).

Parkkila

More than 10 bodies of fine- to medium-grained, massive granodiorite and quartz-monzodiorite have been mapped in the Parkkila area of SE Finland (Figure 1; Simonen and Niemelä 1980). Sporadic K-feldspar phenocrysts occur, as well as biotite phenocrysts, in some relatively coarse varieties. Occasional thin granitic veins cut the intrusion. The larger bodies are a few kilometres long and some hundreds of metres wide (Simonen and Niemelä 1980). An age of 1794 ± 5 million years has been obtained from one of these (Simonen 1982). The Parkkila intrusions have entrained partly dissolved xenoliths of country-rock mica-gneiss and granite.

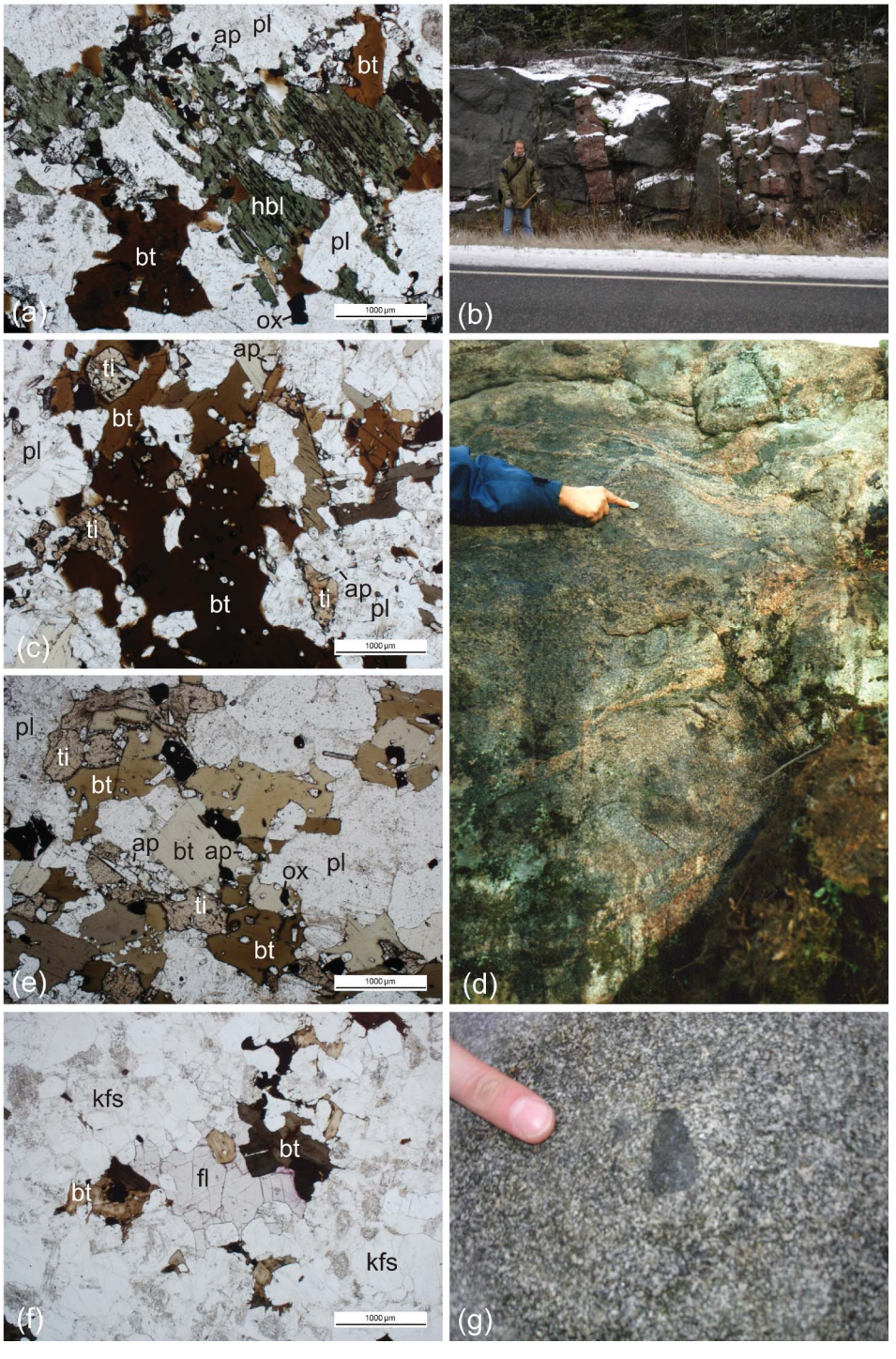

Figure 2. Photomicrographs (in plane-polarized light; mineral abbreviations as in Table 1) and field photographs: (a) Turku monzodiorite (sample #1a in Tables 1–3) with abundant apatite, amphibole (hornblende), and biotite. (b) Granite dikes, cross-cutting (back-veining) into the Renko quartz-monzodiorite intrusion. (c) Renko monzodiorite (sample #2a) with major amounts of titanite,

The principal minerals in the granodiorite are plagioclase, quartz, K-feldspar, biotite, and green hornblende. Titanite and apatite are abundant. Accessory minerals are oxides, sulphides, zircon, muscovite, and allanite (Table 1; Simonen 1982).

Luonteri

The 1802 ± 22 Ma Luonteri intrusion (Korsman *et al.* 1984), approximately 20 km east of Parkkila, is a semi-circular (2.0 × 2.5 km) polymodal complex (Figure 1). The rock types are determined on petrographical grounds as quartz-diorite, quartz-monzodiorite, granodiorites, and granites (Table 1), whereas geochemically all tend to be monzodioritic/monzonitic to monzogranitic in character (cf. Figure 4; Rutanen 2001). The rocks are essentially unfoliated, but sporadically the feldspars show flow foliation. Granodiorite is found as ghost-like enclaves within the mafic rock types (Figure 2d), suggesting magma mingling processes, whereas the granite cuts all the other rock types (Pitkänen 1985).

The principal minerals of the rocks are quartz, K-feldspar, plagioclase, biotite, and green hornblende (Table 1). Apatite and titanite occur abundantly (Figure 2e), as well as magnetite in such amounts that the intrusion shows a positive anomaly on aeromagnetic maps. Zircon is a common accessory mineral, and fluorite is found in those rocks that have a relatively high content of K-feldspar (Korsman and Lehijärvi 1973). Pyrite, allanite, and molybdenite occur occasionally (Pitkänen 1985).

The Luonteri granodiorites and quartz-diorites also intrude the country rocks. Pegmatitic and aplitic dikes cut the main intrusion (Korsman and Lehijärvi 1973; Pitkänen 1985). The country-rock schists and metaigneous rocks have been deformed before and during the Luonteri intrusion (Korsman and Lehijärvi 1973). The schistosity of these surrounding gneisses is conformable with the contacts and dips gently towards the centre of the intrusion (Pitkänen 1985).

Pirilä

The 1815 ± 7 Ma Pirilä intrusion (Vaasjoki and Sakko 1988) is a semi-circular (1.0 × 1.5 km) undeformed granite intrusion in SE Finland, approximately 50 km north of Luonteri (Figure 1). The rock is even-grained, light grey, and locally a bit reddish. The principal minerals are quartz, K-feldspar, biotite, and plagioclase, and the accessories include monazite, muscovite, apatite, fluorite, zircon, allanite, and opaques (Table 1 and Figure 2f). The country rock consists of K-feldspar-sillimanite-metapelite and garnet-diopside-amphibolite with pillow structures (Korsman 1973).

Petravaara

The 1811 ± 6 Ma (SIMS; see below) undeformed Petravaara granite intrusion is located in SE Finland (Figure 1; Nykänen 1968). The intrusion is approximately 1.5 km in diameter and cuts andalusite–mica-schists. It was emplaced within the part of the Karelian Domain

Figure 2. apatite, and biotite. (d) Ghost-like mingling structures in the Luonteri intrusion. (e) Luonteri quartz-diorite (sample #4a) with major amounts of titanite, apatite, and biotite. (f) Pirilä granite (sample #5) with biotite and fluorite. (g) Small mafic enclaves in the Petravaara granite, in support of the former presence of coeval mafic magmas.

Table 1. Localities, coordinates, rock types (cf. Figure 4), and mineralogy of the analysed 1.8 Ga post-collisional rocks in southern Finland. The sample numbers correspond to those in Figure 1a, as well as in Tables 2 and 3 (bold denotes isotopically analysed samples).

No.	Locality	Sample name	Lat. N*	Long. E*	Rock type from petrography	Rock type from geochem.	hbl	pl	bt	kfs	qtz	ox	ti	ap	Other
1a	**Turku**	**Urusvuori 1**	**671049**	**157109**	**qtz diorite**	**monzogabbro**	**x**	**x**	**x**		**x**	**x**		**x!**	**sul, zr**
1b		**Urusvuori 2**	**671028**	**157150**	**granite**	**syenogranite**		**x**	**x**	**x**	**x**	**x**			**gt,ms,zr,myrm**
2a	**Renko**	**Renko**	**675674**	**251821**	**qtz diorite**	**monzodiorite**		**x**	**x**	**(x)**	**x**	**x**	**x**	**x**	**sul,zr,chl**
2b		**Renko gr**	**675670**	**251817**	**granite dike**	**syenogranite**		**x**	**x**	**x**	**x**	**(x)**		**(x)**	**chl, zr,myrm**
3	**Parkkila**	**A826 (GTK)**	**683584**	**352368**	**granodiorite**	**monzonite**	**x**	**x**	**x**	**x**	**x**	**x**	**x!**	**x!**	**sul,all,zr,ms**
4a	**Luonteri**	**1.6b-HAR-96D**	**683083**	**354569**	**qtz diorite**	**monzodiorite**		**x**	**x**	**(x)**	**x**	**x**	**x!**	**x!**	**chl,sul,zr,myrm**
4b		1.1-HAR-96	683011	354642	fine-grained qtz diorite	monzodiorite	(x)	x	x	(x)	x	x	x	x	chl,sul,fl,all,zr
4c		1.9-HAR-96D	683018	354632	tonalite	monzonite		x	x	x	x	x	x	x	zr,sul
4d		1.7B-HAR-96	683090	354694	qtz monzodiorite	monzodiorite	x	x	x	x	x	x	x	x	zr,sul
4e		1.8B-HAR-96	682999	354654	porphyritic granodiorite	monzonite	x	x	x	x	x	x	x	x	chl,ser/sau,fl,zr,sul,ru,all
4f		**1.10-HAR-96D**	**683174**	**354615**	**granite**	**qtz monzonite**		**x**	**x**	**x**	**x**	**x**	**(x)**	**x**	**zr,sul,ms**
4g		1.11B-HAR-96	683092	354521	granite dike	qtz monzonite		x	x	x	x	x	x	x	zr,chl,ms,all,ru
5	**Pirilä**	**3.4-HAR-96**	**688045**	**355493**	**granite**	**syenogranite**		**x**	**x**	**x**	**x**	**x**		**x**	**ms,fl,zr,mz,all**
6	**Petravaara**	**4.1-HAR-96**	**689376**	**452328**	**granite**	**monzogranite**		**x**	**x**	**x**	**x**	**x**		**x**	**zr,mz,ms,all,myrm**

Note: GTK, sampled by Geological Survey of Finland; hbl, hornblende; pl, plagioclase; bt, biotite; kfs, K-feldspar; qtz, quartz; ox, Fe-Ti oxides; ti, titanite; ap, apatite; sul, sulphides; zr, zircon; gt, garnet; ms, muscovite; myrm, myrmekite; chl, chlorite; all, allanite; fl, fluorite; ser/sau, strongly sericite and saussurite altered (when noted ms, only sparsely altered); ru, rutile; mz, monazite; !, abundant; in brackets, scarce.
*Finnish KKJ national grid coordinate system.

where Palaeoproterozoic 2.06–1.97 Ga metasedimentary rocks cover the Archaean basement (Kohonen 1995; Laajoki 2005; Sorjonen-Ward 2006). The intrusion age, its undeformed nature, and the fact that it cuts the presumably Svecofennian structural pattern of the country rocks clearly puts it into the post-kinematic group. The principal minerals are plagioclase, quartz, biotite, and microcline. The accessories are muscovite, apatite, zircon, allanite, monazite, and myrmekite, as well as oxides. Occasionally small mafic enclaves are found, suggesting the presence of coeval, mafic magma (Figure 2g). Additionally, small xenoliths of the country rock can be found.

Analytical techniques

Samples for whole-rock geochemistry were selected to reflect the petrographical variation in each intrusion. Geochemical (Table 2) analyses of samples #1a, #1b, #2b, #3, #4a, #4c, and #4f were performed at Acme Analytical Laboratories Ltd., Canada. The major elements and Sc were determined by inductively coupled plasma optical emission spectrometry (ICP-OES) and the other trace elements by ICP-MS, except carbon and sulphur, which were analysed by Leco (combustion + infrared spectroscopy) and fluorine by a specific ion electrode method. The whole-rock geochemistry of samples #4b, #4d, #4e, #4g, #5, and #6 were analysed at Activation Laboratories Ltd., Canada. The major elements were determined by fusion ICP-OES. Sc and Be analyses were determined by ICP-MS and the other trace elements, except Cl, by fusion ICP-MS. Cl was determined by INAA. Sample #2a was analysed at the same laboratory but by ICP-MS for all the trace elements. A case hardened mild steel swingmill was used for grinding the samples. A swingmill may introduce some contamination for Fe, Cr, Ni, and Cu (cf. e.g. Johnson *et al.* 1999), which may have had a small impact on the concentration of these elements, especially in the more felsic samples. However, relatively large batches were ground, which should have minimized these effects.

Nine of the samples were analysed for Sr and Nd isotopes (Table 3). The analyses were made in the Laboratory for Isotope Geology at the Museum of Natural History in Stockholm, Sweden. Sm and Nd concentrations were determined by isotope dilution, using a mixed ^{147}Sm–^{150}Nd spike. Sm, Nd and Sr were loaded on double Re filaments and analysed as metal ions on a Finnigan MAT 261 thermal ionization MS. The Nd and Sr isotopic compositions were measured in multidynamic, and Sm in static mode. The Nd compositions were corrected for spike, Sm-interference, and fractionation using $^{146}Nd/^{144}Nd = 0.7219$. Sm-interference was monitored by measurements at mass 149. The Nd samples were measured during three sessions over about 1 year. Measured $^{143}Nd/^{144}Nd$ ratios of the LaJolla Nd-standard were 0.511852 ± 9 and 0.511847 ± 8 ($2\sigma_m$) during the first analytical session, 0.511849 ± 7 during the second session, and 0.511857 ± 15 and 0.511847 ± 6 during the third session. The differences are thus small and the values sufficiently close to the preferred value of 0.511854. The same holds true for the analysed standard sample BCR-2, with a value of 0.512638 ± 20 ($2\sigma_m$; Table 3), overlapping the preferred value of 0.512639 (Mahoney *et al.* 2003). No corrections of the measured values were thus necessary.

Reported $^{87}Rb/^{86}Sr$ ratios (Table 3) were calculated from measured $^{87}Sr/^{86}Sr$ and the Rb and Sr whole-rock analyses in Table 2. Precisions for Rb and Sr were reported by Acme Analytical Laboratories and Activation Laboratories at approximately ±5% (2σ) or better. The Sr isotope ratios were corrected for Rb-interference and normalized to $^{86}Sr/^{88}Sr = 0.1194$. Two measurements of the SRM 987 Sr standard during a first session of sample analyses yielded 0.710231 ± 10 and 710229 ± 11 ($2\sigma_m$) and during a second session 0.710243 ± 19 ($2\sigma_m$), which was within error overlap with the preferred value (0.710240;

Table 2. Geochemistry and normative mineral contents (SIN norms) of the analysed rocks. The sample numbers correspond to Figure 1a, as well as in Tables 1 and 3 (bold denotes isotopically analysed samples).

Rock suite	Turku		Renko		Parkkila	Luonteri							Pirilä	Petravaara
Sample	**1a**	**1b**	**2a**	**2b**	**3**	**4a**	4b	4c	4d	4e	**4f**	4g	**5**	**6**
SiO_2, %	**46.88**	**73.65**	**52.83**	**72.62**	**51.17**	**51.89**	53.64	54.85	54.99	56.25	**64.95**	64.70	**71.09**	**65.21**
TiO_2	**2.83**	**0.13**	**2.45**	**0.15**	**2.57**	**2.65**	2.33	2.01	2.26	2.00	**1.10**	1.09	**0.31**	**0.75**
Al_2O_3	**14.60**	**14.40**	**15.00**	**14.34**	**14.24**	**15.46**	15.34	16.26	15.44	15.23	**14.76**	14.82	**13.54**	**14.68**
$Fe_2O_3^t$	**14.65**	**1.58**	**11.00**	**1.53**	**11.47**	**10.81**	10.78	9.47	9.86	8.52	**5.65**	5.21	**2.81**	**4.88**
MnO	**0.13**	**0.04**	**0.12**	**0.01**	**0.13**	**0.09**	0.11	0.10	0.10	0.09	**0.04**	0.05	**0.04**	**0.05**
MgO	**4.79**	**0.18**	**3.95**	**0.34**	**3.38**	**3.08**	2.80	2.55	2.66	2.27	**1.34**	1.22	**0.27**	**1.30**
CaO	**7.71**	**0.87**	**6.83**	**0.88**	**6.20**	**6.37**	5.57	4.08	5.39	4.37	**2.66**	2.70	**1.12**	**2.06**
Na_2O	**2.74**	**3.20**	**2.99**	**3.07**	**3.36**	**3.41**	3.40	3.49	3.44	3.44	**3.08**	3.38	**3.23**	**3.38**
K_2O	**1.85**	**5.29**	**2.73**	**6.40**	**2.92**	**2.72**	2.91	4.35	3.31	3.77	**4.02**	4.64	**5.53**	**4.42**
P_2O_5	**2.24**	**0.10**	**1.43**	**0.17**	**1.90**	**1.46**	1.29	1.24	0.95	0.78	**0.52**	0.44	**0.05**	**0.22**
CO_2	**0.62**	**0.51**	**n.a.**	**0.11**	**0.51**	**0.18**	n.a.	0.15	n.a.	n.a.	**0.29**	n.a.	**n.a.**	**n.a.**
SO_2	**0.70**	**0.02**	**n.a.**	**0.02**	**0.26**	**0.36**	n.a.	0.08	n.a.	n.a.	**0.12**	n.a.	**n.a.**	**n.a.**
LOI	**1.00**	**0.50**	**0.85**	**0.40**	**1.20**	**1.10**	0.94	0.70	0.84	1.52	**1.20**	0.67	**0.65**	**0.59**
Total	**99.42**	**99.94**	**100.18**	**99.91**	**98.54**	**99.04**	99.11	99.10	99.24	98.24	**99.32**	98.92	**98.64**	**97.54**
Mg#	**43.3**	**21.0**	**45.6**	**34.1**	**40.7**	**39.9**	37.7	38.6	38.6	38.3	**35.6**	35.3	**18.3**	**38.3**
F, ppm	**3040**	**100**	**n.a.**	**n.a.**	**n.a.**	**7380**	n.a.	6560	n.a.	n.a.	**3090**	n.a.	**n.a.**	**n.a.**
Ba	**1194**	**845**	**1547**	**627**	**6276**	**3361**	4251	3918	2402	2563	**2299**	2469	**1392**	**1982**
Rb	**42**	**222**	**128**	**231**	**70**	**111**	135	210	106	133	**176**	128	**296**	**172**
Sr	**2105**	**166**	**1646**	**423**	**5811**	**2241**	2520	2350	1260	1084	**941**	1027	**623**	**528**
Cs	**1.1**	**1.4**	**4.2**	**1.8**	**1.8**	**1.2**	1.3	1.7	2.4	2.5	**4.6**	2.1	**3.4**	**4.6**
Ga	**24.2**	**21.4**	**28.0**	**16.4**	**24.4**	**28.5**	29.0	31.2	30.0	31.0	**26.1**	25.0	**26.0**	**28.0**
Ta	**1.1**	**0.6**	**1.8**	**0.3**	**1.1**	**1.9**	2.1	1.0	2.0	2.3	**1.0**	1.7	**1.3**	**0.8**
Nb	**22.8**	**10.4**	**33.2**	**6.8**	**29.0**	**47.5**	58.2	39.8	65.9	61.9	**27.9**	28.3	**36.2**	**24.5**
Hf	**6.8**	**3.6**	**4.6**	**5.1**	**11.2**	**15.8**	12.7	8.0	17.9	16.9	**10.8**	11.6	**13.0**	**10.7**
Zr	**264**	**108**	**331**	**152**	**551**	**756**	590	404	773	757	**477**	469	**431**	**425**
Y	**31.1**	**5.8**	**23.8**	**10.3**	**42.0**	**37.3**	40.0	18.3	36.0	30.6	**15.8**	17.1	**17.1**	**16.1**

Th	**5.6**	**12.5**	**5.2**	**15.6**	**14.5**	**16.9**	12.9	5.0	9.4	11.5	**7.3**	10.3	**63.1**	**20.3**
U	**1.70**	**4.40**	**2.65**	**7.30**	**6.20**	**5.60**	4.86	1.70	1.07	2.32	**3.00**	2.56	**14.02**	**2.28**
Cr	**95**	**14**	**40**	**14**	**14**	**54**	23	27	42	35	**20**	28	**87**	**57**
Ni	**37.7**	**2.2**	**n.d.**	**3.9**	**6.5**	**12.1**	7.0	6.7	11.0	7.0	**4.3**	5.0	**n.d.**	**17.0**
Co	**35.1**	**1.7**	**27.0**	**2.1**	**20.8**	**19.1**	18.7	15.5	16.8	13.6	**8.7**	7.9	**0.8**	**6.8**
Sc	**15.0**	**2.0**	**11.0**	**2.0**	**12.0**	**11.0**	13.0	9.0	14.0	11.0	**2.0**	1.0	**3.0**	**8.0**
V	**239**	**11**	**121**	**6**	**145**	**131**	111	90	96	82	**48**	53	**10**	**56**
Cu	**67.6**	**2.9**	**60.0**	**10.7**	**32.9**	**38.8**	32.0	22.5	24.0	13.0	**20.1**	8.0	**n.d.**	**n.d.**
Pb	**3.3**	**3.8**	**11.0**	**4.4**	**27.2**	**6.3**	38.0	6.3	18.0	23.0	**2.2**	30.0	**112.0**	**25.0**
Zn	**150**	**29**	**240**	**30**	**197**	**205**	190	190	206	171	**126**	91	**69**	**83**
W	**10.7**	**16.2**	**7.0**	**9.2**	**6.1**	**7.2**	7.2	6.0	7.5	7.1	**11.4**	10.6	**11.4**	**8.4**
Mo	**2.40**	**1.90**	**2.00**	**0.90**	**1.70**	**1.70**	3.47	1.40	2.46	2.93	**1.10**	2.75	**6.46**	**1.93**
Be	**3**	**1**	**2**	**n.d.**	**3**	**n.a.**	3	n.a.	3	3	**n.a.**	2	**3**	**4**
La	**128**	**44**	**117**	**45**	**343**	**235**	320	121	233	227	**141**	161	**370**	**164**
Ce	**308**	**85**	**253**	**91**	**830**	**545**	620	265	430	410	**303**	292	**596**	**288**
Pr	**34.8**	**8.0**	**30.8**	**9.2**	**82.1**	**56.3**	58.2	25.4	38.9	36.8	**28.2**	24.6	**53.2**	**24.2**
Nd	**143**	**29**	**112**	**29**	**294**	**222**	230	94	154	146	**103**	85	**178**	**87**
Sm	**19.9**	**4.2**	**16.5**	**4.4**	**32.5**	**26.9**	29.9	11.8	22.0	21.9	**12.4**	9.4	**20.4**	**10.6**
Eu	**4.41**	**0.68**	**4.38**	**0.82**	**7.95**	**5.61**	6.57	2.37	4.21	4.43	**2.83**	2.51	**2.16**	**1.96**
Gd	**11.4**	**2.1**	**12.3**	**2.4**	**17.3**	**13.7**	19.6	6.1	15.8	14.8	**6.0**	6.5	**4.8**	**7.6**
Tb	**1.42**	**0.28**	**1.21**	**0.41**	**2.12**	**1.73**	1.85	0.78	1.62	1.53	**0.82**	0.60	**0.73**	**0.64**
Dy	**6.38**	**1.40**	**5.24**	**1.90**	**8.79**	**7.69**	8.31	3.46	7.80	7.00	**3.37**	2.83	**3.77**	**2.86**
Ho	**1.05**	**0.18**	**0.82**	**0.30**	**1.13**	**1.11**	1.31	0.52	1.27	1.06	**0.48**	0.52	**0.60**	**0.49**
Er	**2.39**	**0.48**	**2.06**	**0.73**	**3.04**	**2.48**	3.47	1.20	3.18	2.66	**1.04**	1.54	**1.41**	**1.47**
Tm	**0.35**	**0.07**	**0.28**	**0.11**	**0.46**	**0.37**	0.32	0.18	0.32	0.27	**0.15**	0.18	**0.20**	**0.18**
Yb	**2.21**	**0.62**	**1.68**	**0.69**	**2.36**	**2.23**	2.14	1.18	2.04	1.80	**0.92**	1.26	**1.22**	**1.10**
Lu	**0.29**	**0.07**	**0.23**	**0.09**	**0.34**	**0.26**	0.35	0.15	0.31	0.32	**0.13**	0.20	**0.24**	**0.20**
La_N/Yb_N	**41**	**51**	**50**	**47**	**104**	**76**	107	73	82	90	**110**	92	**218**	**107**

(*Continued*)

Table 2. (*Continued*)

Rock suite	Turku		Renko		Parkkila	Luonteri							Pirilä	Petravaara
Sample	**1a**	**1b**	**2a**	**2b**	**3**	**4a**	4b	4c	4d	4e	**4f**	4g	**5**	**6**
SIN norms:														
qtz, %	**0.3**	**32**	**6**	**28**	**4**	**6**	7	7	7	9	**24**	20	**28**	**22**
or	**11**	**32**	**16**	**38**	**18**	**16**	18	26	20	23	**24**	28	**33**	**27**
ab	**24**	**27**	**26**	**26**	**29**	**29**	29	30	30	30	**26**	29	**28**	**29**
an	**23**	**4.0**	**20**	**3.6**	**16**	**19**	19	10	17	16	**9**	12	**6**	**10**
di	**1.5**	**-**	**5.0**	**-**	**5.4**	**0.3**	2.5	-	3.8	2.1	**-**	-	**-**	**-**
hy	**26**	**1.7**	**15**	**2.0**	**14**	**15**	14	13	11	10	**7**	6	**2.8**	**7**
mt	**3.3**	**0.7**	**3.9**	**0.7**	**4.1**	**3.8**	3.8	3.7	3.9	3.4	**2.2**	2.4	**1.3**	**2.3**
il	**5.5**	**0.2**	**4.7**	**0.3**	**5.0**	**5.1**	4.5	3.9	4.4	3.9	**2.1**	2.1	**0.6**	**1.5**
ap	**5.5**	**0.2**	**3.4**	**0.4**	**4.8**	**3.6**	3.2	3.1	2.3	1.9	**1.3**	1.1	**0.1**	**0.5**
zr	**0.1**	**0.02**	**0.1**	**0.03**	**0.1**	**0.1**	0.1	0.1	0.2	0.2	**0.1**	0.1	**0.1**	**0.1**
fl	**0.2**	**0.002**	**-**	**-**	**-**	**1.3**	-	1.2	-	-	**0.6**	-	**-**	**-**
chr	**0.1**	**0.002**	**0.04**	**0.004**	**0.03**	**0.04**	0.03	0.03	0.03	0.03	**0.01**	0.02	**0.02**	**0.02**

Note: LOI, loss of ignition; Mg#, Mg number (100×(MgO×0.603 / 24.305)) / (MgO×0.603 / 24.305+((0.85×FeO^t)×0.777 / 55.847)); n.d., not detected; n.a., not analysed. Normative minerals were calculated using the SINCLAS program of Verma *et al*. (2002), employing the Fe-recalculation scheme by Middlemost (1989). qtz, quartz; or, orthoclase; ab, albite; an, anorthite; di, diopside; hy, hypersthene; mt, magnetite; il, ilmenite; ap, apatite; zr, zircon; fl, fluorite; chr, chromite.

Table 3. Sm-Nd and Rb-Sr isotopic data of the selected 1.8 Ga post-collisional rocks in southern Finland and the Columbia River basalt standard BCR-2. The sample numbers correspond to those in Figure 1a, as well as in Tables 1 and 2.

No.	t (Ma)	Sm (ppm)[a]	Nd (ppm)[a]	$^{147}Sm/^{144}Nd$[a]	$^{143}Nd/^{144}Nd \pm 2\sigma_m$[b]	$\varepsilon_{Nd}(t)$[c]	T_{DM}[d] (Ga)	$^{87}Rb/^{86}Sr$[e]	$^{87}Sr/^{86}Sr \pm 2\sigma_m$[b]	$^{87}Sr/^{86}Sr(t)$	$\varepsilon_{Sr}(t)$[f]	T_{UR}[f] (Ga)
1a	1815	19.67	135.5	0.0878	0.511380 ± 5	+0.8	2.02	0.0576	0.704178 ± 7	0.7027	+4.8	0.90
1b	1814	3.80	26.02	0.0883	0.511373 ± 5	+0.6	2.03	3.8931	0.807773 ± 6	0.7062	+54.8	1.88
2a	1812	16.91	118.3	0.0864	0.511393 ± 9	+1.4	1.98	0.2250	0.707755 ± 7	0.7019	−6.5	1.59
2b	1812	4.83	35.05	0.0832	0.511281 ± 10	−0.1	2.06	1.5860	0.746091 ± 9	0.7048	+34.3	1.92
3	1794	34.82	279.7	0.0753	0.511212 ± 6	+0.1	2.02	0.0348	0.704029 ± 17	0.7031	+10.9	0.69
4a	1802	26.62	199.6	0.0806	0.511289 ± 5	+0.5	2.01	0.1430	0.706531 ± 6	0.7028	+6.7	2.33
4f	1802	12.05	94.94	0.0767	0.511245 ± 6	+0.6	2.00	0.5404	0.716881 ± 11	0.7029	+7.4	1.88
5	1815	18.89	172.9	0.0660	0.511101 ± 11	+0.5	2.01	1.3811	0.733770 ± 9	0.6977	−65.9	1.57
6	1811	10.52	89.13	0.0713	0.511002 ± 13	−2.8	2.19	0.9477	0.728031 ± 6	0.7033	+14.2	1.89
BCR-2		6.55	28.53	0.1388	0.512638 ± 20				0.704982 ± 11			

[a]Sm and Nd concentrations and $^{147}Sm/^{144}Nd$ ratio from isotope dilution. Estimated analytical uncertainty of $^{147}Sm/^{144}Nd$ ratio is ≤ ±0.5 %.
[b]Error given as 2 standard error of the mean from the mass spectrometer run in the last digits.
[c]Initial ε_{Nd} value calculated, according to Jacobsen and Wasserburg (1984): present-day chondritic $^{147}Sm/^{144}Nd$ ratio 0.1967, present-day chondritic $^{143}Nd/^{144}Nd$ ratio 0.512638.
[d]Model age calculated relative to the depleted mantle curve (DM) of DePaolo (1981).
[e]Calculated from ICP-MS data (Table 2) and measured $^{87}Sr/^{86}Sr$ ratio.
[f]ε_{Sr} value and T_{UR} Sr model age calculated using the UR values of McCulloch and Chappell (1982): present-day $^{87}Rb/^{86}Sr = 0.0827$; present-day $^{87}Sr/^{86}Sr = 0.7045$.

Gladney *et al.* 1990). One analysis of the BCR-2 standard yielded a value of 0.704982 ± 11 ($2\sigma_m$; Table 3), falling in between the two reported preferred values of 0.704958 (Raczek *et al.* 2003) and 0.705024 (Mahoney *et al.* 2003). No corrections of the measured samples were considered necessary.

Zircons were recovered from the Petravaara granite (sample #6 in Tables 1–3), after sample crushing, by heavy liquid (methylene iodide, CH_2I_2; $D = 3.32$) and magnetic separation, before handpicking. Crystals were mounted in epoxy and subjected to CL/BSE imaging using a JEOL JSM 5900LV scanning electron microscope at the Geological Survey of Finland (GTK) in Espoo. U–Pb analyses were made at the Nordsim facility at the Swedish Museum of Natural History using a Cameca IMS 1270 high-spatial resolution SIMS. The spot-diameter for the 9 nA primary O_2^- ion beam was approximately 25 μm. Oxygen flooding in the sample chamber was used to increase the production of Pb^+ ions. Three counting blocks, each including four cycles of the Zr, Pb, Th, and U species of interest, were measured from each spot. The mass resolution ($M/\triangle M$) was 5400 (10%). The raw data were calibrated against a zircon standard 91500 (Wiedenbeck *et al.* 1995) and corrected for modern common lead ($T = 0$; Stacey and Kramers 1975). The procedure followed essentially those reported in Whitehouse *et al.* (1999) and Whitehouse and Kamber (2005). The age calculation was done using Isoplot/Excel v. 3.05 (Ludwig 2003).

Lu-Hf isotope analyses were performed on zircon grains selected among those analysed by SIMS from the Petravaara sample (#6). A Nu Plasma HR multicollector (MC)-ICP-MS in the SIGL facility (Finland Isotope Geosciences Laboratory) at the Geological Survey of Finland (GTK) was used, with a technique similar to that of Rosa *et al.* (2009), except for the utilization of a New Wave UP193 Nd:YAG laser microprobe in the present case. Samples were ablated in He gas (gas flow = 1.0 L/min) in the standard laminar flow ablation cell provided by New Wave. The He aerosol was mixed with Ar (gas flow = 0.7 L/min) in a teflon mixing cell prior to entry into the plasma. The gas mixture was optimized daily for maximum sensitivity. All analyses were made in static ablation mode using the following parameters: beam diameter 45 μm, pulse frequency 10 Hz, and beam energy density 1 J/cm^2. Each ablation was preceded by a 30s on-mass background measurement. The MC-ICP-MS was equipped with 9 Faraday detectors and amplifiers with 10^{11} Ω resistors. During the ablation, the data were collected in static mode (^{173}Yb, ^{175}Lu, ^{176}Hf-Yb-Lu, ^{177}Hf, ^{178}Hf, ^{179}Hf). The total Hf signal obtained for zircons with normal Hf concentration was 1.0–2.0 V. Under these conditions, 120 s of ablation are needed to obtain an internal precision of $\leq \pm 0.000040$ ($1\sigma_m$). Isotopic ratios were measured using the Nu Plasma analysis software and recalculated off-line using an Excel spreadsheet. The raw data were filtered at 2σ in three passes and corrected for mass discrimination using an exponential law. The mass discrimination factor for Hf was determined assuming $^{179}Hf/^{177}Hf = 0.7325$ (Patchett *et al.* 1981). It has been noted before that the Yb interference correction is crucial for precise and accurate $^{176}Hf/^{177}Hf$ obtained by laser ablation (LA) analysis (e.g. Woodhead *et al.* 2004; Kemp *et al.* 2009). However, in the present study the moderate Yb/Hf ratios of the studied zircons, below 0.06, propagate into shifts in $^{176}Hf/^{177}Hf$ similar to the analytical uncertainty (cf. Kemp *et al.* 2009). A range of Yb isotope ratios are reported in the literature (e.g. Chu *et al.* 2002; Segal *et al.* 2003; Vervoort *et al.* 2004) and we have used the $^{176}Yb/^{173}Yb$ value of 0.796218 from Chu *et al.* (2002) for the correction of the ^{176}Yb interference on ^{176}Hf. The $^{176}Lu/^{175}Lu$ value of 0.02656 has also been used for the correction of the ^{176}Lu interference on ^{176}Hf (Scherer *et al.* 2001; Vervoort *et al.* 2004). A value for the decay constant of ^{176}Lu of 1.867×10^{-11} a^{-1} has been used in all calculations (Scherer *et al.* 2001, 2007; Söderlund *et al.* 2004). For the calculation of ε_{Hf} values we used present-day chondritic $^{176}Hf/^{177}Hf = 0.282785$

and $^{176}Lu/^{177}Hf = 0.0336$ (Bouvier *et al.* 2008). Monte Carlo simulation was applied for the propagation of errors to the initial ratios. Standards/reference zircons 91500 and GJ-1 were run as unknowns at frequent intervals. Multiple LA-MC-ICP-MS analyses, using the same instrumental parameters of the reference zircon 91500 and GJ-1, over a period of 1 year yielded a $^{176}Hf/^{177}Hf$ of 0.28231 ± 12 (2σ, $n = 112$) and 0.28204 ± 10 (2σ, $n = 45$), respectively, which are within error to results obtained by solution MC-ICP-MS analyses (0.282306 ± 8 for 91500; Woodhead and Hergt 2005, and 0.281998 ± 7 for GJ-1; Gerdes and Zeh 2006).

Major elements

Table 2 reports the whole-rock geochemical data of 14 samples, including calculated normative mineral contents (Standard Igneous Norm) using the SINCLAS software of Verma *et al.* (2002). In addition to the data reported here, plotted data from the presently studied intrusions are from Hackman (1931), Nykänen (1968), Pitkänen (1985), Eklund *et al.* (1998), Väisänen *et al.* (2000), and Nironen (2005 and references therein). The Harker diagrams (Figure 3) show a wide variation in composition of the rocks; from the most basic at 43–53 wt.% SiO_2 and Mg# of 46–40 to the most silicic granites at 71–74 wt.% SiO_2, with Mg# of 21–18. For comparison, rocks from the other ca. 1.8 Ga post-kinematic intrusions in SW Finland and Russian Karelia and the late-orogenic granites of southern Finland are included in Figure 3.

The basic-intermediate rocks (<61 wt.% SiO_2) range in composition from monzogabbro/alkali gabbro to monzonite (Figure 4) and are found in the Turku, Renko, Parkkila, and Luonteri intrusions. They are evolved rocks with <6 wt.% MgO, and TiO_2, $Fe_2O_3^t$, and P_2O_5 ranging up and above 3, 15, and 3 wt.%, respectively (Figure 3). CaO is typically between 4 and 9 wt.% and K_2O up to 4 wt.% for the most basic rocks.

The granitoids can be grouped into three compositional sub-groups: (i) the most silicic (>71 wt.% SiO_2), alkali-rich (syeno-)granites, consisting of most of the Turku granites, the Pirilä granite, and the Renko granitic dike; (ii) those with SiO_2 close to 65 wt.%, and quartz monzonitic to tonalitic in compositions, comprising most granitoids from Luonteri and one from Petravaara; and (iii) a group intermediate between the other two, around 70 wt.% SiO_2, with granodioritic to (monzo-)granitic in compositions, including the most silicic rocks at Luonteri, one sample from Turku, and two from Petravaara (Figure 4).

All the granites are peraluminous, whereas the basic and intermediate rocks are metaluminous and hornblende-dominated (Figure 5). Samples #1b and #2b classify as muscovite-dominated leucogranites, whereas the rest of the peraluminous samples plot as biotite-granites, according to the classification of Debon and Le Fort (1983).

Generally, the rocks plot in the shoshonitic fields in the K_2O-Na_2O and the K_2O-SiO_2 diagrams (Figure 6), except some of the Turku and Petravaara rocks that plot in the calc-alkaline and high-K calc-alkaline fields. According to the alkali-lime classification, a majority of the mafic rocks, as well as most felsic rocks, are alkali-calcic, whereas most of the intermediate rocks are calc-alkalic (Figure 7). Among the mafic rocks of the individual intrusions, Luonteri, Renko, and Parkkila are more coherently shoshonitic and alkali-calcic in composition (Figure 7) and are typically monzonitoid in R_1–R_2 space (Figure 4). In contrast, the intrusive bodies of the Turku complex show a much wider compositional spread, from undersaturated, alkalic, syenogabbroic compositions among the most mafic rocks towards more distinctly calc-alkaline for the intermediate representatives.

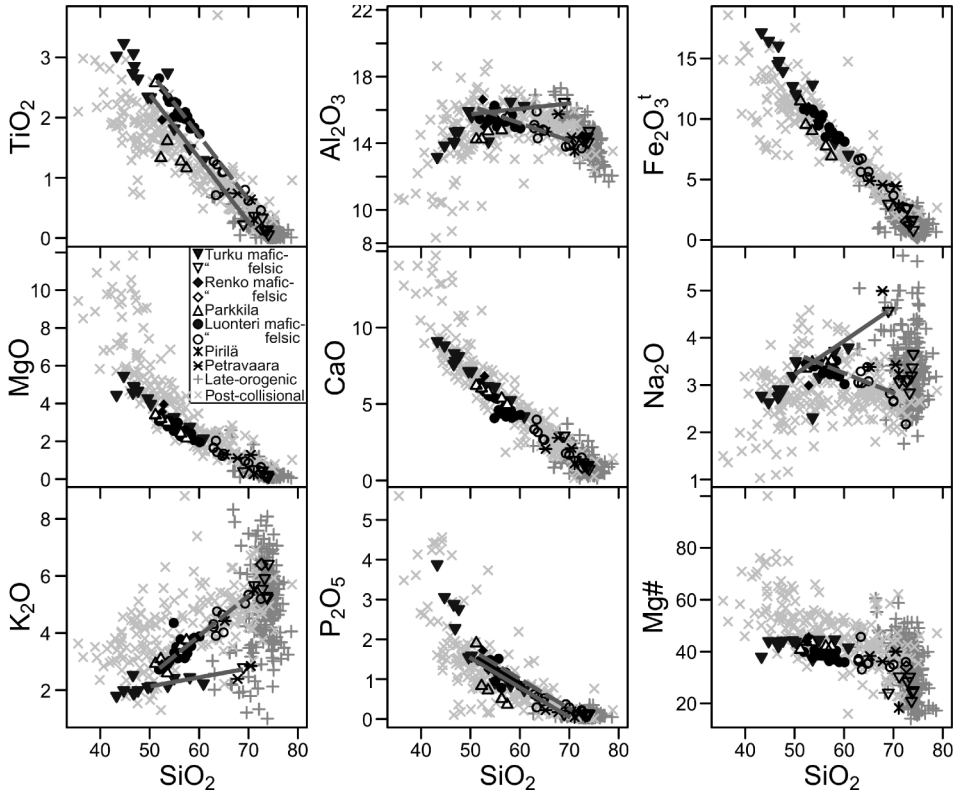

Figure 3. SiO_2 variation diagrams of major elements. Straight lines, to highlight the mixing trends, have been added: unbroken lines for Turku and broken lines for Luonteri. In addition to the data reported here, plotted data from these studied intrusions are from Hackman (1931), Nykänen (1968), Pitkänen (1985), Eklund *et al.* (1998), Väisänen *et al.* (2000), and Nironen (2005 and references therein). The reference data of the late-orogenic granitoids in southern Finland and 1.8 Ga post-collisional rocks from southern Finland and Russian Karelia are collected from Rutanen *et al.* (1997 and references therein), Eklund *et al.* (1998), Nironen (2005), Andersson *et al.* (2006a), Stålfors and Ehlers (2006), and the Rock Geochemical Database of Finland (see in the reference list). Some of these analyses were also received from the late-Matti Vaasjoki (Geological Survey of Finland) in 2003.

Trace elements

Selected trace elements are plotted in Harker diagrams in Figure 8. Some of the mafic-intermediate rocks of the Parkkila and Luonteri intrusions are strongly enriched, for example, in Ba (>3500 ppm), Sr (>3000 ppm), Nb (>50 ppm), Zr (>700 ppm), F (>6000 ppm), Ce (>500 ppm), and Nd (>200 ppm), whereas mafic-intermediate rocks from all intrusions are fairly high in Eu (>4 ppm). The Turku monzodiorites have slightly more primitive compositions, compared to the other samples, being higher in Ni, Cr, and V. The Petravaara granite shows similarities with the Luonteri granites, but is higher in Ni, Cr, and Th. The Pirilä syenogranite is markedly high in Rb, Th, Pb, LREE, and Cr.

In the discrimination diagram by Whalen *et al.* (1987; Figure 9), the Renko granitic dike and most of the Turku granites plot as fractionated felsic I/S/M-granites together with many late-orogenic Svecofennian granites of southern Finland. The latter extends into the A-type field, where also the Pirilä and the remainder of the Turku granites are found. The Petravaara

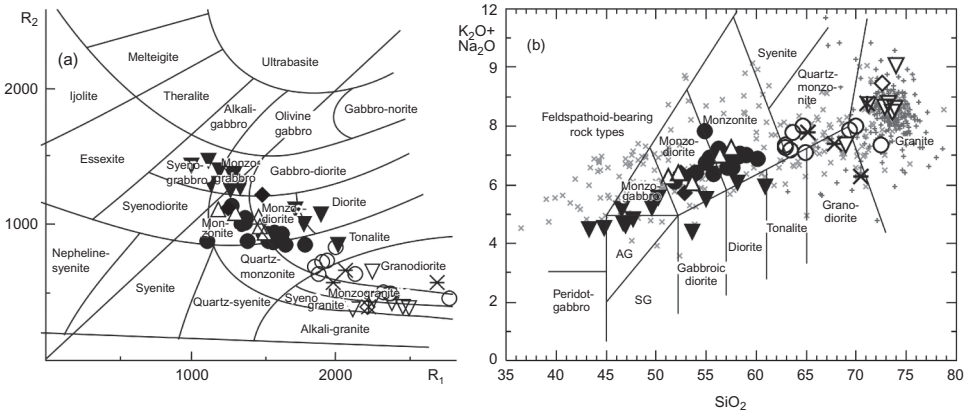

Figure 4. (a) R_1–R_2 diagram after De la Roche *et al.* (1980). $R_1 = 4Si–11(Na + K)–2(Fe + Ti)$, $R_2 = 6Ca + 2Mg + Al$. (b) TAS classification diagram, after Middlemost (1994). The feldspathoid-bearing rocks come from the post-collisional Vuoksi intrusion in Russian Karelia. AG = alkalic gabbro, SG = subalkalic gabbro. Symbols as in Figure 3.

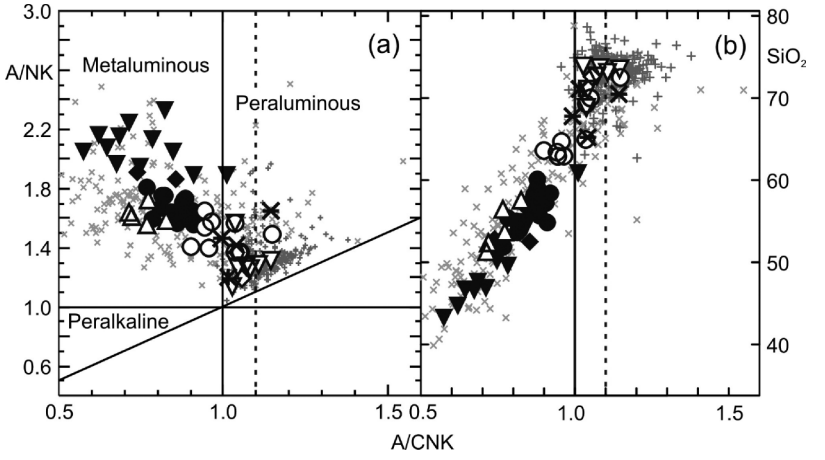

Figure 5. (a) A/NK (molecular $Al_2O_3/(Na_2O + K_2O)$) versus A/CNK (molecular $Al_2O_3/(CaO + Na_2O + K_2O)$) diagram, after Maniar and Piccoli (1989). (b) SiO_2-A/CNK diagram demonstrating the variation in Al_2O_3 saturation with silica. A/CNK > 1.1 suggests an S-type granite composition after Chappell and White (1974) and Clarke (1992). Symbols as in Figure 3.

and Luonteri granitoids plot within the A-type field, but at lower $(K_2O + Na_2O)/CaO$ values, overlapping with other post-collisional and TIB granites. In the Rb versus Y + Nb diagram (Figure 10), the Renko and Turku anatectic granites plot in or close to the syn-collisional field, whereas the other granitoids plot in the volcanic-arc/post-collisional field, except the Pirilä granite with higher Rb, placing it on the border to the syn-collisional field.

Despite the considerable differences between the intrusions, the mafic-intermediate rocks, together with other ca. 1.8 Ga, post-kinematic rocks in southern Finland and Russian Karelia (Konopelko 1997; Eklund *et al.* 1998; Väisänen *et al.* 2000; Andersson *et al.* 2006a), show elevated abundances of, in particular, K_2O, P_2O_5, Pb, Ba, Sr, Zr, Hf, LREE-middle REE (MREE), and F, and, to a relatively lesser extent, for example, TiO_2, Cs, Rb,

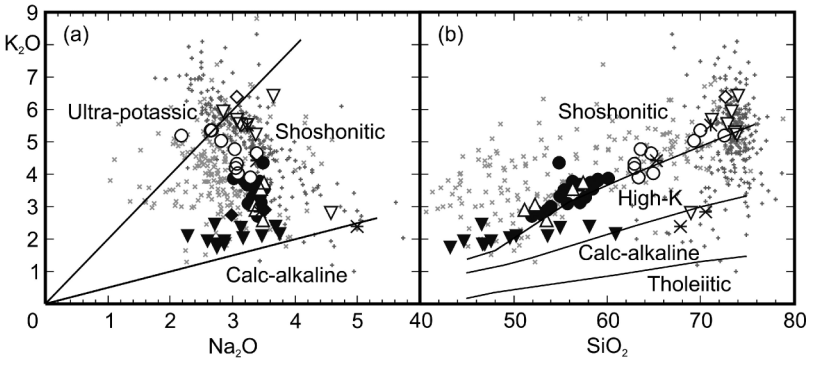

Figure 6. (a) The Svecofennian 1.8 Ga post-collisional rocks in southern Finland in a K_2O versus Na_2O diagram after Turner *et al.* (1996). (b) The samples demonstrate shoshonitic and high-K calc-alkaline trends in a K_2O versus SiO_2 variation diagram after Rickwood (1989). Symbols as in Figure 3.

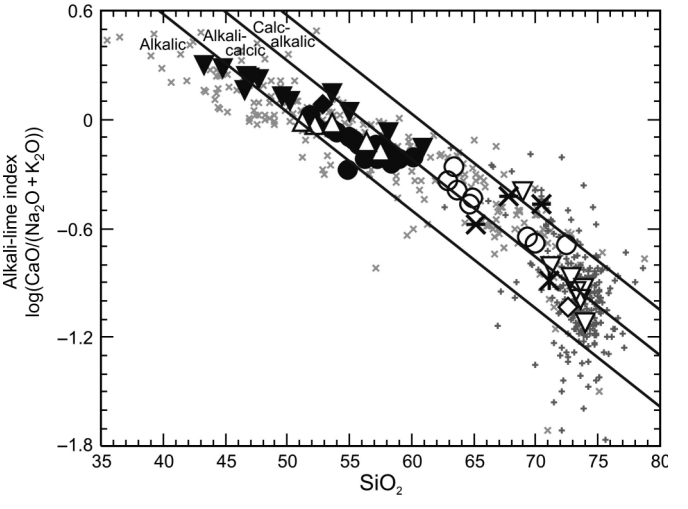

Figure 7. Alkali-lime index diagram, following Peacock (1931) and, for example, Brown (1982). Symbols as in Figure 3.

Th, U, and Nb relative to MORB, but significant negative relative anomalies for Nb, Ta, Y, and heavy rare earth elements (HREE) (Figures 3, 8, and 11a–c). In detail, Luonteri and Parkkila intrusions are the most enriched. Parkkila is more enriched in Sr and less enriched in Rb, Zr, and Hf compared with the Luonteri rocks. The Turku and Renko intrusions are geochemically similar, but Renko is somewhat richer in Cs and Rb.

Figure 11 shows a combination of multi-element diagrams and REE patterns for the post-collisional rocks, to detect spatial variations in elemental characteristics. All the rocks show high abundances of the large ion lithophile elements (LILE) and LREE (e.g. high La_N/Yb_N, from 41 to 218; Table 2), combined with low relative abundances of high field strength elements (HFSE) and particularly low contents of the HREE. Such patterns are characteristic for arc rocks (e.g. Rollinson 1993; Pearce 1996a). In detail, however, enrichment levels vary both locally and regionally. In general, the concentrations of essentially all elements in the mafic rocks, except the HREEs, are much higher than for tholeiitic to calc-alkaline island (oceanic) arc rocks and, in many cases, significantly higher than for continental andesitic

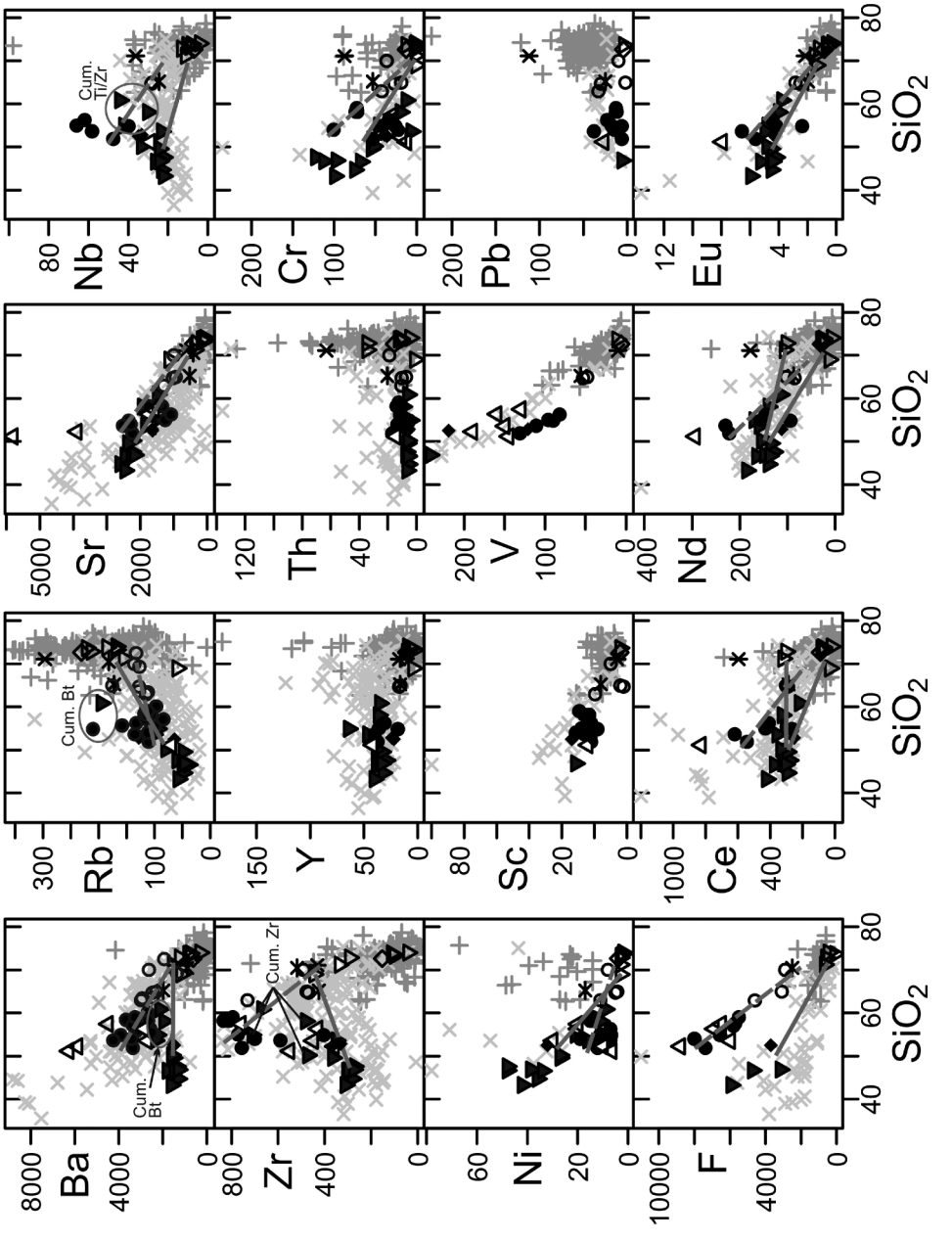

Figure 8. Selected SiO_2 versus trace element variation diagrams. The concentrations of the elements are in ppm. Straight lines, to highlight the mixing trends, have been added: unbroken lines for Turku and broken lines for Luonteri. Cum. Bt = cumulated biotite; Ti = titanite; Zr = zircon. Data collection and symbols as in Figure 3.

arcs, but overlapping with shoshonitic rocks from various settings. Compared to asthenosphere-derived ocean island basalt (OIB) rocks, LILE and LREE are strongly enriched, whereas HFSE and HREE are similar (including Nb and Ta). The mafic samples show no Eu anomalies, and the granitoid rocks none or only minor ones.

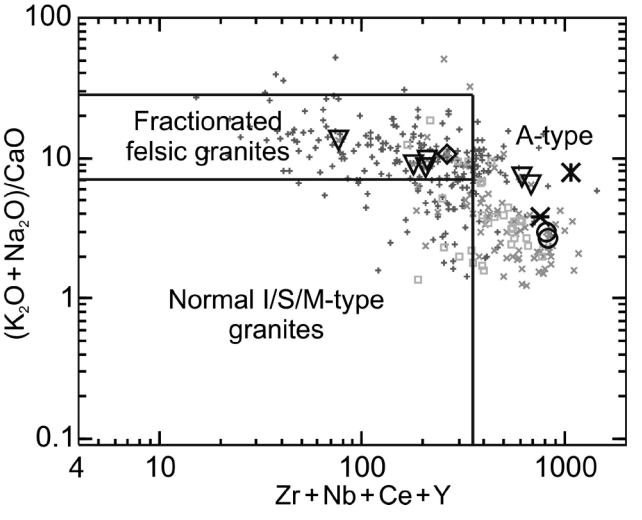

Figure 9. I-, S-, M-, and A-type granite discrimination diagram (≥60 wt.% SiO_2) after Whalen *et al.* (1987) with the addition of Transscandinavian Igneous Belt granites (as light grey squares; data from Andersson 1997). Other symbols as in Figure 3.

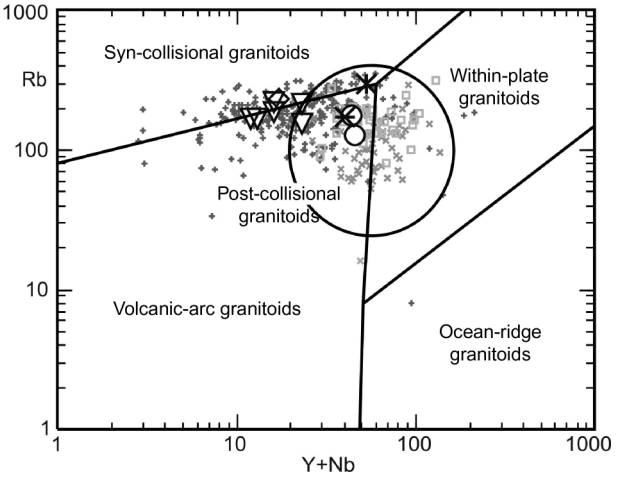

Figure 10. Tectonic settings of granitoids, after Pearce (1996b). Symbols as in Figure 9.

In the Th/Yb versus Ta/Yb diagram (Figure 12), the Turku rocks are distinctly more calc-alkaline compared to the other complexes that are shoshonitic. However, the post-kinematic rocks fall in the field defined for active continental-margin magmatism, apart from two samples from Turku with anomalously elevated Ta contents that fall in the field of enriched OIB-type mantle.

In the Th-Ta-Hf diagram (Figure 13), most samples plot within the field of calc-alkaline volcanic-arc basalts (in the section for most enriched continental-arc compositions), whereas two Turku samples stray off to more relative Ta enrichment in the field for enriched mid-ocean ridge basalts (E-MORB) and within-plate basalts.

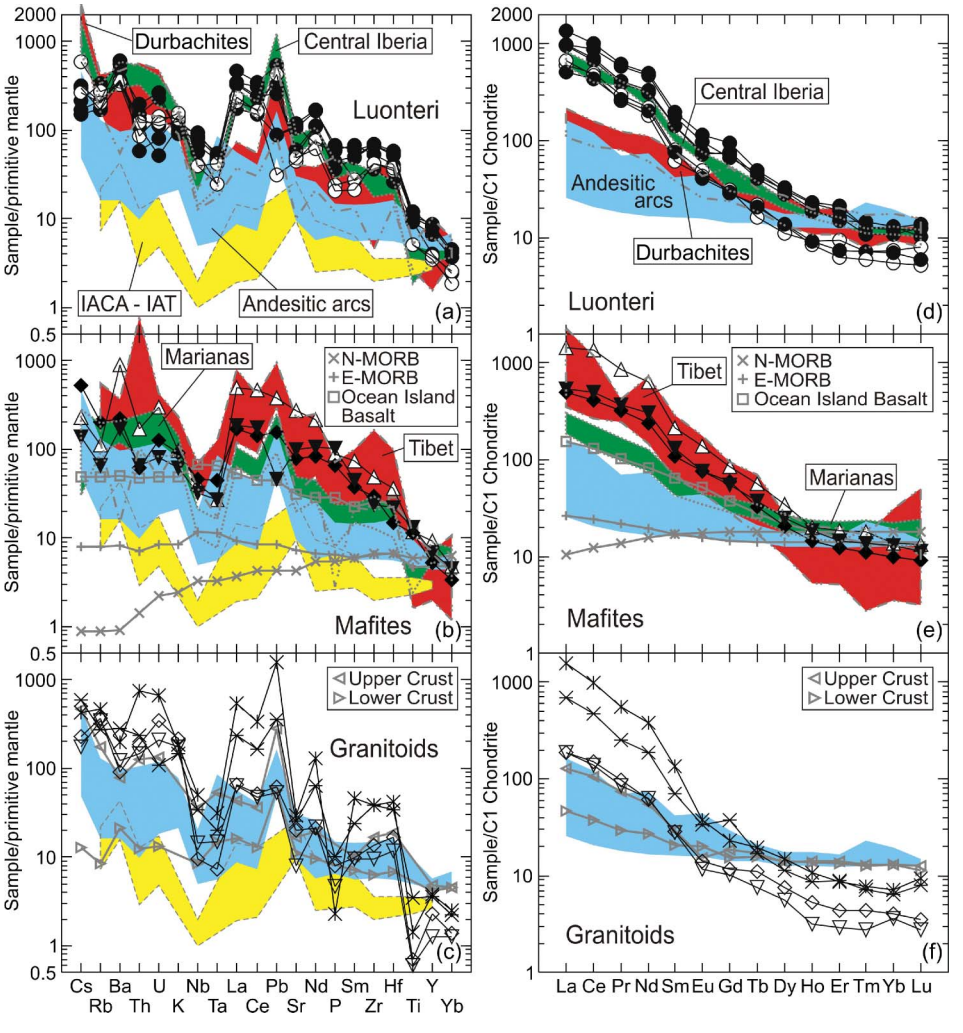

Figure 11. Multi-element diagrams for (a) the Luonteri rocks, (b) other mafic rocks, and (c) other granites of the studied intrusions, normalized to primitive mantle (Sun and McDonough 1989). N-MORB, E-MORB, and ocean island basalts from Sun and McDonough (1989), and upper and lower crust from Taylor and McLennan (1985). IACA-IAT = field between average composition of calc-alkaline island-arc basalts and island-arc tholeiites (after Sun 1980), Andesitic Arcs = field between average composition of most depleted and most enriched andesitic arc rocks, calculated from the data in the file 'Av-Andesite2.xls' in http://www.geokem.com/earths_average_composition.html, by Dr Bernard M. Gunn, 2004. Durbachite data from Bowes and Košler (1993) and Janoušek *et al.* (2000), shoshonites from Central Iberia from López-Moro and López-Plaza (2004), Mariana shoshonites from Sun *et al.* (1998) and Sun and Stern (2001), and Tibet shoshonites from Turner *et al.* (1996) and Zhang *et al.* (2008). (d–f) REE diagrams of the same data as in (a–c). Normalization after Sun and McDonough (1989). Symbols as in Figure 3.

In Figure 14, the post-kinematic rocks can be separated from within-plate and MOR basalts by their distinctly high La/Nb ratios. In fact, most samples have La/Nb ratios significantly higher than those of crustal compositions, as well as higher than continental and oceanic arcs. A few samples trend towards higher Ba/La ratios.

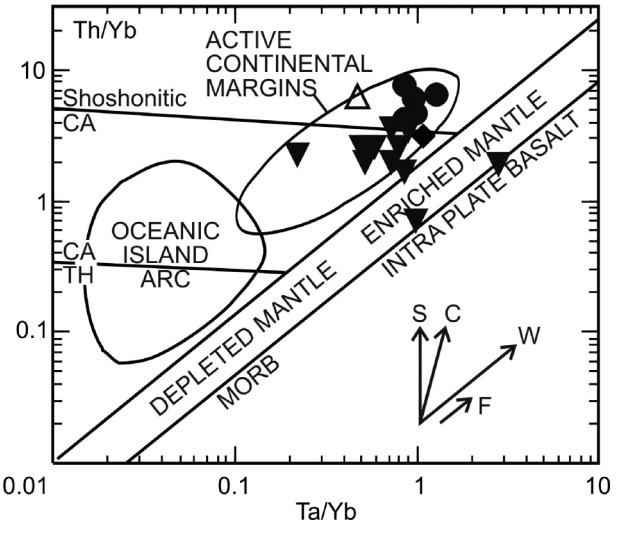

Figure 12. A Th/Yb versus Ta/Yb diagram shows calc-alkaline active continental margin (continental arc) setting for the mafic (<60 wt.% SiO_2) Svecofennian 1.8 Ga post-collisional rocks in southern Finland. CA = calc-alkaline, TH = tholeiitic. The arrows indicate effects of (i) the influence of subduction components (S), (ii) crustal contamination (C), (iii) within-plate enrichment (W), and (iv) fractional crystallization (F) (the diagram after Pearce 1983 and Wilson 1989). Symbols as in Figure 3.

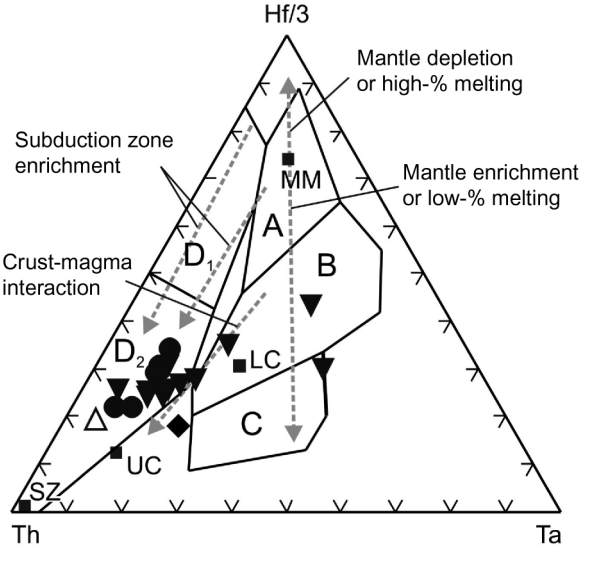

Figure 13. Th-Ta-Hf diagram for mafic rocks (<60 wt.% SiO_2). A = N-MORB, B = E-MORB and within-plate tholeiites, C = alkaline within-plate basalts, D = volcanic-arc/destructive plate-margin basalts (D_1 = primitive arc tholeiites, D_2 = calc-alkaline), MM = N-MORB mantle source, LC = lower crust, UC = upper crust, SZ = subduction zone component (after Wood *et al.* 1979; Wood 1980; Pearce 1996a). Almost all samples plot inside or close to the field of calc-alkaline volcanic-arc rocks. The arrows mark the directions of the trends for mantle source regions. The mafic rocks of the present study show indications of being strongly influenced by subduction zone enrichment, except a few of the Turku rocks that show within-plate signals. Symbols as in Figure 3.

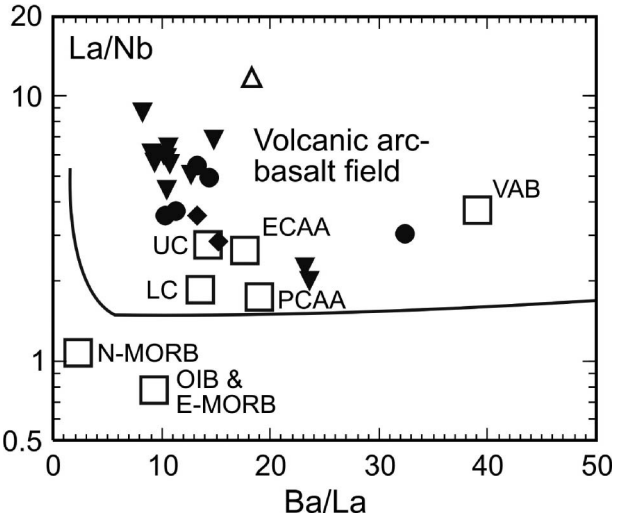

Figure 14. La/Nb versus Ba/La diagram for mafic rocks (<60 wt.% SiO_2). High La/Nb distinguishes arc basalts from those of other sources (e.g. Hawkesworth *et al.* 1995). UC = upper crust; LC = lower crust, ECAA = evolved continental andesitic arcs, PCAA = primitive continental andesitic arcs, VAB = volcanic arc basalts (oceanic), OIB = ocean island basalts. The reference data from Taylor and McLennan (1985), Sun and McDonough (1989), Hawkesworth *et al.* (1991, 1995), Condie (1993), and the file 'Av-Andesite2.xls' in http://www.geokem.com/earths_average_composition.html, by Dr Bernard M. Gunn (2004). Symbols as in Figure 3.

Nd isotopes

Nine samples were selected for Nd and Sr isotopic data characterization (Table 3). The Sm and Nd contents show large differences, from 3.8 to 35 ppm Sm and from 26 to 280 ppm Nd.

The $^{147}Sm/^{144}Nd$ values are all low, even for the most mafic rocks, ranging from approximately 0.07 to 0.09, that is, far from the chondritic value of 0.1967 (Jacobsen and Wasserburg 1984). The measured $^{143}Nd/^{144}Nd$ ratios are correspondingly low and range between 0.511002 and 0.511393 (cf. chondritic uniform reservoir, CHUR: 0.512638; Wasserburg *et al.* 1981).

The initial $\varepsilon_{Nd}(t)$ values have been calculated at the reported age for each intrusion: 1815 million years for Turku monzodiorite and 1814 million years for the granite (Väisänen *et al.* 2000), 1812 million years for Renko (Vaasjoki 1995), 1794 million years for Parkkila (Simonen 1982), 1802 million years for Luonteri (Korsman *et al.* 1984), 1815 million years for Pirilä (Vaasjoki and Sakko 1988), and 1811 million years for Petravaara (this study). Except for the considerably more enriched isotopic signature of the Petravaara granite at −2.8, the initial $\varepsilon_{Nd}(t)$ values range from chondritic to mildly depleted (0–1.4), where the Renko quartz-monzodiorite has the highest value. The present data confirm the previous few data available from some of these intrusions (Patchett and Kouvo 1986; Lahtinen and Huhma 1997; Nironen and Rämö 2005).

Sr isotopes

The Sr isotopic data of the nine selected samples are reported in Table 3. Because of the strong variation in major element geochemistry of the samples, the contents of both Rb and Sr in these plutonic rocks vary from approximately 40 to 300 ppm Rb and from

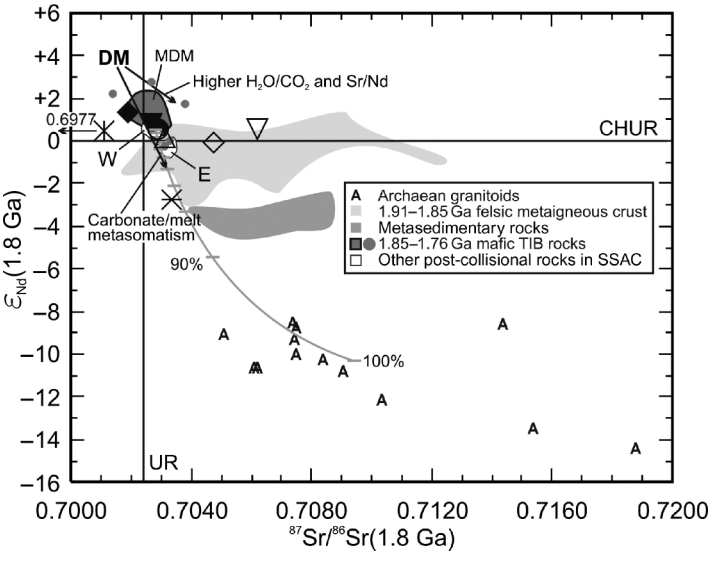

Figure 15. $\varepsilon_{Nd}(t)$–$^{87}Sr/^{86}Sr(t)$ diagram for post-collisional rocks in southern Finland and Russian Karelia, and for possible contaminants and sources. All values recalculated to 1.80 Ga. Symbols as in Figure 3. CHUR = chondritic uniform reservoir. DM (depleted mantle) has ε_{Nd}(1.80 Ga) of +3.9 (DePaolo 1981) and $^{87}Sr/^{86}Sr$(1.80 Ga) of 0.7014 (Taylor and McLennan 1985), and UR (uniform reservoir) has $^{87}Sr/^{86}Sr$(1.80 Ga) of 0.7024 (McCulloch and Chappell 1982; Faure 2001). The 1.85–1.76 Ga mafic TIB rocks define a field with the isotopic composition of a 'mildly depleted mantle' (MDM); the data for the 1.91–1.85 Ga felsic metaigneous crust are from the central and southern Svecofennian Domain in Finland and Sweden; the Svecofennian metasedimentary rocks are from the central and southern Svecofennian Domain in Sweden; additional 1.8 Ga post-collisional rocks from the SSAC are subdivided into rocks from the westernmost SSAC (W) and from Russian Karelia in the eastern SSAC (E). Explanation of the grey mixing line and the evolution arrows in the text. The reference data are collected from Martin *et al.* (1983), Wilson *et al.* (1986), Valbracht (1991), O'Brien *et al.* (1993), Valbracht *et al.* (1994), Claesson and Lundqvist (1995), Billström and Weihed (1996), Andersson (1997), Kononova *et al.* (1999, 2000), Rämö *et al.* (2001), Andersson *et al.* (2002, 2006a, 2007), Högdahl *et al.* (2008), Rutanen and Andersson (2009 and references therein), Woodard and Huhma (in review).

approximately 160 to 5800 ppm Sr (Table 2). The more mafic samples have the lowest Rb contents and conversely the highest Sr contents.

The $^{87}Rb/^{86}Sr$ values are thus low for mafic rocks and higher for the felsic samples. The values range from 0.035 to 3.90, where the latter value was obtained for the S-type granite in the Turku area (sample #1b).

The measured $^{87}Sr/^{86}Sr$ values fall in the range 0.7040–0.8078, which, when recalculated to the intrusive age of each rock type (cf. Chapter 8), results in initial $^{87}Sr/^{86}Sr(t)$ values between the unrealistically low 0.6977 (sample #5) and 0.7062. All except two samples (#2a and #5) have values higher than that estimated for the uniform reservoir at 1.80 Ga (0.7024; McCulloch and Chappell 1982; Faure 2001; Figure 15), resulting in positive $\varepsilon_{Sr}(t)$ values (Table 2), whereas only sample #5 is below that of the depleted mantle ($^{87}Sr/^{86}Sr$(1.80 Ga) = 0.7014 and ε_{Sr}(1.80 Ga) = –14; Taylor and McLennan 1985; Figure 15). Errors in the initial ratios for samples with high Rb/Sr are relatively high and should be viewed with caution.

U–Pb zircon SIMS geochronology of the Petravaara granite

Light brown, transparent, mostly short prismatic, and relatively crack-free zircons, with fairly well-developed crystal forms were chosen from the 75–150 μm size fraction of sample #6. The crystals showed concentric oscillatory zoning in BSE and CL images (Figure 16a). A few CL images indicated lighter cores with darker rims; however, no significant age differences could be detected. Some crystals showed very thin metamict rims. Inclusions of apatite, pyrite, and quartz were observed.

Altogether, 50 crystals were analysed. Th/U ratios were all relatively high (0.25–0.93; Table 4), suggesting that the zircons crystallized from a magma. A weighted average $^{207}Pb/^{206}Pb$ age of all the analysed spots yielded an age of 1809 ± 8 million years (MSWD = 1.8). However, many of the analyses are normally or reversely discordant and have suffered recent or ancient Pb loss, or result from analytical artefacts. Additionally, some spots have hit cracks resulting in discordancy or large errors. At least one zircon, showing an older $^{207}Pb/^{206}Pb$ age (1877 Ma; n2167-50 in Table 4), is possibly inherited. Omitting these from the age calculation and using 36 concordant or near concordant analytical spots resulted in a weighted average $^{207}Pb/^{206}Pb$ age of 1810.6 ± 6.5 million years (2σ, MSWD = 1.2; Figure 16b) and a concordia age of 1810.9 ± 6.0 million years (95% confidence interval, MSWD = 1.4 of concordance and equivalence; Figure 16c); 1811 ± 6 million years is thus considered as the best estimate for the crystallization age of the Petravaara granite.

Hf isotopes in zircon from the Petravaara granite

Forty-five analyses of Lu–Hf isotopes (Table 5) were performed in the same set of crystals that was previously analysed by SIMS (Figure 16a). For the concordant spots, initial ε_{Hf} values were calculated for each analysis from the individual concordia ages (Table 4). For discordant points deemed to have crystallized from the Petravaara magma, the initial ratios were calculated at 1811 million years; that is, the concordia age determined from the SIMS data (Figure 16). For the few grains that appear to be older than the intrusion age, the $^{207}Pb/^{206}Pb$ ages were used for calculating the initial ε_{Hf}. The ε_{Hf} values show a range of almost 15 ε-units, from −11.9 to +2.8 ($\pm 2\sigma_m$ from 2.1 to 5.3, with the average of 3.3; Table 5, Figure 17), that is, from Archaean crust to 'mildly depleted' mantle values.

Discussion

Geochemistry

Basic-intermediate rocks. The basic-intermediate rocks of this study exhibit low Mg#, below 46, and MgO below 5.4 wt.%. In fact, the evolutionary level varies only between Mg# 46 and 36 (Figure 3). This, and the accompanying low contents of Cr and Ni (<125 and <50 ppm, respectively), strongly suggests that the compositions do not represent primary mantle magmas, but have been modified by pre-emplacement fractionation of olivine and/or pyroxenes, and possibly spinel (cf. e.g. Tatsumi and Eggins 1995; Leat *et al.* 2002; Kelemen *et al.* 2007; Zhang *et al.* 2008). Sc contents <20 ppm further emphasize the role of previous clinopyroxene extraction.

Contamination of more primitive basaltic magmas by average Earth's upper crust, or by local granites in Turku and Renko, cannot explain the high concentrations of many elements

Table 4. U-Th-Pb SIMS isotopic results of the Petravaara granite. Analyses used for calculating the age are marked in bold.

		Concentrations					Isotope ratios									Age (million years)							
Spot No.	Comment	[U] ppm	[Th] ppm	[Pb] ppm	Th/U meas.[a]	f_{206}%[b]	$^{238}U/^{206}Pb$	±1σ %	$^{207}Pb/^{206}Pb$	±1σ %	$^{207}Pb/^{235}Pb$	±1σ %	Disc. % 2σ lim.[c]	Disc. % conv.[d]	ρ[e]	$^{207}Pb/^{206}Pb$	±1σ	$^{206}Pb/^{238}U$	±1σ	$^{207}Pb/^{235}Pb$	±1σ Ma	Conc.	±1σ
n2167-1	crack	122	61	49	0.50	6.70	3.145	1.02	0.1067	2.57	4.677	2.77		2.36	0.37	1744	46	1780	16	1763	23	1776	15
n2167-2		**93**	**39**	**37**	**0.42**	**{0.07}**	**3.100**	**1.11**	**0.1124**	**1.02**	**4.998**	**1.51**		**−2.22**	**0.74**	**1838**	**18**	**1802**	**17**	**1819**	**13**	**1819**	**13**
n2167-3		**61**	**38**	**26**	**0.62**	**{0.00}**	**3.092**	**1.04**	**0.1124**	**1.32**	**5.015**	**1.68**		**−2.03**	**0.62**	**1839**	**24**	**1807**	**16**	**1822**	**14**	**1817**	**14**
n2167-4	crack	120	72	51	0.60	0.10	3.009	1.03	0.1087	1.18	4.979	1.57		4.71	0.66	1777	21	1850	17	1816	13	1822	440*
n2167-5		**141**	**83**	**59**	**0.59**	**{0.05}**	**3.076**	**1.04**	**0.1122**	**0.87**	**5.029**	**1.35**		**−1.28**	**0.77**	**1835**	**16**	**1815**	**16**	**1824**	**12**	**1825**	**11**
n2167-6	discordance	41	16	16	0.38	{0.18}	3.041	1.05	0.1056	1.58	4.789	1.89		7.17	0.55	1725	29	1833	17	1783	16	1804	590*
n2167-7		**150**	**89**	**61**	**0.59**	**{0.08}**	**3.141**	**1.02**	**0.1093**	**0.95**	**4.796**	**1.40**		**−0.34**	**0.73**	**1787**	**17**	**1782**	**16**	**1784**	**12**	**1784**	**12**
n2167-8	discordance	164	120	68	0.73	1.85	3.229	1.07	0.1155	1.71	4.930	2.02	−0.97	−8.97	0.53	1887	30	1739	16	1807	17	–	–
n2167-9	discordance	128	59	44	0.46	5.83	3.721	1.06	0.1194	2.89	4.424	3.07	−10.93	−23.80	0.34	1947	51	1534	14	1717	26	–	–
n2167-10		**91**	**53**	**37**	**0.58**	**0.16**	**3.144**	**1.06**	**0.1114**	**1.18**	**4.886**	**1.58**		**−2.67**	**0.67**	**1823**	**21**	**1780**	**16**	**1800**	**13**	**1796**	**13**
n2167-11		**95**	**38**	**38**	**0.40**	**0.48**	**3.095**	**1.04**	**0.1136**	**1.19**	**5.061**	**1.58**		**−3.29**	**0.66**	**1858**	**21**	**1805**	**16**	**1830**	**13**	**1824**	**330***
n2167-12	Pb loss	67	45	27	0.67	{0.00}	3.233	1.04	0.1087	1.32	4.638	1.68		−2.64	0.62	1778	24	1737	16	1756	14	1749	13
n2167-13		**92**	**64**	**38**	**0.69**	**{0.13}**	**3.152**	**1.04**	**0.1131**	**1.18**	**4.945**	**1.58**		**−4.51**	**0.66**	**1849**	**21**	**1776**	**16**	**1810**	**13**	**1802**	**450***
n2167-14		**47**	**23**	**19**	**0.50**	**{0.07}**	**3.085**	**1.05**	**0.1095**	**1.69**	**4.895**	**1.99**		**1.21**	**0.53**	**1791**	**31**	**1810**	**17**	**1801**	**17**	**1806**	**15**
n2167-15		**85**	**41**	**33**	**0.48**	**0.16**	**3.169**	**1.13**	**0.1114**	**1.33**	**4.847**	**1.75**		**−3.39**	**0.65**	**1822**	**24**	**1768**	**18**	**1793**	**15**	**1786**	**14**
n2167-16a	crack/Pb loss	40	19	14	0.48	1.16	3.467	1.68	0.1093	3.61	4.346	3.99		−9.74	0.42	1788	64	1634	24	1702	33	1649	630*
n2167-17b	discordance	176	45	73	0.25	0.04	2.861	2.01	0.1091	0.82	5.258	2.17	3.65	9.56	0.93	1785	15	1932	34	1862	19	–	–
n2167-18b	crack/ discordance	52	19	22	0.37	0.20	2.882	2.02	0.1095	1.20	5.240	2.35	1.09	8.30	0.86	1792	22	1920	34	1859	20	1830	740*

n2167-19		**148**	**130**	**65**	**0.88**	**0.47**	**3.127**	**2.01**	**0.1102**	**0.83**	**4.859**	**2.17**	**−0.88**	**0.92**	**1803**	**15**	**1789**	**31**	**1795**	**18**	**1800**	**14**
n2167-20	crack	83	42	36	0.50	19.42	3.146	2.05	0.1113	7.38	4.879	7.66	−2.62	0.27	1821	128	1779	32	1799	67	1782	31
n2167-21		**68**	**31**	**28**	**0.46**	**0.09**	**3.012**	**2.01**	**0.1110**	**1.10**	**5.080**	**2.29**	**2.04**	**0.88**	**1816**	**20**	**1848**	**32**	**1833**	**20**	**1825**	**17**
n2167-22		**55**	**19**	**21**	**0.34**	**0.19**	**3.097**	**2.01**	**0.1075**	**1.24**	**4.786**	**2.36**	**3.00**	**0.85**	**1758**	**23**	**1804**	**32**	**1782**	**20**	**1773**	**18**
n2167-23		**176**	**164**	**80**	**0.93**	**0.05**	**3.054**	**2.01**	**0.1108**	**0.65**	**5.004**	**2.11**	**0.82**	**0.95**	**1813**	**12**	**1826**	**32**	**1820**	**18**	**1815**	**11**
n2167-24		**157**	**99**	**68**	**0.63**	**0.05**	**2.997**	**2.01**	**0.1095**	**0.68**	**5.039**	**2.12**	**4.16**	**0.95**	**1791**	**12**	**1856**	**32**	**1826**	**18**	**1800**	**12**
n2167-25		**65**	**23**	**26**	**0.36**	**{0.06}**	**2.994**	**2.01**	**0.1108**	**1.03**	**5.101**	**2.26**	**2.88**	**0.89**	**1812**	**19**	**1858**	**32**	**1836**	**19**	**1824**	**16**
n2167-26		**53**	**24**	**21**	**0.46**	**0.61**	**3.078**	**2.01**	**0.1114**	**1.42**	**4.989**	**2.46**	**−0.52**	**0.82**	**1822**	**26**	**1814**	**32**	**1818**	**21**	**1819**	**20**
n2167-27		**87**	**50**	**35**	**0.57**	**0.14**	**3.146**	**2.31**	**0.1112**	**1.25**	**4.873**	**2.62**	**−2.49**	**0.88**	**1819**	**22**	**1779**	**36**	**1798**	**22**	**1808**	**19**
n2167-28		**104**	**57**	**43**	**0.54**	**1.72**	**3.105**	**2.01**	**0.1097**	**1.29**	**4.872**	**2.39**	**0.32**	**0.84**	**1795**	**23**	**1800**	**32**	**1797**	**20**	**1797**	**19**
n2167-29		**99**	**63**	**42**	**0.64**	**0.32**	**3.056**	**2.01**	**0.1091**	**0.98**	**4.923**	**2.24**	**2.58**	**0.90**	**1785**	**18**	**1825**	**32**	**1806**	**19**	**1794**	**16**
n2167-30		**79**	**54**	**34**	**0.68**	**0.12**	**3.067**	**2.01**	**0.1099**	**1.31**	**4.940**	**2.40**	**1.38**	**0.84**	**1798**	**24**	**1819**	**32**	**1809**	**20**	**1805**	**19**
n2167-31	Pb loss	629	417	226	0.66	9.99	3.715	2.05	0.1121	6.27	4.161	6.59	−18.20	0.31	1834	109	1537	28	1666	55	1547	820*
n2167-32	Pb loss	57	33	23	0.58	2.40	3.219	2.04	0.1088	2.20	4.658	3.00	−2.24	0.68	1779	40	1744	31	1760	25	1757	25
n2167-33		**105**	**68**	**45**	**0.65**	**0.43**	**3.030**	**2.01**	**0.1108**	**0.98**	**5.042**	**2.24**	**1.65**	**0.90**	**1813**	**18**	**1839**	**32**	**1826**	**19**	**1819**	**16**
n2167-34		**41**	**18**	**17**	**0.45**	**{0.05}**	**3.124**	**2.01**	**0.1130**	**1.38**	**4.986**	**2.43**	**−3.54**	**0.82**	**1848**	**25**	**1790**	**31**	**1817**	**21**	**1825**	**20**
n2167-35		**50**	**24**	**21**	**0.48**	**0.13**	**3.028**	**2.01**	**0.1093**	**1.32**	**4.977**	**2.40**	**3.33**	**0.84**	**1788**	**24**	**1840**	**32**	**1815**	**21**	**1806**	**19**
n2167-36		**67**	**42**	**28**	**0.63**	**0.89**	**3.120**	**2.01**	**0.1090**	**1.93**	**4.815**	**2.79**	**0.65**	**0.72**	**1782**	**35**	**1792**	**32**	**1787**	**24**	**1788**	**23**
n2167-37		**52**	**22**	**21**	**0.42**	**0.22**	**2.994**	**2.02**	**0.1087**	**1.44**	**5.007**	**2.48**	**5.14**	**0.81**	**1778**	**26**	**1858**	**33**	**1820**	**21**	**1810**	**20**
n2167-38		**83**	**38**	**34**	**0.46**	**0.19**	**3.023**	**2.02**	**0.1091**	**1.11**	**4.976**	**2.31**	**3.74**	**0.88**	**1784**	**20**	**1842**	**33**	**1815**	**20**	**1801**	**17**
n2167-39		**106**	**78**	**45**	**0.74**	**1.16**	**3.118**	**2.01**	**0.1109**	**1.46**	**4.904**	**2.49**	**−1.33**	**0.81**	**1814**	**26**	**1793**	**32**	**1803**	**21**	**1806**	**20**
n2167-40		**109**	**64**	**46**	**0.59**	**0.09**	**2.997**	**2.01**	**0.1105**	**0.92**	**5.081**	**2.21**	**3.12**	**0.91**	**1807**	**17**	**1856**	**32**	**1833**	**19**	**1817**	**15**
n2167-41		**71**	**34**	**30**	**0.48**	**{0.08}**	**2.989**	**2.01**	**0.1090**	**1.46**	**5.029**	**2.48**	**4.98**	**0.81**	**1783**	**26**	**1860**	**33**	**1824**	**21**	**1814**	**21**
n2167-42		**62**	**30**	**25**	**0.48**	**0.84**	**3.090**	**2.01**	**0.1115**	**1.55**	**4.974**	**2.54**	**−1.02**	**0.79**	**1823**	**28**	**1807**	**32**	**1815**	**22**	**1816**	**21**

(*Continued*)

Table 4. (*Continued*).

		Concentrations					Isotope ratios									Age (millian years)							
Spot No.	Comment	[U] ppm	[Th] ppm	[Pb] ppm	Th/U meas.[a]	f_{206}%[b]	$^{238}U/^{206}Pb$	±1σ %	$^{207}Pb/^{206}Pb$	±1σ %	$^{207}Pb/^{235}Pb$	±1σ %	Disc. % 2σ lim.[c]	Disc. % conv.[d]	ρ[e]	$^{207}Pb/^{206}Pb$	±1σ	$^{206}Pb/^{238}U$	±1σ	$^{207}Pb/^{235}Pb$	±1σ	Conc.	±1σ
n2167-43		**192**	**141**	**87**	**0.74**	**0.11**	**2.925**	**2.01**	**0.1108**	**0.87**	**5.224**	**2.19**		**5.28**	**0.92**	**1813**	**16**	**1896**	**33**	**1857**	**19**	**1829**	**410***
n2167-44		**78**	**60**	**34**	**0.77**	**0.52**	**3.061**	**2.01**	**0.1128**	**1.32**	**5.081**	**2.40**		**−1.43**	**0.84**	**1845**	**24**	**1822**	**32**	**1833**	**21**	**1837**	**19**
n2167-45	discordance	63	36	28	0.57	0.22	2.892	2.01	0.1082	1.35	5.158	2.42	1.60	9.50	0.83	1769	25	1914	33	1846	21	–	–
n2167-46		**156**	**92**	**66**	**0.59**	**0.09**	**3.003**	**2.01**	**0.1116**	**0.82**	**5.127**	**2.17**		**1.69**	**0.93**	**1826**	**15**	**1853**	**32**	**1841**	**19**	**1831**	**14**
n2167-47		**137**	**87**	**60**	**0.64**	**0.10**	**2.958**	**2.01**	**0.1100**	**0.95**	**5.129**	**2.22**		**4.95**	**0.90**	**1800**	**17**	**1877**	**33**	**1841**	**19**	**1817**	**410***
n2167-48		**68**	**30**	**29**	**0.45**	**0.16**	**2.927**	**2.01**	**0.1089**	**1.29**	**5.131**	**2.39**		**7.33**	**0.84**	**1782**	**23**	**1895**	**33**	**1841**	**20**	**1820**	**670***
n2167-49		**71**	**35**	**29**	**0.48**	**{0.06}**	**3.050**	**2.01**	**0.1121**	**1.23**	**5.068**	**2.36**		**−0.34**	**0.85**	**1834**	**22**	**1828**	**32**	**1831**	**20**	**1832**	**18**
n2167-50	inherited?	51	28	21	0.54	{0.00}	3.036	2.02	0.1148	1.48	**5.215**	**2.51**		−2.55	0.81	1877	26	1835	32	1855	22	1860	21

Note: Isotope ratios corrected for present-day common lead according to the model of Stacey and Kramers (1975). Age calculations use the routines of Ludwig (2003) and follow the decay constant recommendations of Steiger and Jäger (1977).

[a]Th/U ratio directly from measured Th and U concentrations; [b]Fraction of ^{206}Pb derived from common lead. Figures in parentheses are given when no correction has been applied; [c]Percent discordance outside 2σ limits: negative value = normal discordant, positive value = reverse discordant; [d]Percent discordance in conventional concordia space: negative value = normal discordant, positive value = reverse discordant; [f]$^{238}U/^{206}Pb$-$^{207}Pb/^{206}Pb$ concordia ages for the separate zicons for the use in initial ε_{Hf}-calculations (Table 5); *$t\sigma\sqrt{}$MSWD-error = 1σ error multiplied by the square root of the MSWD and by the 'Student's-*t* factor'; [e]Error correlation in conventional concordia space;.

Table 5. Lu-Hf LA-MC-ICP-MS isotopic results of the Petravaara granite.

Sample	t (Ma)[a]	$^{176}Hf/^{177}Hf$	$\pm1\sigma_m$	$^{178}Hf/^{177}Hf$	$\pm1\sigma_m$	$^{176}Lu/^{177}Hf$	$\pm1\sigma_m$	$^{176}Yb/^{177}Hf$	$\pm1\sigma_m$	$^{176}Hf/^{177}Hf(t)$	$\pm2\sigma_m$	$\varepsilon_{Hf}(t)$	$\pm2\sigma_m$
n2167-2	**1819**	**0.281412**	**0.000043**	**1.467375**	**0.000083**	**0.000206**	**0.000001**	**0.008164**	**0.000058**	**0.281405**	**0.000086**	**−7.80**	**3.05**
n2167-3	**1817**	**0.281468**	**0.000050**	**1.467388**	**0.000117**	**0.000256**	**0.000003**	**0.010373**	**0.000126**	**0.281459**	**0.000096**	**−5.90**	**3.59**
n2167-4_1	1811	0.281347	0.000029	1.467305	0.000060	0.000167	0.000002	0.006780	0.000079	0.281341	0.000057	−10.25	2.06
n2167-4_2	1811	0.281488	0.000036	1.467431	0.000083	0.000211	0.000006	0.007762	0.000178	0.281481	0.000070	−5.29	2.60
n2167-5	**1825**	**0.281543**	**0.000041**	**1.467397**	**0.000078**	**0.000217**	**0.000005**	**0.010774**	**0.000295**	**0.281536**	**0.000081**	**−3.01**	**2.90**
n2167-6	1811	0.281429	0.000029	1.467350	0.000060	0.000124	0.000001	0.004664	0.000019	0.281424	0.000056	−7.29	2.05
n2167-7	**1784**	**0.281472**	**0.000041**	**1.467427**	**0.000077**	**0.000124**	**0.000001**	**0.004702**	**0.000028**	**0.281468**	**0.000083**	**−6.36**	**2.90**
n2167-8_1	*1887*	*0.281670*	*0.000062*	*1.467656*	*0.000111*	*0.000365*	*0.000020*	*0.011348*	*0.000477*	*0.281657*	*0.000122*	*2.74*	*4.36*
n2167-8_2	*1887*	*0.281675*	*0.000059*	*1.467604*	*0.000105*	*0.000417*	*0.000025*	*0.014676*	*0.000559*	*0.281660*	*0.000117*	*2.84*	*4.05*
n2167-9	*1947*	*0.281495*	*0.000048*	*1.467441*	*0.000093*	*0.000195*	*0.000005*	*0.007374*	*0.000135*	*0.281488*	*0.000094*	*−1.90*	*3.40*
n2167-10	**1796**	**0.281318**	**0.000069**	**1.467370**	**0.000120**	**0.000394**	**0.000008**	**0.019332**	**0.000100**	**0.281305**	**0.000138**	**−11.88**	**4.62**
n2167-11	1811	0.281512	0.000042	1.467742	0.000102	0.000210	0.000005	0.008722	0.000108	0.281504	0.000081	−4.44	2.97
n2167-12	1811	0.281470	0.000047	1.467495	0.000091	0.000276	0.000011	0.009907	0.000306	0.281461	0.000095	−5.98	3.14
n2167-13	1811	0.281624	0.000055	1.467538	0.000100	0.000149	0.000004	0.007531	0.000092	0.281619	0.000110	−0.37	3.81
n2167-14	**1806**	**0.281387**	**0.000034**	**1.467213**	**0.000077**	**0.000134**	**0.000000**	**0.005027**	**0.000027**	**0.281382**	**0.000069**	**−8.90**	**2.35**
n2167-15	**1786**	**0.281616**	**0.000052**	**1.467362**	**0.000093**	**0.000168**	**0.000003**	**0.008692**	**0.000150**	**0.281610**	**0.000105**	**−1.26**	**3.65**
n2167-16a	1811	0.281559	0.000037	1.467466	0.000080	0.000118	0.000002	0.006058	0.000106	0.281555	0.000077	−2.64	2.61
n2167-17b	1811	0.281467	0.000044	1.467401	0.000096	0.000217	0.000004	0.011187	0.000271	0.281460	0.000091	−6.03	3.04
n2167-18b	1811	0.281496	0.000045	1.467449	0.000096	0.000182	0.000004	0.009866	0.000205	0.281490	0.000093	−4.96	3.15
n2167-19	**1800**	**0.281457**	**0.000046**	**1.467365**	**0.000087**	**0.000127**	**0.000003**	**0.005494**	**0.000154**	**0.281453**	**0.000097**	**−6.53**	**3.34**
n2167-20	**1782**	**0.281456**	**0.000041**	**1.467485**	**0.000094**	**0.000264**	**0.000003**	**0.014436**	**0.000146**	**0.281447**	**0.000085**	**−7.16**	**2.92**
n2167-21	**1825**	**0.281597**	**0.000051**	**1.467461**	**0.000107**	**0.000147**	**0.000002**	**0.006998**	**0.000093**	**0.281592**	**0.000107**	**−1.00**	**3.58**
n2167-22	**1773**	**0.281442**	**0.000036**	**1.467372**	**0.000090**	**0.000127**	**0.000001**	**0.006148**	**0.000092**	**0.281438**	**0.000073**	**−7.69**	**2.54**
n2167-23	**1815**	**0.281521**	**0.000050**	**1.467349**	**0.000101**	**0.000360**	**0.000017**	**0.016378**	**0.000343**	**0.281509**	**0.000105**	**−4.19**	**3.56**

(*Continued*)

Table 5. (*Continued*).

Sample	t (Ma)[a]	$^{176}Hf/^{177}Hf$	$\pm1\sigma_m$	$^{178}Hf/^{177}Hf$	$\pm1\sigma_m$	$^{176}Lu/^{177}Hf$	$\pm1\sigma_m$	$^{176}Yb/^{177}Hf$	$\pm1\sigma_m$	$^{176}Hf/^{177}Hf(t)$	$\pm2\sigma_m$	$\varepsilon_{Hf}(t)$	$\pm2\sigma_m$
n2167-24	**1800**	**0.281483**	**0.000049**	**1.467348**	**0.000111**	**0.000463**	**0.000020**	**0.018816**	**0.000318**	**0.281467**	**0.000096**	**−6.02**	**3.56**
n2167-25	**1824**	**0.281413**	**0.000048**	**1.467438**	**0.000099**	**0.000208**	**0.000002**	**0.010638**	**0.000066**	**0.281405**	**0.000103**	**−7.66**	**3.45**
n2167-26	**1819**	**0.281489**	**0.000049**	**1.467445**	**0.000092**	**0.000164**	**0.000003**	**0.008517**	**0.000185**	**0.281483**	**0.000095**	**−5.02**	**3.55**
n2167-27	**1808**	**0.281497**	**0.000048**	**1.467395**	**0.000094**	**0.000181**	**0.000001**	**0.009450**	**0.000037**	**0.281491**	**0.000100**	**−5.00**	**3.42**
n2167-28	**1797**	**0.281488**	**0.000051**	**1.467397**	**0.000096**	**0.000212**	**0.000004**	**0.010915**	**0.000201**	**0.281481**	**0.000105**	**−5.61**	**3.63**
n2167-29	**1794**	**0.281435**	**0.000053**	**1.467442**	**0.000090**	**0.000206**	**0.000002**	**0.010700**	**0.000125**	**0.281428**	**0.000112**	**−7.55**	**3.70**
n2167-30	**1805**	**0.281515**	**0.000047**	**1.467482**	**0.000096**	**0.000172**	**0.000002**	**0.008977**	**0.000073**	**0.281509**	**0.000098**	**−4.40**	**3.39**
n2167-32	1811	0.281425	0.000046	1.467159	0.000097	0.000310	0.000008	0.015875	0.000398	0.281414	0.000094	−7.65	3.25
n2167-33	**1819**	**0.281528**	**0.000042**	**1.467415**	**0.000082**	**0.000293**	**0.000007**	**0.015796**	**0.000385**	**0.281517**	**0.000084**	**−3.80**	**3.09**
n2167-34	**1825**	**0.281522**	**0.000049**	**1.467325**	**0.000090**	**0.000208**	**0.000003**	**0.011002**	**0.000130**	**0.281515**	**0.000100**	**−3.74**	**3.54**
n2167-35	**1806**	**0.281516**	**0.000041**	**1.467398**	**0.000092**	**0.000441**	**0.000019**	**0.021518**	**0.000805**	**0.281501**	**0.000083**	**−4.68**	**3.11**
n2167-36	**1788**	**0.281541**	**0.000043**	**1.467526**	**0.000080**	**0.000194**	**0.000002**	**0.010359**	**0.000104**	**0.281534**	**0.000085**	**−3.92**	**3.03**
n2167-37	**1810**	**0.281456**	**0.000040**	**1.467472**	**0.000096**	**0.000117**	**0.000001**	**0.005855**	**0.000050**	**0.281452**	**0.000079**	**−6.32**	**3.00**
n2167-38	**1801**	**0.281572**	**0.000051**	**1.467618**	**0.000101**	**0.000207**	**0.000002**	**0.010809**	**0.000131**	**0.281565**	**0.000101**	**−2.54**	**3.65**
n2167-40	**1817**	**0.281483**	**0.000046**	**1.467333**	**0.000088**	**0.000110**	**0.000001**	**0.005594**	**0.000055**	**0.281479**	**0.000090**	**−5.20**	**3.29**
n2167-42	**1816**	**0.281463**	**0.000044**	**1.467422**	**0.000084**	**0.000153**	**0.000001**	**0.007938**	**0.000080**	**0.281458**	**0.000086**	**−5.98**	**3.11**
n2167-44	**1837**	**0.281493**	**0.000072**	**1.467856**	**0.000126**	**0.000456**	**0.000020**	**0.016149**	**0.000421**	**0.281477**	**0.000140**	**−4.80**	**5.27**
n2167-46	**1831**	**0.281601**	**0.000047**	**1.467309**	**0.000104**	**0.000224**	**0.000002**	**0.011717**	**0.000099**	**0.281594**	**0.000088**	**−0.82**	**3.31**
n2167-47	1811	0.281408	0.000053	1.467188	0.000094	0.000214	0.000007	0.011154	0.000312	0.281401	0.000104	−8.13	3.87
n2167-49	**1832**	**0.281475**	**0.000044**	**1.467361**	**0.000073**	**0.000251**	**0.000003**	**0.013246**	**0.000167**	**0.281466**	**0.000081**	**−5.31**	**3.13**
n2167-50	*1877*	*0.281520*	*0.000044*	*1.467495*	*0.000083*	*0.000182*	*0.000002*	*0.009428*	*0.000098*	*0.281514*	*0.000091*	*−2.59*	*3.25*

[a]Concordia ages for the individual zircons in bold. Those written in italics are given at their $^{207}Pb/^{206}Pb$ ages, whereas those written in plain font are assumed as 1811 million years.

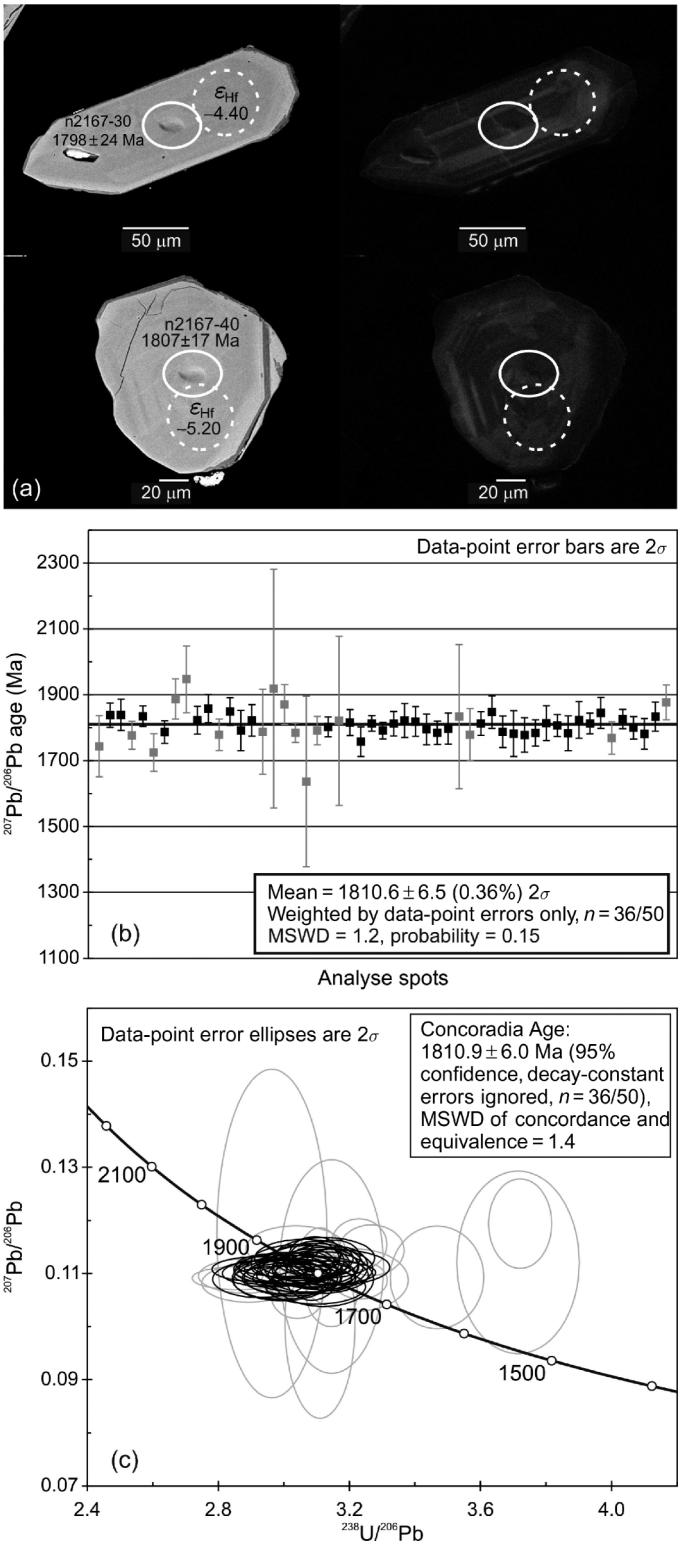

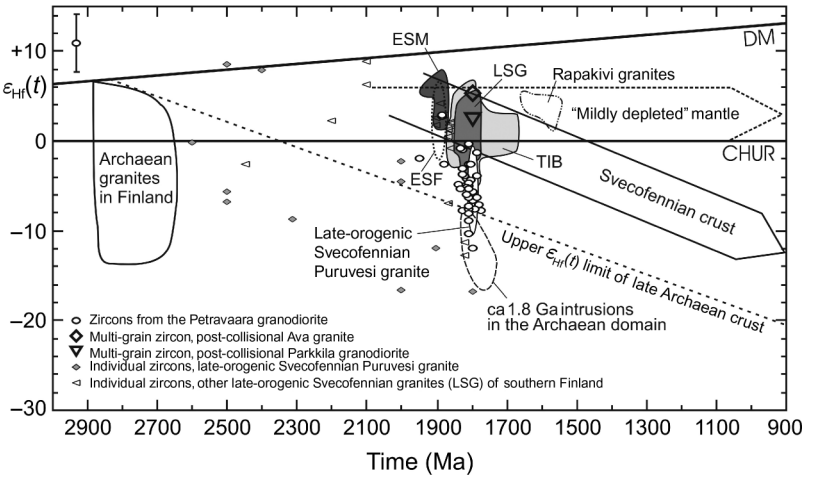

Figure 17. ε_{Hf} versus time diagram for the Petravaara intrusion, modified from Andersen *et al.* (2009) and Kurhila *et al.* (2010). Chondritic uniform reservoir (CHUR) and depleted mantle (DM) growth curves follow those in Andersen *et al.* (2009), with CHUR from Bouvier *et al.* (2008) and DM modified from Griffin *et al.* (2000). Ranges of variation are shown for Archaean granites, early Svecofennian mafic rocks (ESM), early Svecofennian felsic rocks (ESF), late-orogenic Svecofennian granites (LSG; Puruvesi granite, near Petravaara, is plotted separately), ca. 1.8 Ga granites in the Archaean Karelian domain, Transscandinavian Igneous Belt rocks (TIB) in Sweden, and anorogenic rapakivi granites in Finland (Patchett *et al.* 1981; Vervoort and Patchett 1996; Andersson *et al.* 2008; Andersen *et al.* 2009; Kurhila *et al*. 2010; Lauri *et al*., in review). The data from Patchett *et al.* (1981), Vervoort and Patchett (1996), and Kurhila *et al.* (2010) are recalculated after Scherer *et al.* (2001, 2007), Söderlund *et al.* (2004), and Bouvier *et al.* (2008). The arrows represent the evolution of juvenile Svecofennian crust and a possible evolution trend for 'mildly depleted' Fennoscandian lithospheric mantle (from Andersen *et al.* 2009). The error bar in the left corner of the figure shows the average $\pm 2\sigma_m$ for the $\varepsilon_{Hf}(t)$ values of Petravaara (cf. Table 5). Discussion in the text.

in the mafic-intermediate rocks, as in most cases granites have lower concentrations (Figure 11). The Pirilä or Petravaara granitoids are also not appropriate as contaminants; Sr, P, and Ti are very low; and Cs, Rb, Ba, Th, U relations are not consistent with such a model. The insignificant role of crustal contamination for the enriched compositions of these rocks is further emphasized in plots of Th/Ta and P_2O_5/TiO_2 versus Ce/Yb (Figure 18). Here we have included data from Svecofennian upper crustal rocks in southern Finland. At corresponding Ce/Yb ratios, the Th/Ta ratios (Figure 18a) of the mafic-intermediate rocks are distinctly lower than in upper crustal rocks in the area. This precludes crustal contamination as a major cause for the compositional variation. The P_2O_5/TiO_2 ratios also tend to be higher than in most crustal rocks (Figure 18b). Furthermore, the La/Nb ratios are significantly higher than in crustal rocks (Figure 14).

Figure 16. (a) BSE and CL images, including $^{207}Pb/^{206}Pb$ ages and ε_{Hf} values, of two selected zircon crystals (analyses n2167-30 and n2167-40 in Tables 4 and 5) from the Petravaara granite. The analytical spots are circled. (b) Pb–Pb weighted age diagram and (c) Tera-Wasserburg (1972) U-Pb concordia diagram for zircons from the Petravaara granite. The grey bars and ellipses are the analyses excluded from the age calculations. MSWD = mean squares of weighted deviates.

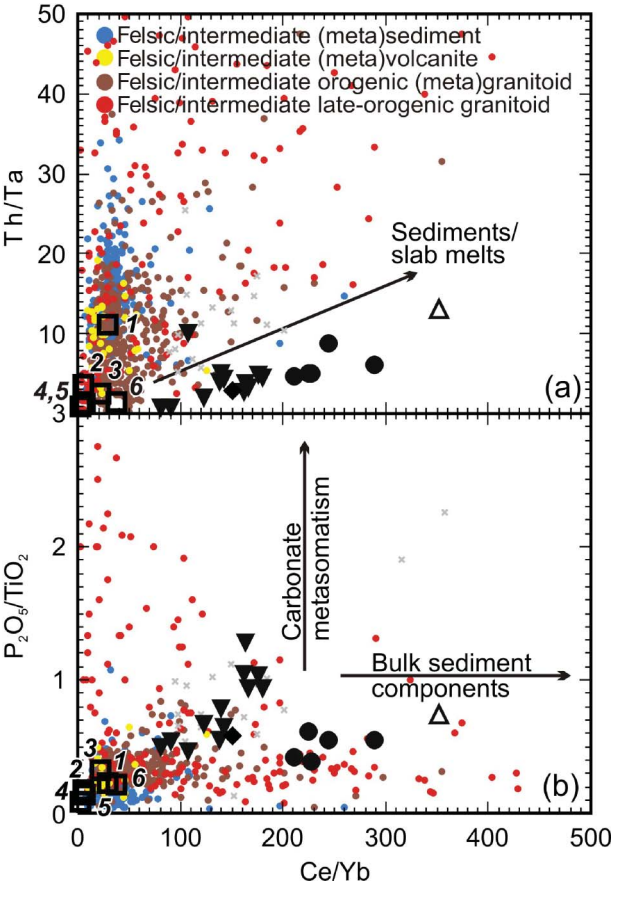

Figure 18. (a) Th/Ta and (b) P_2O_5/TiO_2 versus Ce/Yb diagrams that highlight the differences in between the mafic post-collisional rocks and their relation to the crustal rocks of the SSAC. 1 = upper crust; 2 = primitive continental andesitic arcs; 3 = evolved continental andesitic arcs; 4 = N-MORB; 5 = E-MORB; 6 = ocean island basalts; data from Sun and McDonough (1989), Condie (1993), and the file 'Av-Andesite2.xls' in http://www.geokem.com/earths_average_composition.html, by Dr Bernard M. Gunn (2004). Symbols as in Figure 3, with the additional SSAC reference data in colours (data from the Rock Geochemical Database of Finland, online database; see in the reference list). Of the elsewhere reported post-collisional rocks from southern Finland and Russian Karelia, only mafic-intermediate rocks (<60 wt.% SiO_2) are included.

A diagram of Rb/Ba versus Ti/Y (Figure 19) effectively separates the post-kinematic mafic-intermediate rocks from other Svecofennian rocks. The former have in general very low Rb/Ba ratios, mostly below 0.07, whereas among the crustal rocks only approximately 5% fall below the line defined in Figure 19. At Ti/Y ratios below 300, elevated Rb/Ba ratios are noted for the post-kinematic rocks, indicating increasing crustal influence. Likewise, Turner *et al.* (1996) showed with the same elemental ratios that crustal contamination was insignificant in shoshonites from the Tibetan plateau.

The strongly enriched trace element patterns, except Ti, Y, and the HREE, are reminiscent of patterns for calc-alkaline, continental-arc rocks, although even more enriched (Figure 11), which is typical for shoshonitic rocks (e.g. Arnaud *et al.* 1992; Sun and Stern 2001). According to Morrison (1980), shoshonitic rocks are characterized by $Na_2O + K_2O > 5$ wt.%, Al_2O_3 between 14 and 19 wt.%, $TiO_2 < 1.3$ wt.% and can be

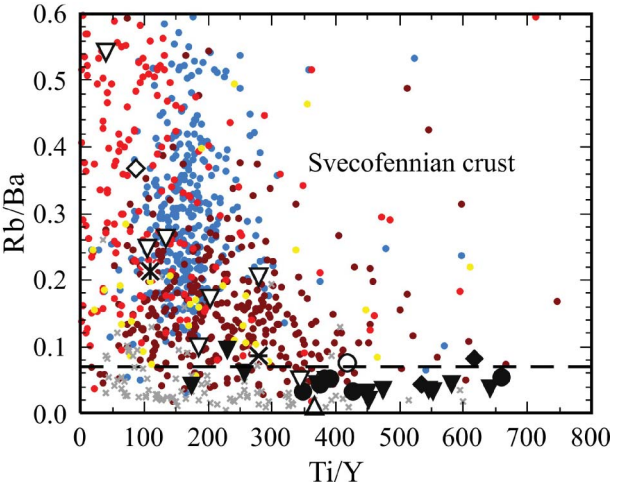

Figure 19. Mafic-intermediate post-collisional rocks show distinctly low Rb/Ba and high Ti/Y ratios, with insignificant overlaps with the Svecofennian crust. In contrast, the granitoid rocks of Turku, Renko, and Pirilä fall within the Svecofennian crustal field. The Luonteri granitoids and the Petravaara granite plot close to the border between the Svecofennian crust and the post-collisional mafic rocks, as does one of the Turku granitoid samples. Symbols as in Figures 3 and 18.

separated from calc-alkaline rocks by higher K_2O/Na_2O and K_2O/SiO_2, features that define post-kinematic rocks in southern Finland as shoshonitic, except for their much higher TiO_2 (Table 2). However, TiO_2 contents >1.3 wt.% is not uncommon among rocks classified as shoshonitic, especially in Tibet (e.g. Turner *et al.* 1996; Carr 1998; Duchesne *et al.* 1998; Williams *et al.* 2004; Zhang *et al.* 2008). The character and level of enrichment are roughly similar in the studied plutons, irrespective of geographical position and evolutionary level, although differing in significant details. Although these rocks are evolved (Mg# < 46), with low contents of Ni and Cr, and pre-emplacement fractionation of at least olivine and pyroxene must have caused increases in the abundance of incompatible elements, this is not enough to explain the extreme enrichment (cf. e.g. Wenzel *et al.* 1997; Becker *et al.* 1999; Gerdes *et al.* 2000; Sun and Stern 2001). Furthermore, the LREE/HREE is not correlated with Mg# (Figure 20). This calls for the presence of strongly enriched mantle sources for these magmas (cf. e.g. Tatsumi and Eggins 1995; Turner *et al.* 1996; Leat *et al.* 2002; Zhang *et al.* 2008). Local variations in the type of source enrichment and degree of melting explain the compositional differences between the plutons. The slab-derived component to the sources of the shoshonitic rocks in the east (Parkkila and Luonteri) appears to have contributed a higher relative input of bulk sedimentary material (melts), compared with those in the west (Turku and Renko), which on the contrary partly seem to have experienced higher input of carbonatitic fluids as indicated by trace element ratios (Figure 18).

Apart from the Renko intrusion, the Nd and Sr isotopic composition of the ca. 1.8 Ga post-kinematic, mafic-intermediate rocks in southern Finland falls within a field defined by initial $^{87}Sr/^{86}Sr$ of 0.7024–0.7033 and $\varepsilon_{Nd}(t)$ of 0–1 (Figure 15; Patchett and Kouvo 1986; Nironen and Rämö 2005; Andersson *et al.* 2006a; this study). This also includes the 1.79 Ga carbonatites at Halpanen (Torppa and Karhu 2007). The $\varepsilon_{Nd}(t)$ values of the ca. 1.80 Ga carbonatites at Naantali show slightly more enriched values, between –0.8 and +0.4, whereas the initial $^{87}Sr/^{86}Sr$ is on 0.7028–0.7032 (Woodard and Huhma, in review).

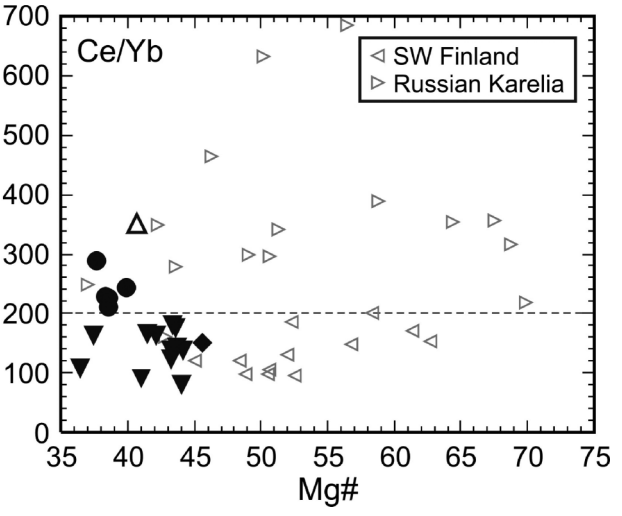

Figure 20. Ce/Yb versus Mg# for mafic rocks (<60 wt.% SiO_2). Symbols as in Figure 3, with the addition of those in the legend. Reference data collected from Rutanen *et al.* (1997 and references therein), Eklund *et al.* (1998), and Andersson *et al.* (2006a). Rocks from SE Finland and Russian Karelia have Ce/Yb > 200, while those from SW Finland are <200.

The coeval post-kinematic, shoshonitic rocks in Russian Karelia also show more enriched compositions: essentially within the ranges 0.7033–0.7035 for initial $^{87}Sr/^{86}Sr$ and 0 to –0.8 for $\varepsilon_{Nd}(t)$ (Kononova *et al.* 2000; Andersson *et al.* 2006a; Woodard and Huhma, in review).

The LREE enrichment is unrelated to the degree of fractionation as is demonstrated by the equally high, or higher, Ce/Yb ratios in more primitive members of the ca. 1.8 Ga post-kinematic suites in Russian Karelia and SW Finland (Figure 20). Here, a clear distinction is observed where the rocks from SW Finland (including Turku and Renko) are much less enriched compared to SE Finland (including Luonteri and Parkkila) and Russian Karelia. This difference is observed also in the isotopic diagram (Figure 15), where Luonteri and Parkkila are slightly more enriched, compared to Renko and Turku. This shows that these magmas cannot have been derived from a 'normal depleted' mantle (ε_{Nd} approximately +3.9 at 1.80 Ga; after DePaolo 1981). Based on the pronounced LILE and LREE enrichment, but depletion in HREE, depleted mantle sources strongly overprinted by mantle metasomatism are indicated (cf. Eklund *et al.* 1998; Väisänen *et al.* 2000; Andersson *et al.* 2006a). The abundances of many elements are too high, higher than in any crustal rocks, to be accounted for by crustal contamination (Figures 8 and 11), and thus crustal influence would rather result in lowering the contents of these elements (cf. e.g. Hegner *et al.* 1998; Miller *et al.* 1999; Wenzel *et al.* 2000; Guo *et al.* 2004). Concerning the isotopes, the high abundances of Sr and Nd in these rocks would effectively mask contamination by Svecofennian crustal material with substantially lower contents. Moreover, the isotopic composition of the Svecofennian, juvenile metaigneous crust partly overlaps that of these enriched, mantle-derived rocks (Figure 15).

The roughly coeval, calc-alkaline to marginally shoshonitic mafic rocks in the TIB further west (Figure 1) show a similar, but less strong enrichment of LILE and LREE, and depletion in HFSE and HREE, compatible with metasomatic enrichment of a previously depleted mantle (e.g. Andersson *et al.* 2004a, 2007 and references therein). The relatively

lesser enrichment of the TIB sources is noticeable also in the isotopic composition, and these rocks roughly define a 'mildly depleted mantle' field of initial ε_{Nd} approximately +0.7 to +2 and $^{87}Sr/^{86}Sr$ 0.7020–0.7033 (Wilson *et al.* 1986; Andersson 1997; Claeson and Andersson 2000; Andersson *et al.* 2004a, 2007; Wikström and Andersson 2004; Rutanen and Andersson 2009), slightly above that of the southern Finland shoshonitic intrusions (Figure 15). The Renko monzodiorite is isotopically overlapping the TIB rocks (Table 3; cf. Nironen and Rämö 2005). With few exceptions, there is thus a progressive increase in the degree of mantle source enrichment going eastwards across the Svecofennian Domain at 1.8 Ga, reflected in both geochemical and isotopic compositions (Andersson *et al.* 2006a).

Direct observations of mantle rocks with such an enrichment have been made, for example, by Beccaluva *et al.* (2004), who reported amphibole-phlogopite-bearing harzburgitic mantle xenoliths with strongly enriched Nd and Sr isotopic signatures inherited by subduction-related metasomatism. Thus, fluids/melts from a subducting slab percolate and enrich the overlying depleted mantle wedge, for example, in Ba, more radiogenic Sr, and less radiogenic Nd (cf. e.g. Menzies *et al.* 1987; Griffin *et al.* 1988; Fitton *et al.* 1991; Thirlwall *et al.* 1996; Becker *et al.* 2000; Xu *et al.* 2003). A large increase in $^{87}Sr/^{86}Sr$ accompanied by a relatively smaller decrease in ε_{Nd} has been interpreted to indicate that H_2O from subducted oceanic crust dominated in the fluids causing a relatively stronger enrichment in LILE than LREE (e.g. Hawkesworth *et al.* 1991, 1994; Thirlwall *et al.* 1996; You *et al.* 1996; Becker *et al.* 2000).

The amount of Th, Ba, and unradiogenic Nd would increase, if the metasomatizing agents were enriched in melts or CO_2 from subducted sediments (e.g. Thirlwall *et al.* 1996; Turner *et al.* 1996; Becker *et al.* 2000; Sun and Stern 2001), as would be the case for a deeply subducted slab in a continental-arc setting (e.g. Pearce 1982; Hoogewerff *et al.* 1997). This is indicated in Figure 15 by a steep enrichment trend at low relative Sr/Nd that includes all the post-kinematic rocks in southern Finland and Russian Karelia. In contrast, many mafic rocks of the TIB in the west tend to show enrichment trends at slightly higher relative Sr/Nd (Rutanen and Andersson 2009 and references therein), suggesting higher H_2O/CO_2 in their mantle sources. Mantle carbonates and carbonate-rich mantle xenoliths are typically enriched in Ba, Sr, and LREE (e.g. Ionov 1998), and melts generated from carbonated lherzolitic mantle are strongly enriched in LREE (Blundy and Dalton 2000). Moreover, carbonatitic melts in the mantle are able to dissolve and transport substantial amounts of P (Green and Wallace 1988; Baker and Wyllie 1992; Rudnick *et al.* 1993; Wyllie 1995). The combination of strong P, Ba, Sr, and LREE enrichment (Figures 8, 11, and 18) in the mafic-intermediate rocks therefore suggests an origin in a carbonate-enriched mantle. Additional strong support for this comes from the existence of coeval carbonatites, the ca. 1.79 Ga Halpanen carbonatite in SE Finland (close to Luonteri and Parkkila), and the ca. 1.80 Ga Naantali carbonatitic dikes (close to Turku) in SW Finland, with isotopic compositions (Torppa and Karhu 2007; Woodard and Huhma, in review) overlapping those of the other post-kinematic rocks.

The generally very high Ce/Yb (mostly >100; Figures 18 and 20) favours a deep origin, within the garnet-bearing mantle (cf. e.g. Turner *et al.* 1996; Doe 2002; Guo *et al.* 2004; Zhang *et al.* 2008). The high abundances of alkali and LIL elements in these rocks suggest that their mantle source lithologies comprised significant amounts of phlogopite and/or amphibole (e.g. Foley 1992; Foley *et al.* 1996; Ionov *et al.* 1997; Williams *et al.* 2004). Variations in the alkali ratios, for example, K_2O/Na_2O (Figure 6a), may partly derive from variations in the phlogopite/amphibole ratios in the mantle source regions of the primary magmas such that K_2O-richer rocks at Luonteri and Parkkila derive from

deeper, phlogopite-dominated sources, whereas the Na_2O-richer Turku magmas should be generated at shallower levels, relatively richer in amphibole (cf. e.g. Wilkinson and Le Maitre 1987; Wilson 1989; Cocherie *et al.* 1994; Bonin 2004).

Between ~43 and 50 wt.% SiO_2, the mafic rocks of the Turku intrusions show an evolution with decreasing TiO_2, $Fe_2O_3^t$, MgO, CaO, and P_2O_5, whereas K_2O, Na_2O, and Al_2O_3 increase (Figure 3). For Al_2O_3, P_2O_5, and Na_2O, a distinct inflection is present at ~50 wt.% SiO_2, indicating a change in petrogenetic evolution. A straight extrapolation of the trend below 50 wt.% SiO_2 to higher SiO_2 values does not extend towards a reasonable felsic end-member. This rules out mixing with a crustal magma and assimilation of upper crustal rocks as explanations for the <50 wt.% SiO_2 part of the chemical spectrum. Instead, fractionation of dominantly amphibole/clinopyroxene, Fe-Ti oxides, and apatite can account for this evolution. The essentially constant Mg# can be explained by the co-precipitation of ferromagnesian silicates and Fe-Ti oxides. The trace elements are in general agreement with this, but the lack of increase in Ba and Rb suggests that biotite also played a role. Further, the slight decrease in REE, Y, and Sr, as well as no significant increase in Th and Nb, supports an important role for apatite and minor titanite. In contrast, the strong increase in Al_2O_3 and Na_2O preclude significant fractionation of plagioclase.

Above the inflection point, at ~50 wt.% SiO_2, either an Al_2O_3- and Na_2O-containing phase starts to precipitate in the Turku suite or some other process was in operation. If plagioclase joined the fractionating assemblage, together with amphibole that might have substituted clinopyroxene because of an increasing volatile content in the crystallizing magma (indicated petrographically), this would potentially explain the change in the trend and further chemical evolution towards silicic compositions. However, prominent fractionation of plagioclase at 50 wt.% SiO_2 would be expected to show up as more significant changes in evolution for most major elements, most notably Na_2O and CaO, which is not observed. Moreover, fractionation of amphibole and plagioclase up to 70 wt.% SiO_2 is negated by the strongly increasing Na_2O. An interesting feature of the evolution >50 wt.% SiO_2 is that the major element trends here follow a straight line between 50 and ~70 wt.% SiO_2, where the silicic end of the range is represented by a K_2O-poor, Na_2O-rich composition similar to a sample of melted wall rock that has mingled and mixed with the mafic rock (Väisänen *et al.* 2000). Such types of calcic/calc-alkaline, tonalitic/granodioritic granitoids are present within the suite of late-orogenic migmatite-related granitoids of southern Finland (Figures 6a and 7) and may thus represent a crustal magma end-member with which the mafic Turku magmas has mixed. Gerdes *et al.* (2000) observed mixing trends between enriched mantle melts and a felsic crustal end-member granodiorite closely similar to that predicted here. This model appears to be contradicted by elevated contents of, for example, Ba, Rb, Zr, and Nb in the intermediate rocks (Figure 8), and low contents of Rb, Y, and REE in the felsic rock. However, these intermediate rocks may contain cumulus biotite, zircon, and titanite. The trace element composition of the felsic end-member thus diverges in some details from that of the melted wall rock sample. This may be related to a better homogenization of biotite and accessory minerals in the actual felsic end-member compared with melted wall rock sample.

Within the suites of mafic-intermediate Luonteri and Parkkila rocks there are no rocks with <50 wt.% SiO_2 and Mg# > 41 (Table 2). Intermediate rocks follow linear trends towards a felsic end-member at ~70 wt.% SiO_2, compatible with a magma-mixing origin (Figures 3 and 8). In particular, mafic-intermediate rocks between 50 and 60 wt.% SiO_2 also obey this linearity and should therefore contain a minor portion of crustal melt admixture. Discrepancies can be noted for Zr and Nb, which appear to indicate accessory mineral cumulation.

The composition of the most mafic Luonteri and Parkkila rocks correspond to highly fractionated magmas (cf. Figure 20), originally derived by small degrees of melting of a strongly metasomatized, garnet-bearing mantle, slightly deeper and more enriched in bulk sedimentary components compared to SW Finland (cf. Figure 18). The fractionation did not affect the Ce/Yb ratio much. The mantle source contained abundant phlogopite, more than in SW Finland, as evidenced by the higher alkali and fluorine contents (Figures 3 and 8). These strongly enriched mantle magmas fractionated and mixed with K_2O-rich, crustal melts to generate the final spectrum of compositions.

Lahtinen (1996) suggested that the negative Nb anomaly in the Renko monzodiorite was the result of fractionation of titanite ± titanomagnetite, rather than a subduction-influenced source. However, the Nb anomaly in the Renko monzodiorite is not more pronounced than in the other post-kinematic intrusions or in shoshonitic rocks worldwide, which have been related to strongly enriched mantle sources (Figure 11). This does not, however, rule out a minor superimposed effect of titanite and Fe-Ti oxide fractionation, as was indicated for the Turku monzodiorites above.

Granitoid rocks. The granitoids associated with the mafic-intermediate rocks are of highly variable character. Those present along the margins of the Turku monzodiorites show intermingling features with the monzodiorites, which together with the geochronology show that these rocks are coeval (Väisänen *et al.* 2000). They are thus slightly younger than the 1.85–1.82 Ga, late-orogenic Svecofennian granites (Kurhila *et al.* 2005 and references therein), but are geochemically indistinguishable from them (Figures 3–10, 19, and below in 22). As their A/CNK index is mostly below 1.1 (Figure 5), they do not qualify as S-type granites s.s. (e.g. Chappell and White 1974; Clarke 1992). Thus their slightly peraluminous, calc-alkaline to alkali-calcic, high-silica (>71 wt.%) geochemistry suggests derivation from mainly, but not exclusively, metasedimentary sources.

The relatively high Rb in the Turku granites and the late-orogenic granites, combined with low Y + Nb, makes them plot transitional between the volcanic-arc and syn-collisional granite fields (Figure 10); the latter being typical for S-type granites (e.g. Pearce *et al.* 1984). This corroborates the hypothesis that these rocks are derived from mixed sources: metasedimentary and metaigneous. Many authors have emphasized mainly metasedimentary sources in the genesis of the late-orogenic Svecofennian granites (e.g. Nurmi and Haapala 1986; Lahtinen 1996). The heterogeneity in geochemistry for the Turku granites, and for the late-orogenic granites in general, is most probably related to variations in source lithology and composition, as these granites are generally locally derived (cf. Andersson 1991; Zuber and Öhlander 1991; Nironen 2005; Stålfors and Ehlers 2006; Nironen and Kurhila 2008), some of them, for example, containing garnet, others not. Moreover, ca. 1.89–1.87 Ga inherited zircons were found in the Turku granite, suggesting the presence of metaigneous source components of this age (Väisänen *et al.* 2000). Most of the late-orogenic and Turku granites plot in the field of fractionated I- and S-type granites, but partly plot transitional into the A-type granite field, at relatively high alkalinity (Figure 9). The increased alkalinity in some granites may be related to variations in source lithologies, including metaigneous protoliths with elevated HFSE contents. Thus, the granites associated with the Turku monzodioritic plutons were formed by melting of the heterogeneous country rocks in response to the heat advected from the mafic intrusions, and the two magma types were occasionally mingled and mixed.

The analysed granitic dike that cuts the monzodiorites of the Renko intrusions has all the geochemical characteristics discussed above for the Turku and the late-orogenic Svecofennian granites in general and is thus formed from similar crustal sources. Lahtinen (1996) reported that monzodiorite and granite show signs of mingling along the contacts of the pluton, giving evidence of a corresponding situation as in the Turku area. We therefore interpret the granitic dikes in the Renko monzodiorites as back-veins of local crustal melts, generated by the heat from the mafic Renko intrusion.

The Turku and Renko granites are distinct from the mafic rocks and compositionally overlap the plotted SSAC rocks (Figure 19). The isotopic data from the Renko and Turku granites (Table 3) show near-chondritic initial ε_{Nd} values, but somewhat elevated initial $^{87}Sr/^{86}Sr$ values (Figure 15). These data are not compatible with entirely metasedimentary protoliths, as Svecofennian metasedimentary rocks normally contain ~30% Archaean detritus (e.g. Claesson *et al.* 1993; Lahtinen *et al.* 2002, 2010; Rutland *et al.* 2004; Sultan *et al.* 2005; Bergman *et al.* 2008) and plot at negative ε_{Nd} values. Instead, these granites must be derived from more juvenile lithologies, presumably with somewhat elevated Rb/Sr ratios. Seawater alteration, weathering, and diagenetic recrystallization of juvenile sediments, for instance, can mobilize and enrich Rb and deplete Sr in these sources, which will enhance the $^{87}Sr/^{86}Sr$, but does not necessarily fractionate Sm and Nd (e.g. McCulloch and Chappell 1982; Staudigel *et al.* 1995). Such protoliths may be represented by Svecofennian metasedimentary rocks with no, or only a very small, Archaean component; or alternatively, juvenile metaigneous crust. In fact, the Turku and Renko granites plot within the same field of Figure 15 as the 1.91–1.85 Ga Svecofennian metaigneous crust. Although this does not preclude metasedimentary source components for these granites, it shows that juvenile, metaigneous rocks may be a major component. Similar conclusions were reached for the late-orogenic Svecofennian granites in Sweden and Finland (Patchett *et al.* 1987; Andersson 1991; Claesson and Lundqvist 1995; Kurhila *et al.* 2010). Mixing of magmas in the source region of similar leucocratic granite batholiths, from metasedimentary and metaigneous protoliths, has recently been documented by Reichardt *et al.* (2010).

The Pirilä granite is in many respects similar to the late-orogenic granites, but is more enriched in Rb, Nb, Th, Pb, and LREE (Figure 8). As it contains abundant fluorite, it is also rich in F (not analysed). Although it is alkali-calcic (Figure 7) and marginally peraluminous (Figure 5), its elevated HFSE content (Figure 11c) makes it plot distinctly within the A-type field in Figure 9, whereas it plots at the border between three fields in Figure 10. This transitional character may be related to a combination of dominantly metaigneous sources and a highly fractionated, F-rich magma. The Pirilä granite shows geochemical similarities with the 1826 ± 11 Ma Karjaa granite further west, but displays higher Rb, LREE, Th, and lower Zr and Hf. The Karjaa granite shows predominantly A-type character, and it was derived from ca. 1.88 Ga metaigneous sources (Jurvanen *et al.* 2005). Similarly, Roberts and Clemens (1993) and Årebäck *et al.* (2008) advocated intermediate, metaluminous lower-middle crustal lithologies as the main source for the genesis of high-K, calc-alkaline to alkali-calcic granitoid rocks. Heilimo *et al.* (2009) summarized earlier works by, for example, Patchett *et al.* (1981), Kouvo *et al.* (1983), and Huhma (1986) by suggesting lower crustal TTG sources for the similar Nattanen granites in northern Finland. A dominantly metaigneous source is also supported for the Pirilä granite by the near-chondritic initial ε_{Nd} value (Table 3; cf. Lahtinen and Huhma 1997). The initial $^{87}Sr/^{86}Sr$ value is very low, unreal, and has suffered disturbance after crystallization (Figure 15).

The Luonteri granitoids are calc-alkaline (Figure 7) and compositionally divided into two groups: quartz-monzonites and granodiorites/granites (Figure 4b). The former group

is essentially metaluminous, whereas the latter is variably peraluminous (Figure 5). The quartz-monzonites fall compositionally intermediate between the quartz-diorites/monzodiorites and the granites for all major and trace elements, and the granites show geochemical characteristics close to or overlapping with those of the late-orogenic granites (Figures 3, 5, 7, and 8). These geochemical features indicate that the Luonteri rocks form a magmatic mixing suite between the highly evolved, mantle-derived monzodioritic magmas and crustally derived, high-silica (>70 wt.% SiO_2) granitic magmas. Such a model was also proposed for the intermediate rocks at Kårtorp in the TIB of southern Sweden which are similar in age and composition (Andersson 1989, 1997; Andersen *et al.* 2009). This model is supported by the gradual transitions between rock types and ghost-like mingling structures (Figure 2d; cf. Pitkänen 1985). Plutonic mixing between highly evolved, lamprophyric/shoshonitic mafic and granitic magmas has been proposed for a number of cases showing continuous straight line trends in elemental bi-variate plots (e.g. Janoušek *et al.* 2000, 2004; Chen *et al.* 2002; Christofides *et al.* 2007). Some of the crustal magmas at Luonteri have remained liquid longer than the intermediate rocks of the main intrusion and form granitic back-veins. The Luonteri granites show roughly overlapping geochemistry with the late-orogenic granites of southern Finland, or they are slightly displaced along the mixing trend towards the monzodiorites (e.g. Figures 3, 5, 7, and 8). The overlapping isotopic data of the Luonteri monzodiorite and quartz-monzonite (Figure 15) cannot be used uncritically to infer a common source in a 'mildly depleted' mantle. In fact, the isotopic composition of the juvenile, metaigneous Svecofennian crust overlaps that of such a 'mildly depleted' mantle source, which makes mantle and crustal sources equally likely.

The Petravaara intrusion is emplaced within crust underlain by Archaean basement (e.g. Laajoki 2005; Sorjonen-Ward and Luukkonen 2005; cf. Korja and Heikkinen 2008), which is reflected in its substantially low initial ε_{Nd} (−2.8, Table 3; Figure 21), as well as a range in ε_{Hf} zircon values to as low as −12, with an average of −4.9 (Table 5; Figure 17). Nearby analysed metasediments show similar ε_{Nd} values (ε_{Nd}(1.9 Ga) between −3.4 and −2.9; Huhma 1987). The Archaean component has, however, not resulted in a complementary increase in the initial $^{87}Sr/^{86}Sr$ value of the Petravaara magma and thus appears unrelated to upper crustal juvenile, Svecofennian metasedimentary rocks (Figure 15). In contrast, a larger Archaean component is indicated within the nearby and coeval (1797 ± 19 Ma; Nykänen 1983), more silicic Puruvesi monzogranite with an initial ε_{Nd}(1.80 Ga) of −6.9 (Figure 21; Huhma 1986) and initial $\varepsilon_{Hf}(t)$ <−15 in some zircon cores, combined with actual inherited Archaean zircons (Figure 17; Kurhila *et al.* 2010).

The geochemistry of the Petravaara sample #6 (Tables 1–3) is alkali-calcic, on the border between met- and peraluminous, and close to that of the Luonteri quartz-monzonites (Figures 5 and 7), indicating a similar petrogenesis. Referring to the model for the Luonteri rocks above, this would imply an origin by mixing of magmas derived from a strongly enriched mantle and mainly metaigneous, low Rb/Sr crustal sources with a significant Archaean component. The crustal component most likely consists of mixed Archaean and Svecofennian contributions, in proportions not possible to constrain because of the isotopic overlap between the Svecofennian crust and the enriched mantle (Figure 15).

Assuming an entirely Archaean metaigneous source component, with a similar isotopic composition as that of the Archaean tonalites north of Petravaara (O'Brien *et al.* 1993) and in northern Finland (Martin *et al.* 1983), and a magma composition similar to that of late-orogenic Svecofennian granites in southern Finland (Nironen 2005; Stålfors and Ehlers 2006; Rock Geochemical Database of Finland), which are partly derived from

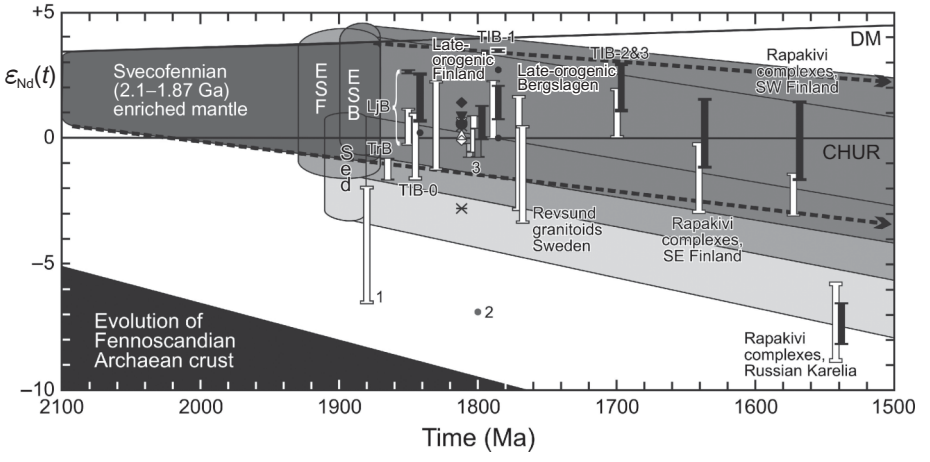

Figure 21. ε_{Nd} versus time diagram. Symbols as in Figure 3. Evolution field for the Archaean crust as compiled in Andersson *et al.* (2002). Evolutionary field (the arrows with broken lines, with $^{147}Sm/^{144}Nd$ in the range 0.14–0.17) for a proposed 'mildly depleted' Svecofennian lithospheric mantle. DM = depleted mantle (DePaolo 1981); CHUR = chondritic uniform reservoir; ESF = early Svecofennian felsic crust in southern Finland (Huhma 1986; Patchett and Kouvo 1986; Lahtinen and Huhma 1997; Rämö *et al.* 2001; Väisänen *et al*. 2008, 2009); ESB = early Svecofennian basic rocks in southern Finland (Huhma 1986, 1987; Patchett and Kouvo 1986; Makkonen 1996; Vaasjoki and 1 1999; Rämö *et al.* 2001; Väisänen *et al*. 2008, 2009); Sed = early Svecofennian metasedimentary rocks in southern Finland (Miller *et al.* 1986; Huhma 1987; Lahtinen *et al.* 2002); 1 = post-kinematic granitoids in the Palaeoproterozoic part of the Karelian Domain (Huhma 1986; Ruotoistenmäki *et al.* 2001; Nironen 2005); 2 = late-orogenic Puruvesi granite in the Palaeoproterozoic part of the Karelian Domain (Huhma 1986); 3 = elsewhere reported analyses of 1.8 Ga post-collisional rocks in the SSAC, of which the black bar demonstrates mafic (Nironen and Rämö 2005; Andersson *et al.* 2006a), the darker grey carbonatite (Torppa and Karhu 2007; Woodard and Huhma, in review), and the white bar felsic (Patchett and Kouvo 1986; Lahtinen and Huhma 1997; Rämö *et al.* 2005; Andersson *et al.* 2006a) analyses from the Finnish part of the SSAC, whereas the lighter grey bar marks rocks in the easternmost SSAC, in Russian Karelia (Kononova *et al.* 1999, 2000; Andersson *et al.* 2006a). The rest of the black (mafic rocks) and white (felsic rocks) bars and smaller circles (single analyses) comprise ca 1.88–1.84 Ga intrusives in the Ljusdal Batholith and the Transition Belt in central Sweden (LjB and TrB, respectively; Högdahl *et al.* 2008); ca. 1.85 Ga TIB-0 basites (Andersson 1997 (recalculated according to data in Andersen *et al.* 2009); Claeson and Andersson 2000); TIB-0 granitoids (Andersson 1997 (recalculated according to data in Andersen *et al.* 2009); Claeson and Andersson 2000; Wikström and Andersson 2004); 1.85–1.82 Ga late-orogenic granites in southern Finland (Huhma 1986; Rämö and Nironen 2001; Rämö *et al.* 2004; Kurhila *et al.* 2005, 2010); ca. 1.80 Ga TIB-1 mafic intrusive rocks of south-central and southern Sweden (Andersson 1997 (recalculated according to data in Andersen *et al.* 2009); Wikström and Andersson 2004; Andersson *et al.* 2007; Rutanen and Andersson 2009); ca. 1.80 Ga TIB-1 granitoids in southern Sweden (Wilson *et al.* 1986; Patchett *et al.* 1987; Andersson 1997 (recalculated according to data in Andersen *et al.* 2009); Mansfeld 2004; Wikström and Andersson 2004); ca. 1.79 Ga late-orogenic granitoids in Bergslagen in south-central Sweden (Patchett *et al.* 1987; Vervoort and Patchett 1996; H. Rutanen, unpublished data); 1.79 Ga Revsund granitoids in north-central Sweden (Wilson *et al*. 1985; Patchett *et al*. 1987; Claesson and Lundqvist 1995; Andersson *et al*. 2002); ca. 1.7 Ga mafic TIB-2&3 rocks (Wilson *et al*. 1985; Nyström 1999; Claeson 2001); ca. 1.7 Ga TIB-2&3 felsic rocks (Wilson *et al*. 1985; Patchett *et al*. 1987; Heim *et al*. 1996; Lundqvist and Persson 1999; Nyström 1999; Appelquist *et al*., submitted); rapakivi-related anorogenic rocks in SE Finland (Rämö 1991), SW Finland (Rämö 1991; Fröjdö *et al*. 1996; Eklund *et al*. 2005) and Russian Karelia (Neymark *et al*. 1994). Discussion in the text.

metaigneous sources, the composition of an Archaean-derived crustal granitic magma may be approximated by ~30 ppm Nd, $\varepsilon_{Nd}(1.81\ Ga) = -10.4$, ~100 ppm Sr, $^{87}Sr/^{86}Sr(1.81\ Ga) = 0.7094$. Magmas from an enriched mantle component may be approximated by: ~220 ppm Nd, $\varepsilon_{Nd}(1.81\ Ga) = +0.5$, ~2200 ppm Sr, $^{87}Sr/^{86}Sr(1.81\ Ga) = 0.7028$, based on Table 3 and data in Eklund *et al.* (1998) and Andersson *et al.* (2006a). When using these end-members, the composition of the Petravaara granite fall on a mixing curve at ~70–75% crustal magma and ~30–25% magma from the enriched mantle (Figure 15).

The presence of numerous small mafic enclaves in the Petravaara granite (Figure 2g) supports the presence of coeval contrasting magmas. A minor contribution by local sediments is suggested by numerous small rusty enclaves of the host rock. Two older analyses of rocks from the Petravaara intrusion (Hackman 1931; Nykänen 1968) deviate significantly from the presently analysed sample, being much lower in K_2O (Figure 7). One of the rocks in the older analyses is also strongly enriched in Na_2O (Figure 3). Whether these analyses are reliable or not is difficult to judge, but compositionally they do fall within the field reported for the late-orogenic Svecofennian granites of southern Finland. They may thus record a large compositional variation within this small intrusion that is due to strongly variable crustal components.

The large range in initial ε_{Hf} of the magmatic Petravaara zircons (–11.9 to +2.8, Table 5; Figure 17) suggests a heterogeneous mixture of magmas. The range from Archaean crust to mildly depleted mantle values supports a mixture between these sources. A significant contribution from juvenile Svecofennian crust is also allowed by the Hf data, whereas an input from a strongly depleted mantle source appears not to be present. Hf isotopic data from the nearby ca. 1.80 Ga Puruvesi monzogranite show a similar range in ε_{Hf} values, but with a higher proportion of inherited old crystals (Kurhila *et al.* 2010), whereas initial ε_{Hf} multi-grain zircon analyses from the post-kinematic Åva and Parkkila intrusions, more to the west (Figure 1), show more depleted values (Patchett *et al.*1981; Figure 17).

In the Hf-Rb-Ta diagram (Figure 22), the Luonteri, Petravaara, Pirilä, and one of the Turku samples, combined with other post-collisional granites from southern Finland and Russian Karelia, and TIB granites, define an area mostly within the field of volcanic-arc granites, but straddling into the late- and post-collisional and within-plate fields. This field is contrasted with a field at higher relative Rb and lower Ta, where the late-orogenic Svecofennian granites plot, including most of the Turku 'S-granites' and the Renko granitic dike. We suggest that this difference (divided with the broken curve in Figure 22) is related to a larger source contribution to the late-orogenic granites by mica-rich metasedimentary rocks, whereas the post-collisional and TIB granites were derived from metaigneous sources.

Geodynamic inferences

The post-kinematic plutons intruded the essentially juvenile (<2.1 Ga) crust of southern Finland at 1.82–1.76 Ga, during the shift from a transpressional to a (trans)tensional tectonic regime (Lahtinen *et al.* 2005; Väisänen and Skyttä 2007). There is a tendency for ages <1.79 thousand million years in southwesternmost Finland and ages >1.79 thousand million years from Turku and eastwards. Furthermore, the oldest 1.815 Ga intrusions have been emplaced deeper, when the surrounding crust was still hot, thus interacting in a ductile way forming mingled zones with anatectic granites (Lahtinen 1996; Väisänen *et al.* 2000). In contrast, some of the youngest intrusions in SW Finland intruded under more brittle conditions after exhumation to crustal levels <10 km (Eklund and Shebanov 2005).

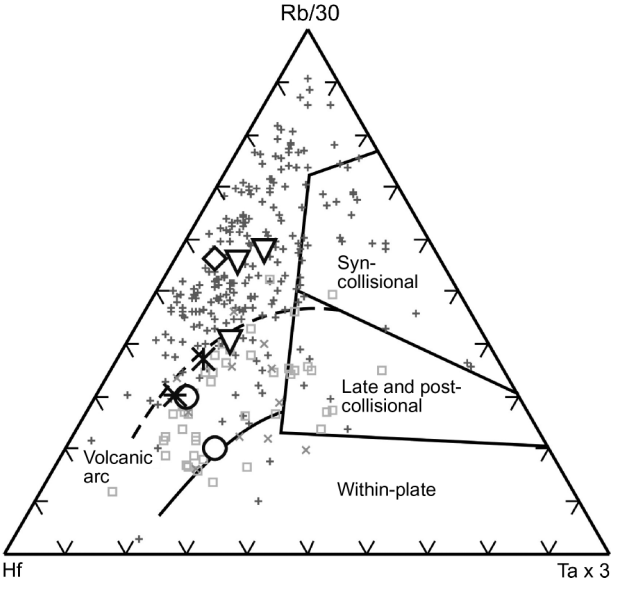

Figure 22. Tectonic settings of granitoids, modified after Harris *et al*. (1986). See in the text for the explanation of the broken line. Symbols as in Figure 9.

High-K calc-alkaline and shoshonitic rocks are found in a variety of tectonic environments, such as oceanic and continental arcs as well as post-collisional and intra-plate settings (e.g. Morrison 1980; Leterrier *et al.* 1990; Müller *et al.* 1992; Sun and Stern 2001). In collisional orogenies, they are often younger than calc-alkaline arc and syn-orogenic/syn-collisional rocks (cf. Barragan *et al.* 1998; Liégeois 1998; Frost *et al.* 2001; Elburg *et al.* 2002; Bonin 2004; Duggen *et al.* 2008). The post-kinematic mafic rocks in southern Finland display strongly enriched subduction-type compositions. However, these rocks clearly post-date active subduction and accretion in the area. The compositions suggest that lithospheric mantle sources, strongly enriched by subduction-derived fluids and/or melts during previous subduction episode/s (cf. e.g. Fitton *et al.* 1991; Feldstein and Lange 1999; Hawkesworth *et al.* 1995; Canning *et al.* 1996; Wilson *et al.* 1997), were tapped by these magmas, during a shift from collision to post-collisional transpression and finally extension in the time frame 1.82–1.76 Ga.

The intrusions in this study fit into the characteristics of post-collisional magmatism given by Bonin *et al.* (1998), Liégeois (1998), and Liégeois *et al.* (1998), which are (a) high-K calc-alkaline to shoshonitic in composition, (b) at least partly related to lateral escape tectonics after collision, and (c) derived from depleted mantle sources, enriched during a previous subduction episode. The pre-enrichment source depletion is evidenced by the depletion in the HREE relative to MORB. In addition, the compositions of the 1.8 Ga post-kinematic intrusions in southern Finland are overlapping with those of shoshonitic, volcanic, and plutonic rocks from elsewhere, typically those from post-collisional settings, for example, in central Iberia (López-Moro and López-Plaza 2004) and particularly those in Tibet (e.g. Guo *et al.* 2006; Zhang *et al.* 2008; Figure 11). The Tibetan shoshonites are normally considered to stem from strongly enriched lithospheric mantle sources that were subjected to melting, after slab break-off and convective erosion of the lower lithosphere (e.g. Turner *et al.* 1996; Miller *et al.* 1999; Mahéo *et al.* 2002; Williams *et al.* 2004).

Roberts and Clemens (1993) suggested that post-collisional magmatism would be a result of mantle upwelling and underplating of the lower crust by mafic magmas because of decompression, after crustal thickening. The 1.8 Ga post-collisional rocks in southern Finland and Russian Karelia have been proposed to be related to upwelling of hot asthenospheric material because of slab break-off (Väisänen *et al.* 2000; Eklund and Shebanov 2002), plume activity (Peltonen *et al.* 2000), or lithospheric unrooting (Kosunen 2004) that caused melting of the strongly enriched lithospheric mantle. In fact, an origin partly as a mixture between strongly enriched lithospheric and asthenospheric magmas is allowed by the data, and larger asthenospheric components appear to be present in the Turku rocks (Figures 12 and 13). However, the dominantly shoshonitic, rather than alkaline within-plate, chemistry argue against a within-plate environment (cf. Pearce *et al.* 1990; Pearce 1996a). It is noteworthy, also, that no 1.8 Ga mafic rocks derived entirely from asthenospheric sources have been found in the Svecofennian Domain.

The absolute timing of the enrichment of the mantle sources for the studied mafic rocks is not known, but the T_{DM} ages are essentially <2.1 Ga (Table 3), and thus do not lend support for a major Archaean influence (except for Petravaara). The mantle enrichment most likely occurred during the preceding Svecofennian ((2.1–)1.95–1.86 Ga) arc magmatism (cf. Andersson 1997; Andersson *et al.* 2006a), when systems of arcs and microcontinents assembled together with underlying slab-enriched mantle sections and accreted to the Archaean craton nucleus in the northeast. The carbonate-rich fluids and melts that percolated the sub-Svecofennian mantle derived from subducted slabs carrying sedimentary detritus. These sediments probably contained a minor component of Archaean material, which is typical for Svecofennian sediments (e.g. Claesson *et al.* 1993; Lahtinen *et al.* 2002; Andersson *et al.* 2004b, 2006b; Bergman *et al.* 2008). This is also evident in their low ε_{Nd} values, intermediate between those of Archaean and Svecofennian metaigneous crust (Figure 15).

During the Svecofennian subduction, the metasomatizing agents added variable amounts of low-radiogenic Nd to the previously depleted mantle, creating a geographically heterogeneous 'mildly depleted mantle' (cf. Andersson *et al.* 2007; Rutanen and Andersson 2009; Figure 15). Analysed samples of enriched mantle have variable, but generally lower $^{147}Sm/^{144}Nd$ compared to DM and mostly also to CHUR (broadly in the range 0.10–0.20; e.g. McDonough and McCulloch 1987; Voshage *et al.* 1987; Gorring and Kay 2000; Schmidberger *et al.* 2001). Variably enriched (varying $^{147}Sm/^{144}Nd$) areas of lithospheric mantle are distributed beneath the Svecofennian Domain of the Fennoscandian Shield. This affects to different degrees post-1.9 Ga mafic magmas extracted from it, or interacting with it while passing through, as shown by their variable initial ε_{Nd} (cf. Andersson *et al.* 2004a; Söderlund *et al.* 2005). Even if individual enriched mantle sections follow their own evolution with time, an average evolutionary slope ($^{147}Sm/^{144}Nd$ 0.14–0.17) in the ε_{Nd} versus time diagram encompasses most of the initial compositions of the younger mafic magmatism between 1.85 and 1.55 Ga (Figure 21), suggesting that they derive from such a 'mildly depleted mantle'. Furthermore, similar 'mildly depleted mantle' evolutions have been postulated from observations of the Lu–Hf isotopic system in Fennoscandian mafic rocks (Söderlund *et al.* 2005; Andersen *et al.* 2009).

Evidence for a widespread and important magmatic event at ca. 1.8 Ga comes from kimberlites and related rocks. Abundant ages around 1.8 Ga in zircon xenocrysts and zircons in lower crustal xenoliths from Palaeozoic kimberlites have shown that significant portions of the mafic lower crust, at least in east-central Finland formed around this age (Hölttä *et al.* 2000; Peltonen and Mänttäri 2001; Peltonen *et al.* 2006). This supports a connection between the small 1.8 Ga middle to upper crustal post-kinematic intrusions

and coeval widespread mafic underplating. These intrusions thus represent higher-level magmatism from widespread layers of enriched mafic magmas underplating the Svecofennian crust in southern Finland and Russian Karelia. In addition to the Petravaara intrusion, the strongly enriched 1.80 Ga mafic Elisenvaara intrusion and Kalto lamprophyres in Russian Karelia (Andersson *et al.* 2006a) and 1.79–1.78 Ga lamprophyres northwest of Petravaara (Woodard *et al.*, submitted) provide evidence that layers of enriched mafic magma underplated also the Archaean Karelian craton margin at this time.

Recent interpretations of the deep seismic reflection profile FIRE 2A that traversed southern Finland in the vicinity of the Renko intrusion (Nironen *et al.* 2006; Korja and Heikkinen 2008) suggest the presence of a major layer of mafic lower crust, interpreted by these authors to indicate a trapped body of oceanic crust. Alternatively, it may comprise layers of mafic magma that underplated the crust at ca. 1.8 Ga.

Simultaneous with the continental collision in southern Finland, continental-margin magmatism was active 1.85–1.75 Ga along the juvenile Svecofennian margin in the west and southwest (in Sweden), creating the TIB (e.g. Andersson 1991; Åhäll and Larson 2000; Andersson *et al.* 2004a, 2007; Johansson *et al.* 2006). NE-directed convergence and subduction resulted in NW-SE-trending lithologies and structures of the southeastermost TIB and the adjoining high-grade Svecofennian crust (Gorbatschev 1980; Rutanen and Andersson 2009). According to magnetic data, these NW-SE-trending structures are deflected southwards in the southeast, close to the Volgo-Sarmatian craton (cf. Bogdanova *et al.* 2006). As in southern Finland, a large number of major dextral, transpressional shear zones developed within the southern and central Svecofennian Domain of Sweden at ca. 1.80 Ga (Beunk and Page 2001; Högdahl and Sjöström 2001; Persson and Sjöström 2003; Högdahl *et al.* 2009). Thus, this complicated palaeotectonic scenario created a convergent stress field presumably as a result of a tectonic interplay between continental collision in the southeast with Volgo-Sarmatia and continental-margin convergence in the southwest (Rutanen and Andersson 2009) that resulted in dextral transpressional tectonics across the southern Svecofennian Domain. The crustal-scale shear zones, initiated by convergence and collision, may have facilitated magma transport and emplacement of the 1.8 Ga post-kinematic intrusions during the post-collisional shift to extension in southern Finland.

Conclusions

(1) The investigated six intrusive complexes in southern Finland, post-kinematic in relation to most of the ductile, pervasive deformation, were emplaced between 1.82 and 1.79 Ga. The age of the easternmost, Petravaara body yielded a U–Pb zircon (SIMS) age of 1811 ± 6 Ma.

(2) The composition ranges from monzogabbro/alkali gabbro to monzo- or syenogranite, but monzodioritic to quartz-monzonitic rocks dominate. The basic to intermediate rocks are alkali-rich ($K_2O + Na_2O > 4$ wt.%), mainly alkali-calcic and shoshonitic, with only a few high-K calc-alkaline compositions. They are strongly enriched in LILE and LREE, but depleted in HREE, and are much less enriched in HFSE relative to N-MORB. They resemble shoshonitic rocks worldwide, in particular those of Tibet. The enriched geochemical character is coupled with a near-chondritic to 'mildly depleted' isotopic composition, with initial ε_{Nd} between +0.1 and +1.4 and initial $^{87}Sr/^{86}Sr$ in the range 0.7027–0.7031, that is,

somewhat more enriched than coeval calc-alkaline, continental-arc rocks located further west in the TIB.

(3) The strongly LILE- and LREE-enriched character of the mafic-intermediate rocks cannot be accounted for by crustal contamination, because of non-crustal trace element signatures, as well as typically higher absolute abundances of elements such as Ba, Sr, Ce, Sm, and P than in the crust. We suggest that previously depleted mantle sources became strongly enriched by CO_2 and/or melt percolation from subducted sediments. Trace elements suggest more carbonated sources in the west and more sediment-influenced sources in the east. Higher Ce/Yb and K_2O/Na_2O ratios in the east indicate a deep, garnet-bearing source in which phlogopite dominated over amphibole, whereas towards the west, more amphibole was present in the source, probably closer to the spinel–garnet transition (i.e. shallower depths). T_{DM} ages <2.1 Ga suggest that the time of mantle enrichment was not more than 300 Ma prior to the magmatism, during the earliest Svecofennian subduction and arc magmatism. Attending subduction and accretion of the Svecofennian crust, a juvenile, heterogeneously enriched mantle was established below the continent. This sub-Svecofennian mantle (isotopically 'mildly depleted') developed with time, largely overlapping the Nd isotopic evolution of the juvenile Svecofennian crust, and acted as a source for many younger mafic rocks in the Svecofennian Domain. Interaction of melts from both lithospheric and asthenospheric sources was also possible inasmuch as the trace element abundances of these rocks are similar or exceed that of typical OIB.

(4) The associated granitoids are more diverse, ranging from calc-alkaline to alkali-calcic and from metaluminous to slightly peraluminous. The granites in the Turku and Renko intrusions are transitional between I- and S-type, volcanic-arc and collisional in character, whereas those of Luonteri, Petravaara, and Pirilä fall between I- and A-type, as well as between volcanic-arc and within-plate in character. The former group distinctly overlaps compositions of the bulk of the late-orogenic Svecofennian granites and shows relatively juvenile isotopic compositions similar to those of the early Svecofennian granitoids. This, and the mixed geochemical character, suggests that they had mixed sedimentary and igneous protoliths. The other group was derived mainly from Svecofennian igneous protoliths. Isotopic evidence strongly suggests mixed Archaean and juvenile sources for the Petravaara intrusion.

(5) Geochemical trends within the mafic Turku intrusions are compatible with the fractionation of mainly clinopyroxene/amphibole, Fe-Ti oxides and apatite, with minor biotite and titanite up to ~50 wt.% SiO_2. Straight line trends between ~50 and 70 wt.% SiO_2 for essentially all elements suggest that rocks in this compositional range represent mixtures between mafic magmas from strongly enriched mantle and magmas derived from the juvenile Svecofennian crust. This holds for both the Turku and Luonteri intrusions, although the end-members differ. Some cumulation of biotite, zircon, and titanite accounts for the scatter in these trends.

(6) The post-kinematic intrusions in southern Finland intruded the juvenile SSAC and the Karelian Domain in the aftermath of the continental collision with the Volgo-Sarmatian craton on the southeast, during a shift from contraction and transpressional shearing to an extensional regime. The setting is thus post-collisional, rather than post-orogenic, which is corroborated by the shoshonitic composition, typical for post-collisional rocks.

Acknowledgements

HR acknowledges the financial support from Magnus Ehrnrooth's Foundation, Agneta and Carl-Erik Olin's Foundation, Nordenskiöld Society in Finland, Oskar Öflund's Foundation, the Research Institute of Åbo Akademi University Foundation, the Principal of Åbo Akademi University (Åbo Akademi University Foundation), The Social Insurance Institution of Finland, and Carl Cedercreuz' stipendiefond (Svenska Kulturfonden). MV was funded by the Academy of Finland (project 117311). The Laboratory for Isotope Geology at the Swedish Museum of Natural History provided the facilities, expertise, and financial support through SYNTHESYS fundings (project acronyms SE TAF 1393 and 2050), which were made available by European Community – Research Infrastructure Action under the FP6 'Structuring the European Research Area' Programme. Martin Whitehouse, Lev Ilyinsky, Chris Kirkland, and Kerstin Lindén from the Nordsim laboratory are thanked for all the help with the SIMS. The Nordsim facility is financed and operated under an agreement between the research councils of Denmark, Norway, and Sweden, the Geological Survey of Finland, and the Swedish Museum of Natural History. This is a Nordsim publication #259, and an SIGL (Finland Isotope Geosciences Laboratory) contribution. Hugh O'Brien at SIGL of the Geological Survey of Finland (GTK) is thanked for letting us make the Hf isotopic analyses and helping us with the analytical procedure and data handling. Hannu Huhma and Bo Johanson from GTK are shown gratitude for lending powder of the Parkkila sample for analysis and for allowing the use of equipments and instructing the CL/BSE imaging. Hannu Huhma and Tom Andersen reviewed an earlier version of the manuscript. Dmitry Konopelko and Shauket Baltybaev are acknowledged for updating the information on the geology of Russian Karelia. Jeremy Woodard is thanked for useful discussions and help in laboratory works. Veikko Grönroos, Juha Kauhanen, and Arto Peltola are acknowledged for preparing the thin sections.

References

Åhäll, K.-I., and Larson, S.Å., 2000, Growth related 1.85–1.55 Ga magmatism in the Baltic Shield; a review addressing the tectonic characteristics of Svecofennian, TIB 1-related, and Gothian events: GFF, v. 122, p. 193–206.

Ahtonen, N., Hölttä, P., and Huhma, H., 2007, Intracratonic Palaeoproterozoic granitoids in northern Finland: Prolonged and episodic crustal melting events revealed by Nd isotopes and U-Pb ages on zircon: Bulletin of the Geological Society of Finland, v. 79, p. 143–174.

Andersen, T., Andersson, U.B., Graham, S., Åberg, G., and Simonsen, S.L., 2009, Granitic magmatism by melting of juvenile continental crust: New constraints on the source of Palaeoproterozoic granitoids in Fennoscandia from Hf isotopes in zircon: Journal of the Geological Society, London, v. 166, p. 233–247.

Andersson, U.B., 1989, Evidence of plutonic magma-mixing, southern Sweden: Rendiconti della Società Italiana di mineralogia e Petrologia, v. 43, p. 831–839.

Andersson, U.B., 1991, Granitoid episodes and mafic-felsic magma interaction in the Svecofennian of the Fennoscandian shield, with main emphasis on the ~1.8 Ga plutonics: Precambrian Research, v. 51, p. 127–149.

Andersson, U.B., 1997, Petrogenesis of some Proterozoic granitoid suites and associated basic rocks in Sweden (geochemistry and isotope geology): Sveriges Geologiska Undersökning, Rapporter och meddelanden, v. 91, 206 pp.

Andersson, U.B., Eklund, O., and Claeson, D.T., 2004a, Geochemical character of the mafic-hybrid magmatism in the Småland-Värmland belt: Geological Survey of Finland, Special Paper, v. 37, p. 47–55.

Andersson, U.B., Eklund, O., Fröjdö, S., and Konopelko, D., 2006a, 1.8 Ga magmatism in the Fennoscandian shield; lateral variations in subcontinental mantle enrichment: Lithos, v. 86, p. 110–136.

Andersson, U.B., Griffin, W.L., Begg, G, and Högdahl, K., 2008, Juvenile and old components in Proterozoic crust; examples from Lu-Hf isotopes in zircon from magmatic Svecofennian and rapakivi rocks in Sweden: 33rd International Geological Congress, Oslo, August 6–14, 2008, Abstract No 1350138 (https://abstracts.congrex.com/scripts/JMEvent/ProgrammeLogic_Abstract_P.asp?PL=Y&Form_Id=8&Client_Id=%27CXST%27&Project_Id=%2708080845%27&Person_Id=1350138, viewed 25th June 2009).

Andersson, U.B., Högdahl, K., Sjöström, H., and Bergman, S., 2004b, Magmatic, detrital, and metamorphic ages in metamorphic rocks from south-central Sweden: GFF, v. 126, p. 16–17.

Andersson, U.B., Högdahl, K., Sjöström, H., and Bergman, S., 2006b, Multistage growth and reworking of the Palaeoproterozoic crust in the Bergslagen area, southern Sweden: Evidence from U-Pb geochronology: Geological Magazine, v. 143, p. 679–697.

Andersson, U.B., Neymark, L.A., and Billström, K., 2002, Petrogenesis of Mesoproterozoic (Subjotnian) rapakivi complexes of central Sweden: Implications from U-Pb zircon ages, Nd, Sr and Pb isotopes: Transactions of the Royal Society of Edinburgh, Earth Sciences, v. 92, p. 201–228.

Andersson, U.B., and Öhlander, B., 2004, The late Svecofennian magmatism: Geological Survey of Finland, Special Paper, v. 37, p. 102–104.

Andersson, U.B., Rutanen, H., Johansson, Å., Mansfeld, J., and Rimša, A., 2007, Characterization of the Paleoproterozoic mantle beneath the Fennoscandian Shield: Geochemistry and isotope geology (Nd, Sr) of ~1.8 Ga mafic plutonic rocks from the Transscandinavian Igneous Belt in southeast Sweden: International Geology Review, v. 49, p. 587–625.

Andersson, U.B., Sjöström, H., Högdahl, K., and Eklund, O., 2004c, The Transscandinavian Igneous Belt, evolutionary models: Geological Survey of Finland, Special Paper, v. 37, p. 104–112.

Appelquist, K., Brander, L., Johansson, Å., Andersson, U.B., and Cornell, D., submitted, Geochemical and Sm-Nd isotope signatures of granitoids from the Transscandinavian Igneous Belt and the Eastern Segment of southcentral Sweden: Geological Journal.

Årebäck, H., Andersson, U.B., and Petersson, J., 2008, Petrological evidence for crustal melting, unmixing, and undercooling in an alkali-calcic, high-level intrusion: The late Sveconorwegian Vinga intrusion, SW Sweden: Mineralogy and Petrology, v. 93, p. 1–46.

Arnaud, N.O., Vidal, Ph., Tapponnier, P., Matte, Ph., and Deng, W.M., 1992, The high K_2O volcanism of northwestern Tibet: Geochemistry and tectonic implications: Earth and Planetary Science Letters, v. 111, p. 351–367.

Baker, M.B., and Wyllie, P.J., 1992, High-pressure apatite solubility in carbonate-rich liquids: Implications for mantle metasomatism: Geochimica et Cosmochimica Acta, v. 56, p. 3409–3422.

Baltybaev, Sh.K., Levchenkov, O.A., Levsky, L.K., Eklund, O. and Kilpeläinen, T., 2006, Two metamorphic stages in the Svecofennian belt: Evidence from isotopic geochronological study of the Ladoga and Sulkava metamorphic complexes: Petrology, v. 14, p. 247–261.

Barragan, R., Geist, D., Hall, M., Larson, P., and Kurz, M., 1998, Subduction controls on the compositions of lavas from the Ecuadorian Andes: Earth and Planetary Science Letters, v. 154, p. 153–166.

Beccaluva, L., Bianchini, G., Bonadiman, C., Siena, F., and Vaccaro, C., 2004, Coexisting anorogenic and subduction-related metasomatism in mantle xenoliths from the Betic Cordillera (southern Spain): Lithos, v. 75, p. 67–87.

Becker, H., Jochum, K.P., and Carlson, R.W., 1999, Constraints from high-pressure veins in eclogites on the composition of hydrous fluids in subduction zone: Chemical Geology, v. 160, p. 291–308.

Becker, H., Jochum, K.P., and Carlson, R.W., 2000, Trace element fractionation during dehydration of eclogites from high-pressure terranes and the implications for element fluxes in subduction zones: Chemical Geology, v. 163, p. 65–99.

Bergman, L., 1986, Structure and mechanism of intrusion of postorogenic granites in the archipelago of southwestern Finland [PhD thesis]: Turku, Finland, Åbo Akademi University, Acta Academiae Aboensis, ser. B, Mathematica et Physica, v. 46, no. 5, 74.

Bergman, S., Högdahl, K., Nironen, M., Ogenhall, E., Sjöström, H., Lundqvist, L., and Lahtinen R., 2008, Timing of Palaeoproterozoic intra-orogenic sedimentation in the central Fennoscandian Shield; evidence from detrital zircon in metasandstone: Precambrian Research, v. 161, p. 231–249.

Bergman, S., Kubler, L., and Martinsson, O., 2001, Description of regional geological and geophysical maps of northern Norrbotten county (east of the Caledonian orogen): Sveriges Geologiska Undersökning Ba, v. 56, 110 p.

Beunk, F.F., and Page, L.M., 2001, The structural evolution of a deeply eroded, accretional continental margin in the Palaeoproterozoic Svecofennian orogen in southern Sweden: Tectonophysics, v. 339, p. 67–92.

Billström, K., and Weihed, P., 1996, Age and provenance of host rocks and ores in the Paleoproterozoic Skellefte District, northern Sweden: Economic Geology, v. 91, p. 1054–1072.

Blundy, J., and Dalton, J., 2000, Experimental comparison of trace element partitioning between clinopyroxene and melt in carbonate and silicate systems, and implications for mantle metasomatism: Contributions to Mineralogy and Petrology, v. 138, p. 356–371.

Bogdanova, S.V., Bingen, B., Gorbatschev, R., Kheraskova, T.N., Kozlov, V.I., Puchkov, V.N., and Volozh, Yu.A., 2008, The East European Craton (Baltica) before and during the assembly of Rodinia: Precambrian Research, v. 160, p. 23–45.

Bogdanova, S., Gorbatschev, R., Grad, M., Guterch, A., Janik, T., Kozlovskaya, E., Motuza, G., Skridlaite, G., Starostenko, V., Taran, L., and EUROBRIDGE and POLONAISE Working Groups, 2006, EUROBRIDGE: New insight into the geodynamic evolution of the East European Craton, *in* Gee, D.G., and Stephenson, R.A., eds., European lithosphere dynamics: London, Geological Society, Memoirs, v. 32, p. 599–624.

Bonin, B., 2004, Do coeval mafic and felsic magmas in post-collisional to within-plate regimes necessarily imply two contrasting, mantle and crustal, sources? Lithos, v. 78, 1–24.

Bonin, B., Azzouni-Sekkal, A., Bussy, F., and Ferrag, S., 1998, Alkali-calcic and alkaline post-orogenic (PO) granite magmatism: Petrologic constraints and geodynamic settings: Lithos, v. 45, p. 45–70.

Bouvier, A., Vervoort, J.D., and Patchett, P.J., 2008, The Lu-Hf and Sm-Nd isotopic composition of CHUR: Constraints from unequilibrated chondrites and implications for the bulk composition of terrestrial planets: Earth and Planetary Science Letters, v. 273, p. 48–57.

Bowes, D.R., and Košler, J., 1993, Geochemical comparison of the subvolcanic appinite suite of the British Caledonides and the durbachite suite of the Central European Hercynides: Evidence for associated shoshonitic and granitic magmatism: Mineralogy and Petrology, v. 48, p. 47–63.

Branigan, N.P., 1987, The role of shearing in the Proterozoic development of the Åland archipelago, S. W. Finland: Bulletin of the Geological Society of Finland, v. 59, p. 117–128.

Brown, G.C., 1982, Calc-alkaline intrusive rocks: Their diversity, evolution, and relation to volcanic arcs, *in* Thorpe, R.S., ed., Andesites: Orogenic andesites and related rocks: Chichester, John Wiley & Sons, p. 437–461.

Cagnard, F., Gapais, D., and Barbey, P., 2007, Collision tectonics involving juvenile crust: The example of the southern Finnish Svecofennides: Precambrian Research, v. 154, p. 125–141.

Canning, J.C., Henney, P.J., Morrison, M.A., and Gaskarth, J.W., 1996, Geochemistry of late Caledonian minettes from northern Britain; implications for the Caledonian sub-continental lithospheric mantle: Mineralogical Magazine, v. 60, p. 221–236.

Carr, P.F., 1998, Subduction-related Late Permian shoshonites of the Sydney Basin, Australia: Mineralogy and Petrology, v. 63, p. 49–71.

Chappell, B.W., and White, A.J.R., 1974, Two contrasting granite types: Pacific Geology, v. 8, p. 173–174.

Chen, B., Jahn, B.-m., and Wei, C., 2002, Petrogenesis of Mesozoic granitoids in the Dabie UHP complex, Central China: Trace element and Nd-Sr isotope evidence: Lithos, v. 60, p. 67–88.

Christofides, G., Perugini, D., Koroneos, A., Soldatos, T., Poli, G., Eleftheriadis, G., Del Moro, A., and Neiva, A.M., 2007, Interplay between geochemistry and magma dynamics during magma interaction: An example from the Sithonia Plutonic Complex (NE Greece): Lithos, v. 95, p. 243–266.

Chu, N.-C., Taylor, R.N., Chavagnac, V., Nesbitt, R.W., Boella, R.M., Milton, J.A., German, C.R., Bayon, G., and Burton, K., 2002, Hf isotope ratio analysis using multi-collector inductively coupled plasma mass spectrometry: An evaluation of isobaric interference corrections: Journal of Analytical Atomic Spectrometry, v. 17, p. 1567–1574.

Claeson, D.T., 2001, Investigation of gabbroic rocks associated with the Småland-Värmland granitoid batholith of the Transscandinavian Igneous Belt [PhD thesis]: Sweden, Earth Sciences Centre, Gothenburg University, A64, 11 p. and 7 appendixes.

Claeson, D.T., and Andersson, U.B., 2000, The 1.85 Ga Nygård pluton, central southern Sweden: An example of early Transscandinavian igneous belt (TIB) noritic magmatism: 24:e Nordiska Geologiska Vintermøte, Trondheim, Norway, January 6–9, 2000, Geonytt, v. 1, p. 50.

Claesson, S., Huhma, H., Kinny, P.D., and Williams, I.S., 1993, Svecofennian detrital zircon ages – implications for the Precambrian evolution of the Baltic shield: Precambrian Research, v. 64, p. 109–130.

Claesson, S., and Lundqvist, Th., 1995, Origins and ages of Proterozoic granitoids in the Bothnian Basin, central Sweden; isotopic and geochemical constraints: Lithos, v. 36, p. 115–140.

Clarke, D.B., 1992, Granitoid rocks: Topics in earth sciences: New York, Chapman and Hall, v. 7, 296 p.

Cocherie, A., Rossi, P., Fouillac, A.M., and Vidal, P., 1994, Crust and mantle contributions to granite genesis – an example from the Variscan batholith of Corsica, France, studied by trace-element and Nd-Sr-O isotope systematics: Chemical Geology, v. 115, p. 173–211.

Condie, K.C., 1993, Chemical composition and evolution of the upper continental crust: Contrasting results from surface samples and shales: Chemical Geology, v. 104, p. 1–37.

Debon, F., and Le Fort, P., 1983, A chemical-mineralogical classification of common plutonic rocks and associations: Transactions of the Royal Society of Edinburgh, Earth Sciences, v. 73, p. 135–149.

De la Roche, H., Leterrier, J., Grand Claude, P., and Marchal, M., 1980, A classification of volcanic and plutonic using R1-R2 diagrams and major element analyses-its relationship with current nomenclature: Chemical Geology, v. 29, p. 183–210.

DePaolo, D.J., 1981, Neodymium isotopes in the Colorado Front Range and crust-mantle evolution in the Proterozoic: Nature, v. 291, p. 193–196.

Doe, B.R., 2002, Further considerations of the Ce/Yb vs. Ba/Ce plot in volcanology and tectonics: International Geology Review, v. 44, p. 877–912.

Duchesne, J.C., Berza, T., Liégeois, J.P., and Vander-Auwera, J., 1998, Shoshonitic liquid line of descent from diorite to granite: The Late Precambrian post-collisional Tismana pluton (South Carpathians, Romania): Lithos, v. 45, p. 281–303.

Duggen, S., Hoernle, K., Klügel, A., Geldmacher, J., Thirlwall, M., Hauff, F., Lowry, D., and Oates, N., 2008, Geochemical zonation of the Miocene Albora'n Basin volcanism (westernmost Mediterranean): Geodynamic implications: Contributions to Mineralogy and Petrology, v. 156, p. 577–593.

Ehlers, C., Lindroos, A., and Selonen, O., 1993, The late Svecofennian granite-migmatite zone of southern Finland-a belt of transpressive deformation and granite emplacement: Precambrian Research, v. 64, p. 295–309.

Ehlers, C., Skiöld, T., and Vaasjoki, M., 2004, Timing of Svecofennian crustal growth and collisional tectonics in Åland, SW Finland: Bulletin of the Geological Society of Finland, v. 76, p. 63–91.

Eklund, O., 1993, Coeval contrasting magmatism and magma mixing in Proterozoic post- and anorogenic granites, Åland, SW Finland [PhD thesis]: Turku, Finland, Department of Geology, Åbo Akademi University, 57 p.

Eklund, O., Fröjdö, S., and Andersson, U.B., 2005, The bimodal highalumina basalt – A-type granite Korsö Dyke, SW Finland, *in* 5th International Dyke Conference (IDC5), Rovaniemi, Finland, July 31–August 3, 2005, Abstracts, p. 10.

Eklund, O., Konopelko, D., Rutanen, H., Fröjdö, S., and Shebanov, A.D., 1998, 1.8 Ga Svecofennian post-collisional shoshonitic magmatism in the Fennoscandian shield: Lithos, v. 45, p. 87–109.

Eklund, O., and Shebanov, A.D., 2002, A slab breakoff model for the differentiation of the Svecofennian crust in southern Finland: Institute of Seismology, University of Helsinki, Finland, Report, v. S-42, p. 9–13.

Eklund, O., and Shebanov, A.D., 2005, The prolonged Svecofennian post-collisional shoshonitic magmatism in the southern part of the Svecofennian domain – a case study of the Åva granite-lamprophyre ring complex: Lithos, v. 80, p. 229–247.

Elburg, A.M., van Bergen, V.M., Hoogewerff, J., Foden, J., Vroon, P., Zulkarnain-Iskandar, I., and Nasution-Asnawir, A., 2002, Geochemical trends across an arc-continent collision zone; magma sources and slab-wedge transfer processes below the Pantar Strait volcanoes, Indonesia: Geochimica et Cosmochimica Acta, v. 66, p. 2771–2789.

Faure, G., 2001, Origin of igneous rocks: The isotopic evidence: Berlin, Springer-Verlag, 496 p.

Feldstein, S.N., and Lange, R.A., 1999, Pliocene potassic magmas from the Kings River region, Sierra Nevada, California: Evidence for melting of a subduction modified mantle: Journal of Petrology, v. 40, p. 1301–1320.

Fitton, J.G., James, D., and Leeman, W.P., 1991, Basic magmatism associated with late Cenozoic extension in the western United States: Compositional variations in space and time: Journal of Geophysical Research, v. 96, p. 13693–13711.

Foley, S., 1992, Petrological characterization of the source components of potassic magmas: Geochemical and experimental constraints: Lithos, v. 28, p. 187–204.

Foley, S.F., Jackson, S.E., Fryer, B.J., Greenough, J.D., and Jenner, G.A., 1996, Trace element partition coefficients for clinopyroxene and phlogopite in an alkaline lamprophyre from Newfoundland by LAM-ICP-MS: Geochimica et Cosmochimica Acta, v. 60, p. 629–638.

Fröjdö, S., Andersson, U.B., and Claesson, S., 1996, Nd isotope geochemistry of some mafic rocks and minerals associated with the Mesoproterozoic Åland and Nordingrå rapakivi batholiths, Fennoscandian shield, *in* International Conference on Proterozoic Evolution in the North Atlantic Realm, Goose Bay, Labrador, Canada, July 29–August 2, 1996, Program and Abstracts, p. 62–63.

Frost, B.R., Barnes, C.G., Collins, W.J., Arculus, R.J., Ellis, D.J., and Frost, C.D., 2001, A geochemical classification for granitic rocks: Journal of Petrology, v. 42, 2033–2048.

Gaál, G., and Gorbatschev, R., 1987, An outline of the Precambrian evolution of the Baltic shield: Precambrian Research, v. 35, p. 15–52.

Gerdes, A., Wörner, G., and Finger, F., 2000, Hybrids, magma mixing and enriched mantle melts in post-collisional Variscan granitoids: The Rastenberg Pluton, Austria: Geological Society, London, Special Publications, v. 179, p. 415–431.
Gerdes, A., and Zeh, A., 2006, Combined U-Pb and Hf isotope La-(MC-)ICPMS analyses of detrital zircons: Comparison with SHRIMP and new constraints for the provenance and age of an Armorican metasediment in Central Germany: Earth and Planetary Science Letters, v. 249, p. 47–61.
Gladney, E.S., Jones, E.A., and Nickell, E.J., 1990, 1988 compilation of elemental concentration data for USGS basalt BCR-1: Geostandards Newsletters, v. 14, p. 209–359.
Gorbatschev, R., 1980, The Precambrian development of southern Sweden: Geologiska Föreningens i Stockholm Förhandlingar, v. 102, p. 129–136.
Gorring, M.L., and Kay, S.M., 2000, Carbonatite metasomatized peridotite xenoliths from southern Patagonia: Implications for lithospheric processes and Neogene plateau magmatism: Contributions to Mineralogy and Petrology, v. 140, p. 55–72.
Green, D.H., and Wallace, M.E., 1988, Mantle metasomatism of basanite magma from garnet peridotite: Earth of Planetary Science Letters, v. 17, p. 456–465.
Griffin, W.L., O'Reilly, S.Y., and Stabel, A., 1988, Mantle metasomatism beneath western Victoria, Australia: II. Isotopic geochemistry of Cr-diopside lherzolites and Al-augite pyroxenites: Geochimica et Cosmochimica Acta, v. 52, p. 449–459.
Griffin, W.L., Pearson, N.J., Belousova, E., Jackson, S.E., van Achterbergh, E., O'Reilly, S.Y., and Shee, S.R., 2000, The Hf isotope composition of cratonic mantle: LAM-MC-ICPMS analysis of zircon megacrysts in kimberlites: Geochimica et Cosmochimica Acta, v. 64, p. 133–147.
Guo, F., Fan, W.M., Wang, Y.J., and Zhang, M., 2004, Origin of early Cretaceous calc-alkaline lamprophyres from the Sulu orogen in eastern China: Implications for enrichment processes beneath continental collisional belt: Lithos, v. 78, p. 291–305.
Guo, Z.F., Wilson, M., Liu, J.Q., and Mao, Q., 2006, Post-collisional, potassic and ultrapotassic magmatism of the northern Tibetan Plateau: Constraints on characteristics of the mantle source, geodynamic setting and uplift mechanisms: Journal of Petrology, v. 47, p. 1177–1220.
Hackman, V., 1931, Geologisk översiktskarta över Finland, sektionen D2, Nyslott. Beskrivning till bergartskartan, 187 p. Espoo: Geological Survey of Finland (in Swedish and summary in French).
Harris, N.B.W., Pearce, J.A., and Tindle, A.G., 1986, Geochemical characteristics of collision-zone magmatism, *in* Coward, M.P., and Reis, A.C., eds., Collision tectonics: Oxford, Blackwell Scientific Publications, Geological Society, Special Publication, v. 19, 67–81.
Hawkesworth, C.J., Gallagher, K., Hergt, J.M., and McDermott, F., 1994, Destructive plate margin magmatism: Geochemistry and melt generation: Lithos, v. 33, p. 169–188.
Hawkesworth, C.J., Hergt, J.M., Ellam, R.M., and McDermott, F., 1991, Element fluxes associated with subduction related magmatism: Philosophical Transactions of the Royal Society of London A, v. 335, p. 393–405.
Hawkesworth, C., Turner, S., Gallagher, K., Hunter, A., Bradshaw, T., and Rogers, N., 1995, Calc-alkaline magmatism, lithospheric thinning and extension in the Basin and range: Journal of Geophysical Research, v. 100, p. 10271–10286.
Hegner, E., Kölbl-Ebert, M., and Loeschke, J., 1998, Post-collisional Variscan lamprophyres (Black Forest, Germany): $^{40}Ar/^{39}Ar$ phlogopite dating, Nd, Pb, Sr isotope, and trace element characteristics: Lithos, v. 45, p. 395–411.
Heilimo, E., Halla, J., Lauri, L.S., Rämö, O.T., Huhma, H., Kurhila, M.I., and Front, K., 2009, The Paleoproterozoic Nattanen-type granites in northern Finland and vicinity – a postcollisional oxidized A-type suite: Bulletin of the Geological Society of Finland, v. 81, p. 7–38.
Heim, M., Skiöld, T., and Wolff, F.C., 1996, Geology, geochemistry and age of the "Tricolor" granite and some other Proterozoic (TIB) granitoids at Trysil, southeast Norway: Norsk Geologisk Tidsskrift, v. 76, p. 45–54.
Högdahl, K., and Sjöström, H., 2001, Evidence for 1.82 Ga transpressive shearing in a 1.85 Ga granitoid in central Sweden: Implications for the regional evolution: Precambrian Research, v. 105, p. 37–56.
Högdahl, K., Sjöström, H., Andersson, U.B., and Ahl, M., 2008, Continental margin magmatism and migmatisation in the west-central Fennoscandian Shield: Lithos, v. 102, p. 435–459.
Högdahl, K., Sjöström, H., and Bergman, S., 2009, Ductile shear zones related to crustal shortening and domain boundary evolution in the central Fennoscandian Shield: Tectonics, v. 28, TC1003, DOI: 10.1029/2008TC002277, 18 p.

Hölttä, P., Huhma, H., Mänttäri, I., Peltonen, P., and Juhanoja, J., 2000, Petrology and geochemistry of mafic granulite xenoliths from the Lahtojoki kimberlite pipe, eastern Finland: Lithos, v. 51, p. 109–133.

Hoogewerff, J.A., van Bergen, M.J., Vroon, P.Z., Hertogen, J., Wordel, R., Sneyers, A., Nasution, A., Varekamp, J.C., Moens, H.L.E., and Mouchel, D., 1997, U-series, Sr-Nd-Pb isotope and trace-element systematics across an active island arc-continent collision zone: Implications for element transfer at the slab-wedge interface: Geochimica et Cosmochimica Acta, v. 61, p. 1057–1072.

Hubbard, F., and Branigan, N.P., 1987, Late Svecofennian magmatism and tectonism, Åland southwest Finland: Precambrian Research, v. 35, p. 241–256.

Huhma, H., 1986, Sm-Nd, U-Pb and Pb-Pb isotopic evidence for the origin of the Early Proterozoic Svecofennian crust in Finland: Geological Survey of Finland, Bulletin, v. 337, 48 p.

Huhma, H., 1987, Provenance of early Proterozoic and Archaean metasediments in Finland: A Sm-Nd isotopic study: Precambrian Research, v. 35, p. 127–143.

Huhma, H., Cliff, R.A., Perttunen, V., and Sakko, M., 1990, Sm-Nd and Pb isotopic study of mafic rocks associated with early Proterozoic rifting: The Peräpohja schist belt in northern Finland: Contributions to Mineralogy and Petrology, v. 104, p. 369–379.

Ionov, D., 1998, Trace element composition of mantle-derived carbonates and coexisting phases in peridotite xenoliths from alkali basalts: Journal of Petrology, v. 39, p. 1931–1941.

Ionov, D.A., O'Reilly, S.Y., and Griffin, W.L., 1997, Volatile-bearing minerals and lithophile trace elements in the upper mantle: Chemical Geology, v. 141, p. 153–184.

Ivanikov, V.V., Konopelko, D.L., Puskarov, Yu.D., Rublov, A.G., and Rungenen, G.I., 1996, Apatite-bearing ultramafic/mafic rocks of NW Ladoga region-Riphean riftorogenic or early Proterozoic postorogenic? Vestnic St. Peterburgskogo Universitera, v. 28, p. 76–81 (in Russian).

Ivanikov, V.V., Konopelko, D.L., and Teterina, T.I., 1995, Geological, geophysical and petrographic features of apatite-bearing Vuoksi pluton (Karelian Isthmus): Vestnic St. Peterburgskogo Universitera, v. 28, p. 44–52 (in Russian).

Ivashchenko, V.I., and Lavrov, O.B., 1993, Lamprophyre dykes of Akionsalmi-Kalto region (Western Lake of Ladoga). Geology and magmatism of Karelia (New results 1992): Petrozavodsk, Institute of Geology, Karelian Research Centre (Russian Academy of Sciences), p. 79–82 (in Russian).

Jacobsen, S.B., and Wasserburg, G.J., 1984, Sm-Nd isotopic evolution of chondrites and achondrites, II: Earth and Planetary Science Letters, v. 67, p. 137–150.

Janoušek, V., Bowes, D.R., Rogers, G., Farrow, C.M., and Jelínek, E., 2000, Modelling diverse processes in the Petrogenesis of a composite batholith: The Central Bohemian Pluton, Central European Hercynides: Journal of Petrology, v. 41, p. 511–543.

Janoušek, V., Braithwaite, C.J.R., Bowes, D.R., and Gerdes, A., 2004, Magma-mixing in the genesis of Hercynian calc-alkaline granitoids: An integrated petrographic and geochemical study of the Sázava intrusion, Central Bohemian Pluton, Czech Republic: Lithos, v. 78, p. 67–99.

Johansson, Å., Bogdanova, S., and Čečys, A., 2006, A revised geochronology for the Blekinge province, southern Sweden: GFF, v. 128, p. 287–302.

Johnson, D.M., Hooper, P.R., and Conrey, R.M., 1999, XRF analysis of rocks and minerals for major and trace elements on a single low dilution Li-tetraborate fused bead: Advances in X-ray Analysis, v. 41, p. 843–867.

Jurvanen, T., Eklund, O., and Väisänen, M., 2005, Generation of A-type granitic melts during the late Svecofennian metamorphism in southern Finland: GFF, v. 127, p. 139–147.

Kähkönen, Y., 2005, Svecofennian supracrustal rocks, *in* Lehtinen, M., Nurmi, P., and Rämö, O.T., eds., Precambrian Geology of Finland – Key to the Evolution of the Fennoscandian Shield: Amsterdam, Elsevier B.V., p. 343–406.

Kaitaro, S., 1953, Geologic structure of the late Pre-Cambrian intrusives in the Åva area. Åland Islands: Bulletin de la Commission Géologique de Finlande, v. 162, p. 1–71.

Kelemen, P.B., Hanghøj, K., and Greene, A.R., 2007 (updated version), One view of the geochemistry of subduction-related magmatic arcs, with an emphasis on primitive andesite and lower crust, *in* Holland, H.D., and Turekian, K.K., eds., Treatise on geochemistry, Volume 3, The crust (Rudnick, R.L., ed.): Oxford, Elsevier – Pergamon, 70 p., DOI: 10.1016/B0–08–043751–6/03035–8.

Kemp, A.I.S., Foster, G.L., Schersten, A., Whitehouse, M.J., Darling, J., and Storey, C., 2009, Concurrent Pb-Hf isotope analysis of zircon by laser ablation multi-collector ICPMS, with implications for the crustal evolution of Greenland and the Himalayas: Chemical Geology, v. 261, p. 242–258.

Kohonen, J., 1995, From continental rifting to collisional crustal shortening – Paleoproterozoic Kaleva metasediments of the Höytiäinen area in North Karelia, Finland: Geological Survey of Finland, Bulletin, v. 380, 79 p.

Koistinen, T., Stephens, M.B., Bogatchev, V., Nordgulen, Ø., Wennerström, M., and Korhonen, J., 2001, Geological map of the Fennoscandian Shield, scale 1:2 000 000: Geological Surveys of Finland, Norway and Sweden and the North-West Department of Natural Recourses of Russia.

Kononova, V.A., Pervov, V.A., Bogatikov, O.A., Parsadanyan, K.S., Zhuravlev, D.Z., and Arakelyants, M.M., 2000, Potassic mafic rocks with megacrysts from the northwestern Ladoga Lake area (Karelia, Russia): A diversity of mantle sources of potassic rocks in the east of the Fennoscandian Shield: Geochemistry International, v. 38, Suppl. 1, p. S39–S58.

Kononova, V.A., Pervov, V.A., and Parsadanyan, K.S., 1999, Heterogeneous mantle of the northern East European platform: Evidence from the isotopic composition of Sr and Nd in high-Mg alkaline rocks: Doklady Earth Sciences, v. 365, p. 227–229.

Konopelko, D.L., 1997, Postorogenic intrusions of the NW Ladoga region with special references to apatite-bearing potassium ultramafic rocks [Unpublished PhD thesis]: Russia, St. Petersburg University, 200 pp (in Russian).

Konopelko, D., and Eklund, O., 2003, Timing and geochemistry of potassic magmatism in the eastern part of the Svecofennian domain, NW Ladoga Lake Region, Russian Karelia: Precambrian Research, v. 120, p. 37–53.

Konopelko, D.L., and Ivanikov, V.V., 1996, Postorogenic intrusions of the NW Ladoga region: IGCP 315, Helsinki University, Abstracts, p. 37.

Korja, A., and Heikkinen, P., 2005, The accretionary Svecofennian orogen – insight from the BABEL profiles: Precambrian Research, v. 136, p. 241–268.

Korja, A., and Heikkinen, P., 2008, Seismic images of Paleoproterozoic microplate boundaries in the Fennoscandian Shield, *in* Condie, K.C., and Pease, V., eds., When did plate tectonics begin on planet Earth? Geological Society of America Special Paper, v. 440, p. 229–248.

Korja, A., Lahtinen, R., and Nironen, M., 2006. The Svecofennian orogen: A collage of microcontinents and island arcs, *in* Gee, D.G., and Stephenson, R.A., eds., European lithosphere dynamics: London, Geological Society, Memoirs, v. 32, p. 561–578.

Korsman, K., 1973, Geological map of Finland, 1:100 000. Sheet 3144-Sulkava: Geological Survey of Finland.

Korsman, K., Hölttä, P., Hautala, T., and Wasenius, P., 1984, Metamorphism as an indicator of evolution and structure of the crust in eastern Finland: Geological Survey of Finland, Bulletin, v. 328, 40 p.

Korsman, K., Koistinen, T., Kohonen, J., Wennerström, M., Ekdahl, E., Honkamo, M., Edman, H., and Pekkala, Y., 1997, Bedrock map of Finland 1:1 000 000; Geological Survey of Finland.

Korsman, K., Korja, T., Pajunen, M., Virransalo, P., and GGT/SVEKA Working group, 1999, The GGT/SVEKA transect: Structure and evolution of the continental crust in the Paleoproterozoic Svecofennian orogen in Finland: International Geology Review, v. 41, p. 287–333.

Korsman, K., and Lehijärvi, M., 1973, Suomen geologinen kartta 3144 Sulkava, 1:100 000. Kallioperäkartan selitykset. Summary: Precambrian rocks of the Sulkava map-sheet area: Geological Survey of Finland, 24 p.

Kosunen, P., 2004, Petrogenesis of mid-Proterozoic A-type granites: Case studies from Fennoscandia (Finland) and Laurentia (New Mexico) [PhD thesis]: Finland, University of Helsinki, 21 p.

Kouvo, O., Huhma, H., and Sakko, M., 1983, Isotopic evidence for old crustal involvement in the genesis of two granites from northern Finland: Terra Cognita, v. 3, p. 135.

Kukkonen, I., and Lauri, L., 2009, Modelling the thermal evolution of a collisional Precambrian orogen: High heat production migmatitic granites of southern Finland: Precambrian Research, v. 168, p. 233–246.

Kurhila, M., Andersen, T., and Rämö, O.T., 2010, Diverse sources of crustal granitic magma: Lu-Hf isotope data on zircon in three Paleoproterozoic leucogranites of southern Finland: Lithos, v. 115, p. 263–271.

Kurhila, M., Vaasjoki, M., Mänttäri, I., Rämö, T., and Nironen, M., 2005, U-Pb ages and Nd isotope characteristics of the lateorogenic, migmatizing microcline granites in southwestern Finland: Bulletin of the Geological Society of Finland, v. 77, p. 105–128.

Laajoki, K., 2005, Karelian supracrustal rocks, *in* Lehtinen, M., Nurmi, P., and Rämö, O.T., eds., Precambrian geology of Finland – Key to the evolution of the Fennoscandian Shield: Amsterdam, Elsevier B. V., p. 279–342.

Lahtinen, R., 1994, Crustal evolution of the Svecofennian and Karelian domains during 2.1–1.79 Ga, with special emphasis on the geochemistry and origin of 1.93–1.91 Ga gneissic tonalites and associated supracrustal rocks in the Rautalampi area, central Finland: Geological Survey of Finland, Bulletin, v. 378, 128 p.

Lahtinen, R., 1996, Geochemistry of Palaeoproterozoic supracrustal and plutonic rocks in the Tampere-Hämeenlinna area, southern Finland: Geological Survey of Finland, Bulletin, v. 389, 113 p.

Lahtinen, R., and Huhma, H., 1997, Isotopic and geochemical constraints on the evolution of the 1.93–1.79 Ga Svecofennian crust and mantle in Finland: Precambrian Research, v. 82, p. 13–34.

Lahtinen, R., Huhma, H., Kontinen, A., Kohonen J., and Sorjonen-Ward, P., 2010, New constraints for the source characteristics, deposition and age of the 2.1–1.9 Ga metasedimentary cover at the western margin of the Karelian Province: Precambrian Research, v. 176, p. 77–93.

Lahtinen, R., Huhma, H., and Kousa, J., 2002, Contrasting source components of the Paleoproterozoic Svecofennian metasediments: Detrital zircon U-Pb, Sm-Nd and geochemical data: Precambrian Research, v. 116, p. 81–109.

Lahtinen, R., Korja, A., and Nironen, M., 2005, Paleoproterozoic tectonic evolution, *in* Lehtinen, M., Nurmi, P., and Rämö, O.T., eds., Precambrian geology of Finland – Key to the evolution of the Fennoscandian Shield: Amsterdam, Elsevier B.V., p. 481–532.

Lauri, L.S., Andersen, T., Hölttä, P., Huhma, H., and Graham, S., in review, Evolution of the Archean Karelian province in the Fennoscandian Shield in the light of U-Pb zircon ages and Sm-Nd and Lu-Hf isotope systematics: Journal of the Geological Society of London.

Leat, P.T., Riley, T.R., Wareham, C.D., Millar, I.L., Kelley, S.P., and Storey, B.C., 2002, Tectonic setting of primitive magmas in volcanic arcs: An example from the Antarctic Peninsula: Journal of the Geological Society, London, v. 159, p. 31–44.

Leterrier, J., Yuwono, Y.S., Soeria-Atmadja, R., and Maury, R.C., 1990, Potassic volcanism in Central Java and South Sulawesi, Indonesia: Journal of Southeast Asian Earth Sciences, v. 4, p. 171–187.

Levin, T., Engström, J., Lindroos, A., Baltybaev, S., and Levchenkov, O., 2005, Late-Svecofennian transpressive deformation in SW Finland – evidence from late-stage D3 structures: GFF, v. 127, p. 129–137.

Liégeois, J.-P., 1998, Preface – Some words on the post-collisional magmatism: Lithos, v. 45, p. XV–XVII.

Liégeois, J.-P., Navez, J., Hertogen, J., and Black, R., 1998, Contrasting origin of post-collisional high-K calc-alkaline and shoshonitic versus alkaline and peralkaline granitoids. The use of sliding normalization: Lithos, v. 45, p. 1–28.

López-Moro, F.-J., and López-Plaza, M., 2004, Monzonitic series from the Variscan Tormes Dome (Central Iberian Zone): Petrogenetic evolution from monzogabbro to granite magmas: Lithos, v. 72, p. 19–44.

Ludwig, K.R., 2003, User's Manual for Isoplot 3.00. A Geochronological Toolkit for Microsoft Excel: Berkeley Geochronology Center, Special Publication, v. 4, 70 p.

Lundqvist, Th., and Persson, P.O., 1999, Geochronology of porphyries and related rocks in northern and western Dalarna, south-central Sweden: GFF, v. 121, p. 307–322.

Mahéo, G., Guillot, S., Blichert-Tofa, J., Rolland, Y., Pêcher, A., 2002, A slab break-off model for the Neogene thermal evolution of Southern Karakorum and South Tibet: Earth Planetary Science Letter, v. 195, p. 45–58.

Mahoney, J.B., Weis, D., Kieffer, B., Friedman, R., Pretorius, W., Scoates, K., Goolaerts, A., and Maerschalk, C., 2003, Abstract GSA Seattle, 2003. Ongoing isotopic characterization of USGS standards: MC-ICPMS and TIMS data from the Pacific Centre for Isotopic and Geochemical Research, University of British Columbia: Geological Society of America, Abstracts with Programs, v. 35, no. 6, p. 243.

Makkonen, H.V., 1996, 1.9 Ga tholeiitic magmatism and related Ni-Cu deposition in the Juva area, SE Finland: Geological Survey of Finland, Bulletin, v. 386, p. 1–101.

Maniar, P.D., and Piccoli, P.M., 1989, Tectonic discrimination of granitoids: Geological Society of America Bulletin, v. 101, p. 635–643.

Mansfeld J., 2004, The Småland-Värmland belt in southeastern Sweden: Geological Survey of Finland, Special Paper, v. 37, p. 20–21.

Martin, H., Chauvel, C., Jahn, B.-M., and Vidal, P., 1983, Rb-Sr and Sm-Nd ages and isotopic geochemistry of Archaean granodioritic gneisses from eastern Finland: Precambrian Research, v. 20, p. 79–91.

McCulloch, M.T., and Chappell, B.W., 1982, Nd isotopic characteristics of S- and I-type granites: Earth and Planetary Science Letters, v. 58, p. 51–64.
McDonough, W.F., and McCulloch, M.T., 1987, The southeast Australian lithospheric mantle: Isotopic and geochemical constraints on its growth and evolution: Earth and Planetary Science Letters, v. 86, p. 327–340.
Menzies, M.A., Rogers, N., Tindle, A., and Hawkesworth, C.J., 1987, Metasomatic and enrichment processes in lithospheric peridotites, an effect of asthenosphere-lithosphere interaction, *in* Menzies, M.A., and Hawkesworth, C.J., eds., Mantle metasomatism: London, Academic Press, p. 313–361.
Middlemost, E.A.K., 1989, Iron oxidation ratios, norms and the classification of volcanic rocks: Chemical Geology, v. 77, p. 19–26.
Middlemost, E.A.K., 1994, Naming materials in the magma/igneous rock system: Earth-Science Reviews, v. 37, p. 215–224.
Miller, C., Schuster, R., Klötzli, U., Frank, W., and Purtscheller, F., 1999, Post-collisional potassic and ultrapotassic magmatism in SW Tibet; geochemical and Sr-Nd-Pb-O isotopic constraints for mantle source characteristics and petrogenesis: Journal of Petrology, v. 40, p. 1399–1424.
Miller, R.G., O'Nions, R.K., Hamilton, P.J., and Welin, E., 1986, Crustal residence ages of clastic sediments, orogeny and continental evolution: Chemical Geology, v. 57, 87–99.
Morrison, G.W., 1980. Characteristics and tectonic setting of the shoshonite rock association: Lithos, v. 13, p. 97–108.
Mouri, H., Väisänen, M., Huhma, H., and Korsman, K., 2005, Sm-Nd garnet and U-Pb monazite dating of high-grade metamorphism and crustal melting in the West Uusimaa area, southern Finland: GFF, v. 127, p. 123–128.
Müller, K., Rock, N.M.S., and Groves, D.I., 1992, Geochemical discrimination between shoshonitic and potassic volcanic rocks in different tectonic settings: A pilot study: Mineralogy and Petrology, v. 46, p. 259–289.
Mutanen, T., and Huhma, H., 2003, The 3.5 Ga Siurua trondhjemite gneiss in the Archaean Pudasjärvi Granulite Belt, northern Finland: Bulletin of the Geological Society of Finland, v. 75, p. 51–68.
Neymark, L.A., Amelin, Yu.V., and Larin, A.M., 1994, Pb-Nd-Sr isotopic constraints on the origin of the 1.54–1.56 Ga Salmi rapakivi granite-anorthosite batholith (Karelia, Russia): Mineralogy and Petrology, v. 50, p. 173–194.
Nironen, M., 1997, The Svecofennian Orogen: A tectonic model: Precambrian Research, v. 86, p. 21–44.
Nironen, M., 2005, Proterozoic orogenic granitoid rocks, *in* Lehtinen, M., Nurmi, P., and Rämö, O. T., eds., Precambrian geology of Finland – Key to the evolution of the Fennoscandian Shield: Amsterdam, Elsevier B. V., p. 443–480.
Nironen, M., Korja, A., Heikkinen, P., and the FIRE Working Group, 2006, A geological interpretation of the upper crust along FIRE 2 and FIRE 2A: Geological Survey of Finland, Special Paper, v. 43, p. 77–103.
Nironen, M., and Kurhila, M., 2008, The Veikkola granite area in southern Finland: Emplacement of a 1.83–1.82 Ga plutonic sequence in an extensional regime: Bulletin of the Geological Society of Finland, v. 80, p. 39–68.
Nironen, M., and Rämö, O.T., 2005, Postorogenic intrusions, *in* Rämö, O.T., Halla, J., Nironen, M., Lauri, L.S., Kurhila, M.I., Käpyaho, A., Sorjonen-Ward, P., Äikäs, O., eds., EUROGRANITES 2005 – Proterozoic and Archean granites and related rocks of the Finnish Precambrian: Helsinki, University of Helsinki, Publications of the Department of Geology, v. A1, p. 47–49.
Nurmi, P.A., and Haapala, I., 1986, The Proterozoic granitoids of Finland: Granite types, metallogeny and relation to crustal evolution: Bulletin of the Geological Society of Finland, v. 58, p. 203–233.
Nykänen, O., 1968, Suomen geologinen kartta, kallioperäkartan selitys. Lehti 4232–4324: Geological map of Finland, explanation to the map of rocks. Sheet 4232–4324, 66 p. Geological Survey of Finland. [English summary.]
Nykänen, O., 1983, Geological map of Finland 1:100 000. Explanation to the maps of pre-Quaternary rocks. Sheets 4124 + 4142 and 4123 + 4114. Pre-Quaternary rocks of the Punkaharju and Parikkala map-sheet areas, 81 p. Geological Survey of Finland. [English summary.]
Nykänen, O., 1988, Geological map of Finland 1:100 000. Explanation to the maps of rocks. Sheet 4121. Pre-Quaternary rocks of the Virmutjoki map-sheet area, 64 p. Geological Survey of Finland. [English summary.]

Nyström, J.-O., 1982, Post-Svecokarelian andinotype evolution in central Sweden: Geologische Rundschau, v. 71, p. 141–157.
Nyström, J.-O., 1999, Origin and tectonic setting of the Dala volcanites: Project 03–889/96, Final report, December 1999, 41 p. + tables. Geological Survey of Sweden.
O'Brien, H.E., Huhma, H., and Sorjonen-Ward, P., 1993, Petrogenesis of the late Archean Hattu schist belt, Ilomantsi, eastern Finland: Geochemistry and Sr, Nd isotopic composition: Geological Survey of Finland, Special Paper, v. 17, p. 147–184.
Öhlander, B., Mellqvist, C., and Skiöld, T., 1999, Sm-Nd isotope evidence of a collisional event in the Precambrian of northern Sweden: Precambrian Research, v. 93, p. 105–117.
Öhlander, B., and Romer, R.L., 1996, Zircon ages of granites occurring along the central Swedish gravity low: GFF, v. 118, p. 217–225.
Öhlander, B., Skiöld, T, Hamilton, P.J., and Claesson, S., 1987, The western border of the Archaean province of the Baltic Shield: Evidence from northern Sweden: Contributions to Mineralogy and Petrology, v. 95, p. 437–450.
Patchett, P.J., Gorbatschev, R., and Todt, W., 1987, Origin of continental crust of 1.9–1.7 Ga age. Nd isotopes in the Svecofennian orogenic terrains of Sweden: Precambrian Research, v. 35, p. 145–160.
Patchett, P.J., and Kouvo, O., 1986, Origin of continental crust of 1.9–1.7 Ga age: Nd isotopes and U-Pb zircon ages in the Svecokarelian terrain of south Finland: Contributions to Mineralogy and Petrology, v. 92, p. 1–12.
Patchett, P.J., Kouvo, O., Hedge, C.E., and Tatsumoto, M., 1981, Evolution of continental crust and mantle heterogeneity: Evidence from Hf isotopes: Contributions to Mineralogy and Petrology, v. 78, p. 279–297.
Peacock, M.A., 1931, Classification of igneous rocks: Journal of Geology, v. 39, 54–67.
Pearce, J.A., 1982. Trace element characteristics of lavas from destructive plate boundaries, *in* Thorpe, R.S., ed., Andesites: Orogenic andesites and related rocks: Chichester, John Wiley & Sons, p. 525–548.
Pearce, J.A., 1983, Role of the sub-continental lithosphere in magma genesis at active continental margins, *in* Hawkesworth, C., and Norry, M.J., eds., Continental basalts and mantle xenoliths: Nantwick, Shiva Press, p. 230–249.
Pearce, J.A., 1996a, A user's guide to basalt discrimination diagrams, *in* Wyman, D.A., ed., Trace element geochemistry of volcanic rocks: Applications for massive sulphide exploration: Geological Association of Canada, Short Course Notes Volume, v. 12, p. 79–113.
Pearce, J.A., 1996b, Sources and settings of granitic rocks: Episodes, v. 19, p. 120–125.
Pearce, J.A., Bender, J.F., De Long, S.E., Kidd, W.S.F., Low, P.J., Guner, Y., Saroglu, F., Ylimaz, Y., Moorbath, S., and Mitchell, J.G., 1990, Genesis of collision volcanism in Eastern Anatolia, Turkey: Journal of Volcanology and Geothermal Research, v. 44, p. 189–229.
Pearce, J.A., Harris, N.B.W., and Tindle, A.G., 1984, Trace element discrimination diagrams for the tectonic interpretation of granitic rocks: Journal of Petrology, v. 25, p. 956–983.
Peltonen, P., Kontinen, A., and Huhma, H., 1996, Petrology and geochemistry of metabasalts from the 1.95 Ga Jormua Ophiolite, northeastern Finland: Journal of Petrology, v. 37, p. 1359–1383.
Peltonen, P., and Mänttäri, I., 2001, An ion microprobe U-Th-Pb study of zircon xenocrysts from Lahtojoki kimberlite pipe, eastern Finland: Bulletin of the Geological Society of Finland, v. 73, p. 47–58.
Peltonen, P., Mänttäri, I., Huhma, H., and Whitehouse, M.J., 2006, Multi-stage origin of the lower crust of the Karelian craton from 3.5 to 1.7 Ga based on isotopic ages of kimberlite-derived mafic granulite xenoliths: Precambrian Research, v. 147, p. 107–123.
Peltonen, P., O'Brien, H., Karhu, J., and Kukkonen, I., 2000, Kimberlites, carbonatites, and their mantle sample: Constraints for the origin and temporal evolution of the lithospheric mantle in Fennoscandia: Institute of Seismology, University of Helsinki, Report, v. S-41, p. 63–69.
Persson, K.S., and Sjöström, H., 2003, Late-orogenic progressive shearing in eastern Bergslagen, central Sweden: GFF, v. 125, p. 23–36.
Pesonen, L.J., Elming, S.-Å., Mertanen, S., Pisarevsky, S., D'Agrella-Filho, M.S., Meert, J.G., Schmidt, P.W., Abrahamsen, N., and Bylund, G., 2003, Palaeomagnetic configuration of continents during the Proterozoic: Tectonophysics, v. 375, p. 289–324.
Pitkänen, P., 1985, Anttolan Luonterin postorogeenisen intruusion petrologia ja geokemia [Unpublished Master thesis]: Finland, University of Helsinki, 81 p. (in Finnish).
Puustinen, K., and Karhu, J.A., 1999, Halpanen calcite carbonatite dike, southeastern Finland: Geological Survey of Finland, Special Paper, v. 27, p. 39–41.

Raczek, I., Jochum, K.P., and Hofmann A.W., 2003, Neodymium and strontium isotope data for USGS reference materials BCR-1, BCR-2, BHVO-1, BHVO-2, AGV-1, AGV-2, GSP-1, GSP-2, and eight MPI-DING reference glasses: Geostandards Newsletter, v. 27, p. 173–179.

Rämö, O.T., 1991, Petrogenesis of Proterozoic rapakivi granites and related basic rocks of southeastern Fennoscandia: Nd and Pb isotopic and general geochemical constraints: Bulletin of the Geological Survey of Finland, v. 355, 161 p.

Rämö, O.T., Halla, J., Nironen, M., Lauri, L.S., Kurhila, M.I., Käpyaho, A., Sorjonen-Ward, P., and Äikäs, O., eds., 2005, EUROGRANITES 2005 – Proterozoic and Archean granites and related rocks of the Finnish Precambrian: Publications of the Department of Geology, v. A1, University of Helsinki, Finland, 128 p.

Rämö, O.T., Kurhila, M., Nironen, M., Vaasjoki, M., Mänttäri, I., and Elliott, B.A., 2004, Nd isotope variation in the lateorogenic microcline granites and their synorogenic country rock granitoids in southern Finland, *in* 26th Nordic Geological Winter Meeting, Uppsala, Sweden, GFF, v. 126, p. 34.

Rämö, O.T., and Nironen, M., 2001, The Oripää granite, SW Finland: Characterization and significance in terms of Svecofennian crustal evolution: Bulletin of the Geological Society of Finland, v. 73, p. 103–109.

Rämö, O.T., Vaasjoki, M., Mänttäri, I., Elliott, B.A., and Nironen, M., 2001, Petrogenesis of the post-kinematic magmatism of the Central Finland Granitoid Complex I; radiogenic isotope constraints and implications for crustal evolution: Journal of Petrology, v. 42, p. 1971–1993.

Reichardt, H., Weinberg, R.F., Andersson, U.B., and Fanning, C.M., 2010, Hybridization of granitic magmas in the source: The origin of the Karakoram Batholith, Ladakh, NW India: Lithos, v. 116, p. 249–272.

Rickwood, P.C., 1989, Boundary lines within petrologic diagrams which use oxides of major and minor elements: Lithos, v. 22, p. 247–263.

Roberts, M.P., and Clemens, J.D., 1993, Origin of high-potassium, calc-alkaline, I-type granitoids: Geology, v. 21, p. 825–828.

Rock Geochemical Database of Finland (online database). Version 1.1 (publication date April 25th 2008; accessed: December 7th 2009). Geological Survey of Finland, available at http://www.gtk.fi/publ/RGDB.

Rollinson, H.R., 1993, Using geochemical data: Evaluation, presentation, interpretation: Essex, Addison Wesley Longman Limited, 352 p.

Romer, R.L., and Öhlander, B., 1995, Tectonic implications of an 1846 ± 1 Ma old migmatitic granite in south-central Sweden: GFF, v. 117, p. 69–74.

Rosa, D.R.N., Finch, A.A., Andersen, T., and Inverno, C.M.C., 2009, U-Pb geochronology and Hf isotope ratios of magmatic zircons from the Iberian pyrite belt: Mineralogy and Petrology, v. 95, p. 47–69.

Rudnick, R.L., McDonough, W.F., and Chappell, B.W., 1993, Carbonate metasomatism in the northern Tanzanian mantle: Petrographic and geochemical characteristics: Earth and Planetary Science Letters, v. 114, p. 463–475.

Rukhlov, A.S., and Bell, K., 2010, Geochronology of carbonatites from the Canadian and Baltic Shields, and the Canadian Cordillera: Clues to mantle evolution: Mineralogy and Petrology, v. 98, p. 11–54.

Ruotoistenmäki, T., Mänttäri, I., and Paavola, J., 2001, Characteristics of Proterozoic late-/post-collisional intrusives in Archaean crust in Iisalmi-Lapinlahti area, central Finland: Geological Survey of Finland, Special Paper, v. 31, p. 105–115.

Rutanen, H., 2001, Geochemistry and petrogenesis of the 1.8 Ga old post-collisional intrusions in southern Finland and Russian Karelia [Unpublished PhLic thesis]: Finland, Åbo Akademi University, 86 p.

Rutanen, H., and Andersson, U.B., 2009, Mafic plutonic rocks in a continental-arc setting: Geochemistry of 1.87–1.78 Ga rocks from south-central Sweden and models of their palaeotectonic setting: Geological Journal, v. 44, p. 241–279.

Rutanen, H., Eklund, O., and Konopelko, D., 1997, Rock and mineral analyses of Svecofennian postorogenic 1.8 Ga intrusions in southern Finland and Russian Karelia: University of Turku and Åbo Akademi University, Finland, Geocenter raportti-Geocenter rapport, v. 15, 8 p. + 58 p, tables.

Rutland, R.W.R., Williams, I.S., and Korsman, K., 2004, Pre-1.91 Ga deformation and metamorphism in the Palaeoproterozoic Vammala migmatite belt, southern Finland, and implications for Svecofennian tectonics: Bulletin of the Geological Society of Finland, v. 76, p. 93–140.

Scherer, E.E., Münker, C., and Mezger, K., 2001, Calibration of the lutetium hafnium clock: Science, v. 293, p. 683–687.
Scherer, E.E., Münker, C., and Mezger, K., 2007, The Lu-Hf systematics of meteorites: Consistent or not: Geochimica et Cosmochimica Acta, v. 71, no. 15, Suppl. 1, Goldschmidt Conference Abstracts, p. A888.
Schmidberger, S.S., Simonetti, A., and Francis, D., 2001, Sr-Nd-Pb isotope systematics of mantle xenoliths from Somerset Island kimberlites: Evidence for lithosphere stratification beneath Arctic Canada: Geochimica et Cosmochimica Acta, v. 65, p. 4243–4255.
Segal, I., Halicz, L., and Platzner, I.T., 2003, Accurate isotope ratio measurements of ytterbium by multiple collection inductively coupled plasma mass spectrometry applying erbium and hafnium in an improved double external normalization procedure: Journal of Analytical Atomic Spectrometry, v. 18, p. 1217–1223.
Simonen, A., 1980, The Precambrian in Finland: Geological Survey of Finland, Bulletin, v. 304, 58 p.
Simonen, A., 1982, Explanation to the maps of rocks 1:100 000. Sheets 3123 and 3142. Mäntyharjun ja Mikkelin kartta-alueiden kallioperä. Summary: Pre-Quaternary rocks of the Mäntyharju and Mikkeli map-sheet areas, Geological Survey of Finland, 36 p.
Simonen, A., and Niemelä, R., 1980, Geological map of Finland 1:100 000. Sheet 3142 – Mikkeli: Geological Survey of Finland.
Skyttä, P., and Mänttäri, I., 2008, Structural setting of late Svecofennian granites and pegmatites in Uusimaa Belt, SW Finland: Age constraints and implications for crustal evolution: Precambrian Research, v. 164, p. 86–109.
Skyttä, P., Väisänen, M., and Mänttäri, I., 2006, Preservation of Palaeoproterozoic early Svecofennian structures in the Orijärvi area, SW Finland – Evidence for polyphase strain partitioning: Precambrian Research, v. 150, p. 153–172.
Söderlund, U., Isachsen, C.E., Bylund, G., Heaman, L.M., Patchett, P.J., Vervoort, J.D., and Andersson, U.B., 2005, U-Pb baddeleyite ages and Hf, Nd isotope chemistry constraining repeated mafic magmatism in the Fennoscandian Shield from 1.6 to 0.9 Ga: Contributions to Mineralogy and Petrology, v. 150, p. 174–194.
Söderlund, U., Patchett, P.J., Vervoort, J., and Isachsen, C.E., 2004, The 176 Lu decay constant determined by Lu-Hf and U-Pb isotope systematics of Precambrian mafic intrusions: Earth and Planetary Science Letters, v. 219, p. 311–324.
Sorjonen-Ward, P., 2006, Geological and structural framework and preliminary interpretation of the FIRE 3 and FIRE 3A reflection seismic profiles, central Finland: Geological Survey of Finland, Special Paper, v. 43, p. 105–159.
Sorjonen-Ward, P., and Luukkonen, E.J., 2005, Archean rocks, *in* Lehtinen, M., Nurmi, P., and Rämö, O.T., eds., Precambrian geology of Finland – Key to the evolution of the Fennoscandian Shield: Amsterdam, Elsevier B.V., p. 19–99.
Stacey, J.S., and Kramers, J.D., 1975, Approximation of terrestrial lead isotope evolution by a two-stage model: Earth and Planetary Science Letters, v. 26, p. 207–221.
Stålfors, T., and Ehlers C., 2006, Emplacement mechanisms of Late-orogenic granites – Structural and geochemical evidence from southern Finland: International Journal of Earth Sciences, v. 95, p. 557–568.
Staudigel, H., Davies, G.R., Hart, S.R., Marchant, K.M., and Smith, B.M., 1995, Large scale isotopic Sr, Nd and O isotopic anatomy of altered oceanic crust: DSDP/ODP sites 417/418: Earth and Planetary Science Letters, v. 130, p. 169–185.
Steiger, R.H., and Jäger, E., 1977, Subcommission of geochronology: Convention on the use of decay constants in geo- and cosmochronology: Earth and Planetary Science Letters, v. 36, p. 359–362.
Sultan, L., Claesson, S., and Plink-Björklund, P., 2005, Proterozoic and Archaean ages of detrital zircon from the Palaeoproterozoic Västervik Basin, SE Sweden: Implications for provenance and timing of deposition: GFF, v. 127, p. 17–24.
Sun, C.-H., and Stern, R., 2001, Genesis of Mariana shoshonites: Contribution of the subduction component: Journal of Geophysical Research, v. 106, p. 589–608.
Sun, C.-H., Stern, R.J., Yoshida, T., and Kimura, J.-I., 1998, Fukutoku-oka-no-ba Volcano: A new perspective on the Alkalic Volcano Province in the Izu-Bonin-Mariana arc: The Island Arc, v. 7, p. 432–442.
Sun, S.-s., 1980, Lead isotopic study of young volcanic rocks from mid-ocean ridges, ocean islands and island arcs: Philosophical Transactions of the Royal Society of London, v. A297, p. 409–445.

Sun, S.-s., and McDonough, W.F., 1989, Chemical and isotopic systematics of oceanic basalts: Implications for mantle composition and processes, *in* Saunders, A.D., and Norry, M.J., eds., Magmatism in the ocean basins: Geological Society Special Publications, v. 42, p. 313–345.
Suominen, V., 1991, The chronostratigraphy of southwestern Finland with special reference to Postjotnian and Subjotnian diabases: Geological Survey of Finland, Bulletin, v. 356, 100 p.
Tatsumi, Y., and Eggins S., 1995, Subduction zone magmatism: Oxford, Blackwell Science, 211 p.
Taylor, S.R., and McLennan, S.M., 1985, The continental crust: Its composition and evolution: Oxford, Blackwell, 312 p.
Tera, F., and Wasserburg, G.J., 1972, U-Th-Pb systematics in three Apollo 14 basalts and the problem of initial Pb in lunar rocks: Earth and Planetary Science Letters, v. 14, p. 281–304.
Thirlwall, M.F., Graham, A.M., Arculus, R.J., Harmon, R.S., and MacPherson, C.G., 1996, Resolution of the effects of crustal assimilation, sediment subduction, and fluid transport in island arc magmas: Pb-Sr-Nd-O isotope geochemistry of Grenada, Lesser Antilles: Geochimica et Cosmochimica Acta, v. 60, p. 4785–4810.
Torppa, O.A., and Karhu, J.A., 2007, Ancient subduction recorded in the isotope characteristics of ~1.8 Ga Fennoscandian carbonatites, *in* Goldschmidt 2007 Conference, Cologne, Germany, August 19–24, 2007, Abstract, p. A1032.
Torvela, T., Mänttäri, I., and Hermansson, T., 2008, Timing of deformation phases within the South Finland shear zone, SW Finland: Precambrian Research, v. 160, p. 277–298.
Turner, S., Arnaud, N., Liu, J., Rogers, N., Hawkesworth, C., Harris, N., Kelley, S., van Calsteren, P., and Deng, Q., 1996, Post-collision, shoshonitic volcanism on the Tibetan plateau: Implication for convective thinning of the lithosphere and source of ocean island basalts: Journal of Petrology, v. 37, p. 45–71.
Vaasjoki, M., 1995, The Rouvinmäki quartzmonzodiorite at Renko: A new posttectonic granitoid: Geologi, v.47, p. 79–81 (in Finnish with English summary).
Vaasjoki, M., 1996, A more precise U-Pb zircon age for the Seglinge ring complex, Åland Islands, SW Finland: Geologi, v. 48, 75–77 (in Finnish with English summary).
Vaasjoki, M., ed., 2001, Radiometric age determinations from Finnish Lapland and their bearing on the timing of Precambrian volcano-sedimentary sequences: Geological Survey of Finland, Special Paper, v. 33, 279 p.
Vaasjoki, M., and Huhma, H., 1999, Lead and neodymium isotopic results from metabasalts of the Haveri Formation, southern Finland: Evidence for Palaeoproterozoic enriched mantle: Bulletin of the Geological Society of Finland, v. 71, p. 143–153.
Vaasjoki, M., and Sakko, M., 1988, The evolution of the Raahe-Ladoga zone in Finland: Isotopic constraints: Geological Survey of Finland, Bulletin, v. 343, p. 7–32.
Väisänen, M., Eklund, O., Johansson, Å., Hölttä, P., and Andersson, U.B., 2009, Palaeoproterozoic adakite-like synorogenic magmatism in SW Finland, *in* Kubischta, F., Kultti, S., and Salonen, V.-P., eds., 6th National Geological Colloquium, Program and Abstracts: Helsinki, University of Helsinki, Publications of the Department of Geology, v. A3, p. 55.
Väisänen, M., and Hölttä, P., 1999, Structural and metamorphic evolution of the Turku migmatite complex, southwestern Finland: Bulletin of the Geological Society of Finland, v. 71, p. 177–218.
Väisänen, M., Johansson, Å., Eklund, O., Ehlers, C., and Andersson, U.B., 2008, Svecofennian synvolcanic magmatism in SW Finland: Examples from Enklinge and Orijärvi: 28th Nordic Geological Wintermeeting, Aalborg, January 7–10, 2008. Abstract Volume, p. 130.
Väisänen, M., and Kirkland, C.L., 2008, U-Th-Pb geochronology of igneous rocks in the Toija and Salittu Formations, Orijärvi area, southwestern Finland: Constraints on the age of volcanism and metamorphism: Bulletin of the Geological Society of Finland, v. 80, 73–87.
Väisänen, M., Mänttäri, I., and Hölttä, P., 2002, Svecofennian magmatic and metamorphic evolution in southwestern Finland as revealed by U-Pb zircon SIMS geochronology: Precambrian Research, v. 116, p. 111–127.
Väisänen, M., Mänttäri, I., Kriegsman, L.M., and Hölttä, P., 2000, Tectonic setting of post-collisional magmatism in the Palaeoproterozoic Svecofennian Orogen, SW Finland: Lithos, v. 54, p. 63–81.
Väisänen, M., and Skyttä, P., 2007, Late Svecofennian shear zones in southwestern Finland: GFF, v. 129, p. 55–64.
Valbracht, P.J., 1991, The origin of the continental crust of the Baltic shield, as seen through Nd and Sr isotopic variations in 1.89–1.85 Ga old rocks from the western Bergslagen, Sweden [PhD thesis]: Amsterdam, Netherlands, GUA papers of geology, Series 1, No. 29, 222 p.

Valbracht, P.J., Oen, I.S., and Beunk, F.F., 1994, Sm-Nd isotope systematics of 1.9–1.8 Ga granites from western Bergslagen, Sweden: Inferences on a 2.1–2.0 Ga crustal precursor: Chemical Geology, v. 112, p. 21–37.

Verma, S.P., Torres-Alvarado, I.S., and Sotelo-Rodríguez, Z.T., 2002, SINCLAS: Standard igneous norm and volcanic rock classification system: Computers & Geosciences, v. 28, p. 711–715.

Vervoort, J.D., and Patchett, P.J., 1996, Behaviour of hafnium and neodymium isotopes in the crust: Controls from Precambrian crustally derived granites: Geochimica et Cosmochimica Acta, v. 60, p. 3717–3733.

Vervoort, J.D., Patchett, P.J., Söderlund, U., and Baker, M., 2004, Isotopic composition of Yb and the determination of Lu concentrations and Lu/Hf ratios by isotope dilution using MC-ICPMS: Geochemistry Geophysics Geosystems, v. 5, Q11002, DOI: 10.1029/2004GC000721.

Voshage, H., Hunziker, J.C., Hofmann, A.W., and Zingg, A., 1987, A Nd and Sr isotopic study of the Ivrea zone, Southern Alps, N-Italy: Contributions to Mineralogy and Petrology, v. 97, p. 31–42.

Wasserburg, G.J., Jacobsen, S.B., DePaolo, D.J., McCulloch, M.T., and Wen, T., 1981, Precise determination of Sm/Nd ratios, Sm and Nd isotopic abundances in standard solutions: Geochimica Cosmochimica Acta, v. 45, p. 2311–2323.

Welin, E., Vaasjoki, M., and Suominen, V., 1983, Age differences between Rb-Sr whole rock and U-Pb zircon ages of syn- and postorogenic Svecokarelian granitoids in Sottunga, SW Finland: Lithos, v. 16, p. 297–305.

Wenzel, T., Mertz, D.F., Oberhansli, R., Becker, T., and Renne, P.R., 1997, Age, geodynamic setting, and mantle enrichment processes of a K-rich intrusion from the Meissen massif (northern Bohemian massif) and implications for related occurrences from the mid-European Hercynian: Geologische Rundschau, v. 86, p. 556–570.

Wenzel, T., Oberhänsli, R., and Mezger, K., 2000, K-rich plutonic rocks and lamprophyres from the Meissen Massif (northern Bohemian Massif): Geochemical evidence for variably enriched lithospheric mantle sources: Neues Jahrbuch für Mineralogie – Abhandlungen, v. 175, p. 249–293.

Whalen, J.B., Currie, K.L., and Chappell, B.W., 1987, A-type granites: Geochemical characteristics, discrimination and petrogenesis: Contributions to Mineralogy and Petrology, v. 95, p. 407–419.

Whitehouse, M.J., and Kamber, B.S., 2005, Assigning dates to thin gneissic veins in high-grade metamorphic terranes: A cautionary tale from Akilia, southwest Greenland: Journal of Petrology, v. 46, p. 291–318.

Whitehouse, M.J., Kamber, B., and Moorbath, S., 1999, Age significance of U-Th-Pb zircon data from early Archaean rocks of west Greenland – a reassessment based on combined ion-microprobe and imaging studies: Chemical Geology, v. 160, p. 201–224.

Wiedenbeck, M., Allé, P., Corfu, F., Griffin, W.L., Meier, M., Oberli, F., von Quadt, A., Roddick, J.C., and Spiegeln, W., 1995, Three natural zircon standards for U-Th-Pb, Lu-Hf, trace element and REE analysis: Geostandards Newsletter, v. 19, p. 1–23.

Wikström, A., and Andersson, U.B., 2004, Geological features of the Småland-Värmland belt along the Svecofennian margin, part I: From the Loftahammar to the Tiveden-Askersund areas. Introduction: Geological Survey of Finland, Special Paper, v. 37, p. 22–25.

Wilkinson, J.F.G., and Le Maitre, R.W., 1987, Upper mantle amphiboles and micas and TiO_2, K_2O and P_2O_5 abundances and 100 $Mg/(Mg+Fe^{2+})$ ratios of common basalts and andesites: Implications for modal mantle metasomatism and undepleted mantle compositions: Journal of Petrology, v. 28, p. 37–73.

Williams, H.M., Turner, S.P., Pearce, J.A., Kelley, S.P., and Harris, N.B.W., 2004, Nature of the source regions for post-collisional, potassic magmatism in southern and northern Tibet from geochemical variations and inverse trace element modelling: Journal of Petrology, v. 45, p. 555–607.

Wilson, M., 1989, Igneous petrogenesis: London, Unwin Hyman, 466 p.

Wilson, M., Tankut, A., and Gulec, N., 1997, Tertiary volcanism of the Galatia province, north-west central Anatolia, Turkey: Lithos, v. 42, p. 105–121.

Wilson, M.R., Fallick, A.E., Hamilton, P.J., and Persson, L., 1986, Magma sources for some mid-Proterozoic granitoids in SE Sweden: Geochemical and isotopic constraints: GFF, v. 108, p. 79–91.

Wilson, M.R., Hamilton, P.J., Fallick, A.E., Aftalion, M., and Michard, A., 1985, Granites and early Proterozoic crustal evolution in Sweden: Evidence from Sm-Nd, U-Pb and O isotope systematics: Earth and Planetary Science Letters, v. 72, p. 376–388.

Wood, D.A., 1980, The application of a Th-Hf-Ta diagram to problems of tectonomagmatic classification and to establishing the nature of crustal contamination of basaltic lavas of the British Tertiary Volcanic Province: Earth and Planetary Science Letters, v. 50, p. 11–30.

Wood, D.A., Joron, J.-L., and Treuil, M., 1979, A re-appraisal of the use of trace elements to classify and discriminate between magma series erupted in different tectonic settings: Earth and Planetary Science Letters, v. 45, p. 326–336.

Woodard, J., and Hetherington, C.J., in review, Primary carbonatite in a post-collisional tectonic setting: Geochronology and emplacement conditions at Naantali, SW Finland: Precambrian Research.

Woodard, J., and Huhma, H., in review, Paleoproterozoic mantle enrichment beneath the Fennoscandian Shield: Isotopic insight from carbonatites and lamprophyres: Lithos.

Woodard, J., Kietäväinen, R., Eklund, O., and Shebanov, A., in review, Svecofennian post-collisional shoshonitic lamprophyres at the margin of the Karelia Craton: implications for mantle metasomatism: Lithos.

Woodhead, J.D., and Hergt, J.M., 2005, A preliminary appraisal of seven natural zircon reference materials for in situ Hf isotope determination: Geostandards Geoanalytical Research, v. 29, p. 183–195.

Woodhead, J., Hergt, J., Shelley, M., Eggins, S., and Kemp, R., 2004, Zircon Hf-isotope analysis with an excimer laser, depth profiling, ablation of complex geometries, and concomitant age estimation: Chemical Geology, v. 209, p. 121–135.

Wyllie, P.J., 1995, Experimental petrology of upper mantle materials, processes and products: Journal of Geodynamics, v. 20, p. 439–468.

Xu, X., O'Reilly, S.Y., Griffin, W.L., and Zhou, X., 2003, Enrichment of upper mantle peridotite: Petrological, trace element and isotopic evidence on xenoliths from SE China: Chemical Geology, v. 198, p. 163–188.

You, C.-F., Castillo, P.R., Gieskes, J.M., Chan, L.H., and Spivack, A.J., 1996, Trace element behaviour in hydrothermal experiments: Implications for fluid processes at shallow depths in subduction zones: Earth and Planetary Science Letters, v. 140, p. 41–52.

Zhang, Z., Xiao, X., Wang, J., Wang, Y., and Kusky, T. M., 2008, Post-collisional Plio-Pleistocene shoshonitic volcanism in the western Kunlun Mountains, NW China: Geochemical constraints on mantle source characteristics and petrogenesis: Journal of Asian Earth Sciences, v. 31, p. 379–403.

Zuber, J., and Öhlander, B., 1991, Gravimetrical and geochemical studies of 1.8 Ga old granites in the Strängnäs-Enköping area, south central Sweden: Geologiska Föreningens i Stockholm Förhandlingar, v. 113, p. 309–318.